Biochemical characterization of physiological age-dependent aggregates in *C. elegans*

Dissertation

zur Erlangung des Grades eines
Doktors der Naturwissenschaften

der Mathematisch-Naturwissenschaftlichen Fakultät
und
der Medizinischen Fakultät
der Eberhard-Karls-Universität Tübingen

vorgelegt
von

Nicole Schlörit (geborene Groh)
aus Erbach, Deutschland

Oktober - 2017

Tag der mündlichen Prüfung: 11.12.2017

Dekan der Math.-Nat. Fakultät: Prof. Dr. W. Rosenstiel

Dekan der Medizinischen Fakultät: Prof. Dr. I. B. Autenrieth

1. Berichterstatter:	Dr. D. David
2. Berichterstatter:	Prof. Dr. T. Stehle
Prüfungskommission:	Dr. D. David
	Prof. Dr. T. Stehle
	Prof. Dr. M. Ueffing
	Prof. Dr. P. Heutink

Erklärung / Declaration:

Ich erkläre, dass ich die zur Promotion eingereichte Arbeit mit dem Titel:

„Biochemical characterization of physiological age-dependent aggregates in *C. elegans*“

selbständig verfasst, nur die angegebenen Quellen und Hilfsmittel benutzt und wörtlich oder inhaltlich übernommene Stellen als solche gekennzeichnet habe. Ich versichere an Eides statt, dass diese Angaben wahr sind und dass ich nichts verschwiegen habe. Mir ist bekannt, dass die falsche Abgabe einer Versicherung an Eides statt mit Freiheitsstrafe bis zu drei Jahren oder mit Geldstrafe bestraft wird.

I hereby declare that I have produced the work entitled “……”, submitted for the award of a doctorate, on my own (without external help), have used only the sources and aids indicated and have marked passages included from other works, whether verbatim or in content, as such. I swear upon oath that these statements are true and that I have not concealed anything. I am aware that making a false declaration under oath is punishable by a term of imprisonment of up to three years or by a fine.

Tübingen, den ....

Datum / Date Unterschrift /Signature

Summary

Aging is the most important risk factor for neurodegenerative diseases associated with pathological protein aggregation such as Alzheimer's disease. Although aging is an important player, it remains unknown which molecular changes are relevant for disease initiation. Recently, we and others demonstrated that several hundred proteins become highly insoluble with age, in the absence of disease. But how these misfolded proteins aggregating with age affect neurodegenerative diseases is not known until today. Importantly, several of these aggregation-prone proteins are found as minor components in disease-associated aggregates such as amyloid-β plaques or neurofibrillary tangles. In this thesis we demonstrate that insoluble protein extracts from aged *Caenorhabditis elegans* or aged mouse brains are able to seed amyloid-β aggregation *in vitro*, whereas protein aggregates formed during the early stages of life did not initiate amyloid-β aggregation. The injection of insoluble protein extracts from aged mouse brains into the hippocampus of APP23 transgenic mice lead to a formation of some amyloid-β plaques in three out of five mice. By mass spectrometry analysis of insoluble protein extracts from *C. elegans* we found late-aggregating proteins that were previously identified as minor components of amyloid-β plaques and neurofibrillary tangles such as 14-3-3, Ubiquitin-like modifier-activating enzyme 1 and Lamin A/C, highlighting these as strong candidates for cross-seeding. Double-transgenic worms overexpressing human amyloid-β in the body-wall muscle together with PAR-5 (*C. elegans* homolog of 14-3-3) showed an increase in paralysis, which demonstrates that PAR-5 (14-3-3) could be a potential seed for the aggregation of amyloid-β.

In conclusion, the results presented here show that physiological protein aggregation with age might constitute a heterologous seed

for disease-associated protein aggregation. To find out why these heterologous seeds form with age would have a major impact in advancing our understanding of aging and its influence on pathophysiology. Targeting the seeds before the onset of the disease would be an important prevention strategy.

Recently, widespread protein aggregation as a common feature of aging has become an important topic of research. We already demonstrated that cross-seeding between different age-dependent aggregating proteins is possible in the absence of disease. The investigation of endogenous age-dependent protein aggregation could give insights into molecular and cellular mechanisms that regulate protein aggregation and into the effect of protein insolubility on organisms health. Therefore, we wanted to analyze whether rapidly-aggregating proteins can act as harmful seeds for the aggregation of other proteins in *C. elegans.* The goal was to crosslink a rapidly-aggregating protein together with its co-aggregating proteins, to purify them and to identify them by mass spectrometry. This thesis presents the establishment of a tandem affinity purification under denaturing conditions to be used to purify rapidly-aggregating proteins tagged with a tandem affinity tag.

Zusammenfassung

Alterung ist der wichtigste Risikofaktor für neurodegenerative Erkrankungen verbunden mit pathologischer Proteinaggregation wie zum Beispiel bei der Alzheimer-Erkrankung. Obwohl Alterung ein wichtiger Akteur ist bleibt es unbekannt welche molekularen Veränderungen relevant für den Krankheitsbeginn sind. Kürzlich demonstrierten wir und andere, dass einige hundert Proteine im Alter, in Abwesenheit einer Krankheit, äußerst unlöslich werden. Aber wie diese missgefalteten Proteine, die im Alter aggregieren, neurodegenerative Erkrankungen beeinflussen, ist bis heute nicht bekannt. Wichtig ist, dass einige von diesen aggregations-anfälligen Proteinen als nebensächliche Komponenten in krankheitsassoziierten Aggregaten, wie Amyloid-β Plaques oder neurofibrillären Bündeln, gefunden wurden. In dieser Arbeit demonstrieren wir, dass unlösliche Proteinextrakte von gealterten *Caenorhabditis elegans* oder gealterten Maushirnen fähig sind *in vitro* Amyloid-β Aggregation zu "seeden" (säen), wohingegen Proteinaggregate, die sich während früher Lebensstadien gebildet haben, keine Amyloid-β Aggregation initiierten. Die Injektion von unlöslichen Proteinextrakten gealterter Maushirne in den Hippocampus von APP23 transgenen Mäusen führte zur Bildung von einigen Amyloid-β Plaques in drei von fünf Mäusen. Mit massenspektrometrischer Analyse von unlöslichen Proteinextrakten von *C. elegans* fanden wir spät-aggregierende Proteine die zuvor als nebensächliche Komponenten von Amyloid-β Plaques und neurofibrillären Bündeln identifiziert wurden, wie zum Beispiel 14-3-3, Ubiquitin-like modifier-activating enzyme 1 und Lamin A/C, was diese als starke Kandidaten für "cross-seeding" hervorhebt. Doppelt-transgene Würmer, die humanes Amyloid-β im sogenannten "body-wall muscle" zusammen mit PAR-5 (*C. elegans* Homolog von 14-3-3) überexprimieren, zeigten eine Erhöhung der

Paralyse, was demonstriert, dass PAR-5 (14-3-3) ein potentieller "Seed" (Keim) für die Aggregation von Amyloid-β sein könnte.

Abschließend lässt sich sagen, dass die Ergebnisse, die hier präsentiert werden, zeigen, dass physiologische Proteinaggregation im Alter einen heterologen "Seed" für krankheitsassoziierte Proteinaggregation bilden könnte. Herauszufinden warum diese heterologen "Seeds" sich im Alter bilden würde eine große Auswirkung auf die Verbesserung unseres Verständnisses von Alterung und deren Einfluss auf die Pathophysiologie haben. Das Abzielen auf die "Seeds" vor dem Beginn der Krankheit wäre eine wichtige Präventionsstrategie.

Kürzlich wurde die weitverbreitete Proteinaggregation als ein häufiges Merkmal von Alterung ein wichtiges Thema in der Forschung. Wir haben bereits demonstriert, dass "cross-seeding" zwischen verschiedenen altersabhängig aggregierenden Proteinen in Abwesenheit einer Krankheit möglich ist. Die Untersuchung von körpereigener, altersabhängiger Proteinaggregation könnte Erkenntnisse über molekulare und zelluläre Mechanismen bringen, welche die Proteinaggregation regulieren und über den Effekt von Proteinunlöslichkeit auf die Gesundheit des Organismus. Deshalb wollten wir untersuchen, ob schnell-aggregierende Proteine als schädliche "Seeds" für die Aggregation von anderen Proteinen in *C. elegans* agieren können. Das Ziel war ein schnell-aggregierendes Protein zusammen mit seinen co-aggregierenden Proteinen zu vernetzen, diese zu reinigen und mittels Massenspektrometrie zu identifizieren. Diese Arbeit präsentiert die Etablierung einer Tandem-Affinitäts-Reinigung unter denaturierenden Bedingungen um diese für die Reinigung schnell-aggregierender Proteine, markiert mit einem Tandem-Affinitäts-Marker, zu nutzen.

Table of contents

1 Introduction

This chapter includes parts of the introduction reproduced from:

Groh N, Bühler A, Huang C, Li KW, van Nierop P, Smit AB, Fändrich M, Baumann F and David DC (2017) Age-Dependent Protein Aggregation Initiates Amyloid-β Aggregation. Front. Aging Neurosci. 9:138. Doi: 10.3389/fnagi.2017.00138

1.1 Protein folding and misfolding

To perform their biological function proteins must fold into their three-dimensional structure, which is encoded by the amino acid sequence. To understand how a protein converts from its unfolded structure to its thermodynamically favorable native state the energy surface or landscape for protein folding has to be considered. In the review of (Dobson 2003) it is shown that "the surface 'funnels' the multitude of denatured conformations to the unique native structure". During the folding process the protein reaches a transition state, which lies on the saddle point of the energy surface. In this state a small number of residues have formed their native like contacts. Once this so called folding nucleus is generated the topology of the native fold is established and the remainder of the structure rapidly condenses (Fersht 2000).

Normally, misfolded proteins are ubiquitinated and degraded in the cytoplasm by the ubiquitin-proteasome system. However, misfolded proteins could also escape the protective mechanisms and form aggregates. (Dobson 1999) explains the formation of a misfolded globular protein. Under physiological conditions a globular protein is folding properly with the polypeptide chain and hydrophobic residues hidden in the interior and is secreted

from the cell. Under conditions like low pH, heating and increased protein concentration the protein tends to unfold and becomes prone to aggregation. In *C. elegans* it was shown that hypertonic stress causes irreversible aggregation of both, endogenous and foreign proteins (Burkewitz, Choe, and Strange 2011).

1.2 Mechanisms to prevent protein aggregation

In a cell many of the proteins, which are synthesized on ribosomes, are intended for secretion to the extracellular space. After synthesis these proteins are translocated to the endoplasmic reticulum (ER), where they fold correctly with the help of molecular chaperones and folding catalysts before they are secreted through the Golgi apparatus (Figure 1.1).

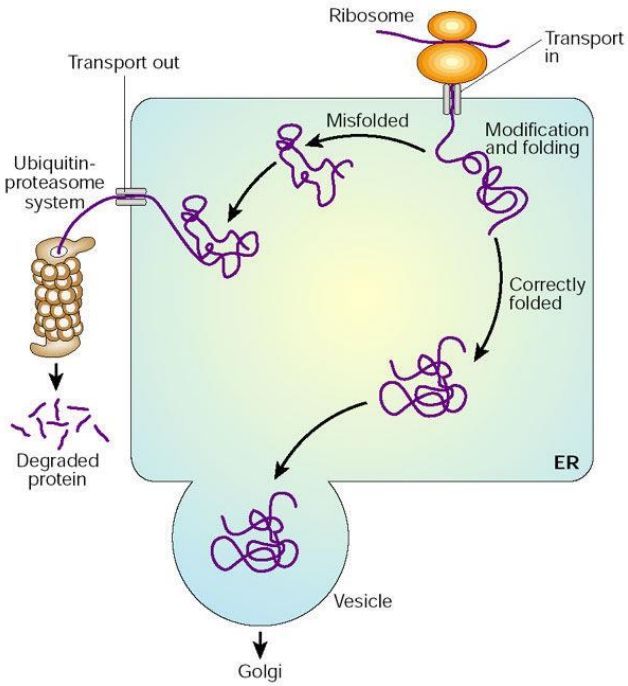

Figure 1.1: Protein folding in the endoplasmic reticulum (ER) (Protein folding and misfolding, Christopher M. Dobson, Nature 426, 884-890 (18 December 2003), doi:10.1038/nature02261).

During aging the regulation of protein homeostasis (proteostasis) is impaired and contributes to the pathological aggregation of proteins in neurodegenerative diseases such as Alzheimer's disease. Moreover, the age-related decline in the proteostasis network suggests, that misfolding of proteins and their accumulation to aggregates are general consequences of aging as we previously showed in *C. elegans* (David et al. 2010).

The proteostasis network, which consists of chaperones and protein degradation machineries, is required for the surveillance

of the proteome, reviewed by (Balchin, Hayer-Hartl, and Hartl 2016). This network includes molecular chaperones which facilitate proper protein folding and refolding as reviewed by (Hartl, Bracher, and Hayer-Hartl 2011). Members of the chaperone family are known as heat-shock proteins (HSPs), because under stress, such as heat stress, protein misfolding increases and the HSPs are upregulated. Moreover, the ubiquitin–proteasome system (UPS) and autophagy system are responsible for the removal of irreversibly misfolded and aggregated proteins (Figure 1.1 and Figure 1.2). Ubiquitination is a post-translational protein modification that governs the degradation of proteins by the proteasome. Furthermore, proteins are degraded in lysosomes through autophagy. Signaling pathways including the cytosolic stress response, which upregulates HSPs during stress (Anckar and Sistonen 2011), and the unfolded protein response (UPR) of the ER and mitochondria (Schulz and Haynes 2015; Walter and Ron 2011) regulate the proteostasis network. The UPR of the ER upregulates ER chaperones, the UPR of mitochondria leads to an increased resistance to oxidative damage.

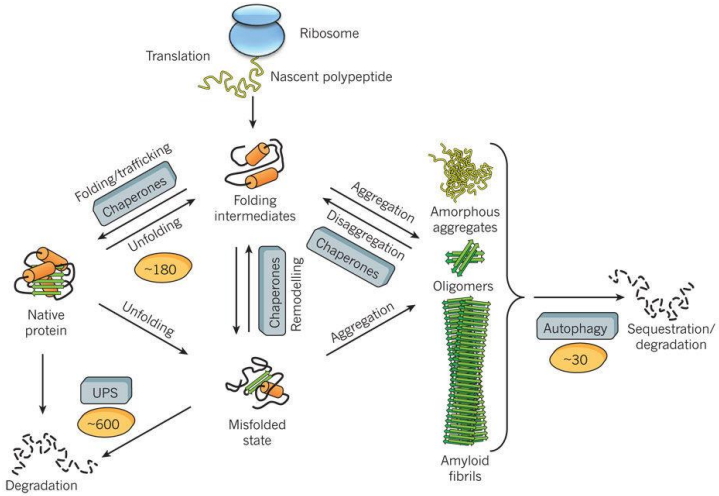

Figure 1.2: The proteostasis network including 180 chaperone components, 600 components of the ubiquitin-proteasome system (UPS) and 30 components of the autophagy system (Molecular chaperones in protein folding and proteostasis, F. Ulrich Hartl, Andreas Bracher & Manajit Hayer-Hartl, Nature 475, 324–332 (21 July 2011), doi:10.1038/nature10317).

With age the chaperone function and availability is reduced as reviewed by (Kaushik and Cuervo 2015). Moreover, age-related modifications on proteins interfere with the target-recognition ability of chaperones. Additionally, autophagy and proteasome activity decrease with age. In *C. elegans* the ectopic expression of RPN-6, a 19S proteasome subunit, leads to proteotoxic stress resistance and extends lifespan (Vilchez et al. 2012). It was also shown that overexpression of the proteasome subunit 20S increases lifespan and resistance to stress (Chondrogianni et al. 2015). Furthermore, the overexpression of the autophagy stimulator HLH-30 extends lifespan in *C. elegans* (Lapierre et al. 2013).

1.3 Protein aggregation in neurodegenerative diseases

A variety of neurodegenerative diseases are associated with the misfolding and aggregation of specific proteins. For example, in Alzheimer's disease (AD), amyloid-β (Aβ) peptides and tau proteins aggregate and ultimately form the characteristic pathological hallmarks: amyloid plaques and neurofibrillary tangles (NTFs) respectively. For Aβ and tau (and also other amyloidogenic proteins) it has been reported that the more toxic species might be small intermediates in the aggregation process, the soluble oligomers (Haass and Selkoe 2007; Spires-Jones et al. 2011). As reviewed by (Haass and Selkoe 2007) some oligomeric species of Aβ are small and soluble enough to diffuse through the brain parenchyma and affect synaptic structure, function and neuronal survival, whereas the insoluble inclusions might function as reservoir for soluble oligomers. The amyloid cascade hypothesis, reviewed by (Haass and Selkoe 2007), explains how Aβ accumulation could result to AD. In the first part of the cascade an increase in the Aβ42/Aβ40 ratio enhances oligomerization of the highly amyloidogenic Aβ42 isoform. The increase of the ratio can be augmented by mutations in β-amyloid precursor protein (APP), presenilin-1 (PS-1) and presenilin-2 (PS-2) that cause familial forms of AD (Scheuner et al. 1996; Suzuki et al. 1994). APP is a single-transmembrane, receptor-like protein that is processed by β-site APP-cleaving enzyme (BACE) and the γ-secretase complex (including PS-1 and PS-2). The γ-secretase cleavage-sites on APP are variable and can occur after amino acids 38, 40 and 42 leading to the liberation of different forms of Aβ into the extracellular space.

In AD and other tauopathies NFTs are formed by intracellular accumulations of hyperphosphorylated tau, reviewed by (Kuret et al. 2005). An ongoing question is whether the tangles are the

toxic species in the brain, but that tau dysfunction can lead to neurodegeneration is generally accepted. It has been shown that the expression of an aggregation-prone tau construct is associated with cell death in cultured cells (Khlistunova et al. 2006; Wang et al. 2007).

In general, knowledge of the nature of aggregate pathogenicity would be important to identify targets for therapeutic interventions. (Bucciantini et al. 2002) demonstrated that aggregates of two different non-disease-related proteins can be inherently cytotoxic suggesting toxicity of aggregated species could be a general phenomenon. The data support the assumption that non-fibrillar aggregates, that precede formation of mature amyloid fibrils, may be the primary toxic species. (Olzscha et al. 2011) generated artificial proteins with β-sheet structures (so called β proteins) that lead to the formation of amyloid-like aggregates and toxicity in HEK293T cells. They showed that the protein with the highest toxicity has the tendency to form prefibrillar aggregates *in vitro*. Moreover, the β proteins co-aggregate with two types of endogenous aggregation-prone proteins with specific sequence features. One group includes the pre-existing proteins that are enriched in intrinsically unstructured regions and are prone to aggregate even in their post-folding state. The other group, the newly synthesized proteins, contain large or multidomain proteins which are prone to aggregate during and shortly after synthesis.

An important and currently understudied question is how aging influences protein aggregation in neurodegeneration. Recently, physiological protein insolubility in the context of aging has become an important topic of research (David 2012; Partridge 2011). Indeed, numerous publications demonstrate that protein aggregation is not restricted to disease but a normal conse-

quence and possibly cause of aging (Ayyadevara, Mercanti, et al. 2016; David et al. 2010; Demontis and Perrimon 2010; Lechler et al. 2017; Ottis et al. 2013; Peters et al. 2012; Reis-Rodrigues et al. 2012; Tanase et al. 2016; Walther et al. 2015). To investigate endogenous age-dependent protein aggregation could give insights into molecular and cellular mechanisms that regulate protein aggregation and into the effect of protein insolubility on organisms health, without the need to ectopically express human disease-associated proteins in model organisms.

Until now it remains unclear whether and how age-dependent protein aggregation and disease-associated protein aggregation influence each other. One possibility is that age-dependent aggregates indirectly accelerate disease-associated protein aggregation by stressing the cell and/or titrating away anti-aggregation factors. Another possibility is a direct interaction whereby disease-associated proteins and age-dependent aggregation-prone proteins co-aggregate. In support of this latter hypothesis, proteins prone to aggregate during normal aging are significantly overrepresented as minor protein components in amyloid plaques and NFTs (Ayyadevara, Balasubramaniam, Parcon, et al. 2016; David et al. 2010). Recent research reveals that the sequestration of these age-dependent aggregation-prone proteins in the disease aggregates is a source of toxicity (Ayyadevara, Balasubramaniam, Parcon, et al. 2016).

1.4 Amyloids and seeding mechanisms

In neurodegenerative diseases specific proteins are aggregating in an amyloid conformation. One of the most known amyloids is amyloid-β (Aβ) peptide which aggregates in Alzheimer's disease. The term amyloid describes multimeric proteinaceous assemblies with a cross-β quaternary structure. Proteins in the amy-

loid state form elongated fibrils which are unbranched and can be found *in vivo* (Eisenberg and Jucker 2012). In all fibrils β-sheets are arranged in parallel to the fibril axis with the β-strands perpendicular to the axis. This formation is stabilized by hydrogen bonds. To prove whether an aggregated protein is in an amyloid state, usually the dye Congo red is used. Congo red binding is monitored by a red shift in the light absorption and a characteristic green birefringence under crossed polarization. Moreover, the cross-β structure is detected in X-ray diffraction and the typical morphology is analysed by electron microscopy. As reviewed by (Eisenberg and Jucker 2012) amyloid formation occurs because the free energy of it is highly favourable. Another reason is an abnormally high protein concentration (Balch et al. 2008).

In recent years, understanding the initiation and spread of hallmark protein aggregates such as Aβ or tau has become a central area of investigation (Jucker and Walker 2011). The current model stipulates that aggregation in disease is initiated by a protein seed that forms a template for further protein aggregation (Jucker and Walker 2013). In detail, an amyloid seed is formed by the aggregation of native proteins through intermediate states during a slow nucleation phase. Then monomers and oligomeric structures are bonded to the end of the initial amyloid seed which leads to a growing fibril that can break during the rapid growth phase. This results to the generation and spreading of new seeds.

In transgenic models for Aß amyloidosis, intracerebral injections of brain extracts containing minute amounts of aggregated Aß seeds are sufficient to instigate the formation of Aß plaques (Kane et al. 2000; Meyer-Luehmann et al. 2006). This process is called homologous seeding (Figure 1.3A). However, whether

misfolded proteins aggregating with age can form heterologous seeds that initiate Aβ aggregation (Figure 1.3A) has not been investigated. Although current research focuses on homologous seeding, there are a few examples of cross-seeding (or heterologous seeding), mostly between different disease-aggregating proteins (Morales, Moreno-Gonzalez, and Soto 2013). For instance, Aβ is a potent seed for the aggregation of human islet amyloid polypeptide involved in type II diabetes (O'Nuallain et al. 2004; Oskarsson et al. 2015); Aβ and prion protein PrP^{Sc} cross-seed each other and accelerate neuropathology (Morales et al. 2010); and both α-synuclein and Aβ co-aggregate with tau and enhance tau pathology *in vivo* (Guo et al. 2013; Vasconcelos et al. 2016). Finally, we recently showed that cross-seeding between different age-dependent aggregating proteins is possible in the absence of disease (Lechler et al. 2017). Until today little is known about heterologous seeding of disease-aggregating proteins by non-disease aggregating proteins. One example is acetylcholinesterase, which is also found in Aß plaques (Alvarez et al. 1998; Jean et al. 2007).

The *in vitro* Aβ seeding assay or FRANK assay (Fibrillisation of Recombinant Aβ Nucleation Kinetic) (Nagarathinam et al. 2013) has been used to analyse if brain-derived Aβ is able to induce the aggregation of monomeric recombinant Aβ. In general, over time Aβ fibrils are formed, detected by the increase in fluorescence of the amyloid dye Thioflavin T (ThT) (Figure 1.3B, red line). The time that is needed to form initial fibril seeds is called the lag time. If brain-derived Aβ is added, the lag time is reduced by the initiation and acceleration of Aβ aggregates (Figure 1.3B, blue line). The investigation whether extracts containing non-disease aggregating proteins (age-dependent protein aggregates) are also able to reduce the lag time has not been done so far.

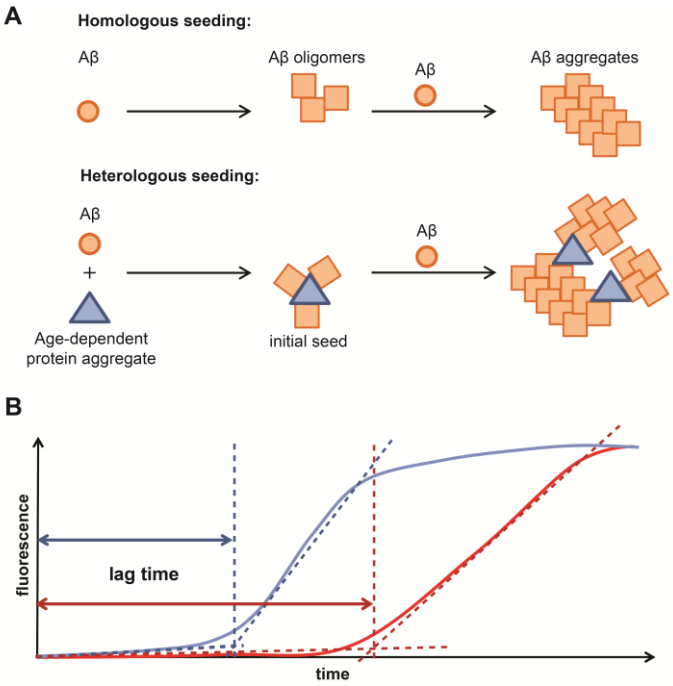

Figure 1.3: Schematic representation of homologous and heterologous Aβ seeding and determination of lag times (reproduced from Frontiers article).
A Homologous seeding (upper part): Aβ monomers very slowly accumulate to metastable intermediate oligomers which act in a succeeding step as a seed for fast Aβ accumulation. Initial seed formation critically depends on exceeding a minimal local concentration of Aβ. This process leads to stable Aβ aggregate formation (fibril formation) which can break and serve as new seeds for further Aβ aggregation.
Heterologous seeding (lower part): Hypothetically during aging, Aβ monomers and age-dependent protein aggregates accumulate and build together an initial seed which leads to a faster accumulation of Aβ aggregates bypassing the slow buildup of homologous seeds from monomeric Aβ. This might be even more important when Aβ concentration never reaches the minimal local concentration for homologous seed formation.
B During the FRANK assay (Fibrillisation of Recombinant Aβ Nucleation Kinetic) protein extracts are measured in the presence of Thioflavin T

(ThT) and recombinant Aβ1-40. Aβ fibrils, which are detected by the incorporation of ThT, are formed after initial fibril seeds develop. After this the ThT fluorescence increases rapidly until a maximum is reached (red line). The time that is needed to form initial seeds is called the lag time. Brain derived Aβ (or hypothetically age-dependent protein aggregates) reduce the lag time by initiating and accelerating Aβ aggregation (blue line).

1.5 *Caenorhabditis elegans* as a model system

The nematode *C. elegans* was developed as a model system to study developmental biology and neurobiology by Sydney Brenner. As described by (Corsi, Wightman, and Chalfie 2015) the small size (length of adults amounts to 1 mm), the transparent body, the simple body plan including pharynx, intestine, gonads and muscles and the well-annotated genome are reasons why it is a useful model system. Moreover, *C. elegans* has a rapid lifecycle: after hatching the worms develop from four larval stages (L1 to L4) to adults that lay eggs in approximately 55 hours at 20°C. They exist primarily as a self-fertilizing hermaphrodite, but also males arise at a low frequency (<0.2%) (Corsi, Wightman, and Chalfie 2015). The free-living nematode can be found worldwide. In the laboratory, they live on agar plates or in liquid culture and are fed with bacteria (*E. coli*). Their nervous system is composed of exactly 302 neurons. As a model system to study aging and age-related diseases, *C. elegans* has a lot of advantages: First of all, the worms have a short lifespan (about 17 days for wild-type worms). Moreover, different longevity pathways are known. Additionally, specific genes can be easily knocked down by RNA interference (RNAi). It was shown by (Fire et al. 1998) that injection of double stranded RNA (dsRNA) into worms resulted to degradation of the corresponding messenger RNA (mRNA) and therefore to potent interference. Moreover, feeding worms with bacteria expressing dsRNA of the gene of interest induces RNAi

response, demonstrated by (Tabara, Grishok, and Mello 1998; Timmons and Fire 1998). Because the complete genomic sequence of *C. elegans* is available, RNAi is a useful technique to study gene function. Another advantage of using *C. elegans* as an *in vivo* system is the possibility to overexpress toxic proteins prone to pathological misfolding. (Teschendorf and Link 2009) reviewed that the expression of specific human proteins linked to neurodegeneration leads to cellular toxicity in worms. One example for using *C. elegans* as transgenic model for neurodegenerative diseases is the expression of human Aβ in the body-wall muscle under the *unc-54* promoter (Link 1995). The group of Christopher Link discovered that Aβ accumulates in muscle cells forming amyloid deposits. Later (McColl et al. 2012) generated a model where Aβ aggregates in muscle cells and results in temperature induced age-progressive paralysis.

1.6 Objectives

1.6.1 Identifying age-dependent heterologous seeds for amyloid-β aggregation

A variety of neurodegenerative diseases are associated with the misfolding and aggregation of specific proteins. To understand the initiation and spread of hallmark protein aggregates such as Aβ or tau has become a central area of investigation. Recently, a model was published stipulating that aggregation in disease is initiated by a protein seed that forms a template for further protein aggregation. Targeting the seeds before the onset of the disease would be an important therapeutic strategy. The thesis presented here describes the investigation whether endogenous proteins, that aggregate with age, can seed the aggregation of Aβ. To address our hypothesis, we wanted to examine detergent-insoluble protein extracts from young and aged wild-type

C. elegans and young and aged wildtype mouse brains. To analyse Aβ aggregation in the presence of the insoluble fraction, we wanted to use an *in vitro* seeding assay (FRANK assay, Fibrillisation of Recombinant Aβ Nucleation Kinetic). Quantitative mass spectrometry with the insoluble proteome of *C. elegans* and mouse brains from different ages should be performed to identify changes in aggregation with age. With the comparison of early- and late-aggregating proteins with the highest change in aggregation with age in *C. elegans* with minor components of Aβ plaques and neurofibrillary tangles we wanted to identify potential candidates for seeding Aβ.

1.6.2 Investigation whether rapidly-aggregating proteins seed the aggregation of other proteins

To characterize endogenous age-dependent protein aggregation could help to understand the molecular and cellular mechanisms that regulate protein aggregation. Moreover, the characterization could give insights into the effect of protein insolubility on organisms health. Therefore, the goal was to investigate whether rapidly-aggregating proteins can act as harmful seeds for the aggregation of other proteins in *C. elegans.* An early-aggregating protein, identified in the first part of the thesis, should be chemically crosslinked together with its co-aggregating proteins. Next, they should be purified and identified by mass spectrometry.

2 Material and Methods

2.1 Identifying age-dependent heterologous seeds for amyloid-β aggregation

This chapter includes parts of the material and methods reproduced from:

Groh N, Bühler A, Huang C, Li KW, van Nierop P, Smit AB, Fändrich M, Baumann F and David DC (2017) Age-Dependent Protein Aggregation Initiates Amyloid-β Aggregation. Front. Aging Neurosci. 9:138. Doi: 10.3389/fnagi.2017.00138

2.1.1 *C. elegans* mutant and transgenics

Table 2.1: C. elegans mutant and transgenic strains used in this study.

Strain name	**Genotype**
CF2253	*gon-2(q388)I*
GMC101	*dvIs100[unc-54p::A-beta-1-42::unc-54 3'-UTR + mtl-2p::GFP]*
UE50	*oaSi10[par-5p::GFP::par-5::par-5 3'UTR + unc-119(+)]*
DCD296 (GMC101;UE50)	*dvIs100[unc-54p::A-beta-1-42::unc-54 3'-UTR + mtl-2p::GFP]; oaSi10[par-5p::GFP::par-5::par-5 3'UTR + unc-119(+)]*

2.1.2 Bacterial strains

Table 2.2: Bacterial strains used in this study as food source for C. elegans.

Strain name	**Description**
OP50	*Escherichia coli* (*E. coli*) strain
OP50-1	OP50 with streptomycin resistance

2.1.3 Mouse strains

Wild-type C57BL/6J (WT) and transgenic APP23 mice (Sturchler-Pierrat et al. 1997) were bred and maintained under pathogen-free conditions at the Hertie Institute for Clinical Brain Research, Tübingen, controlled by Dr. Frank Baumann. All studies were performed in accordance with German animal welfare legislation and with approval from the Ethical Commission for animal experimentation of Tübingen, Germany. Age and sex of mice used for the FRANK assay (Fibrillization of Recombinant Aβ Nucleation Kinetic) and mass spectrometry are listed in Table 2.3.

Table 2.3: Mice used for FRANK assay (Fibrillization of Recombinant Aβ Nucleation Kinetic) and mass spectrometry# (mainly reproduced from Frontiers article).*

Number	**Sex**	**Age (months)**
7519*	male	2
8418*	female	2
8419*	female	2
8628*#	male	3
8629*#	male	3
8916*	female	2
8951#	female	2
8070#	female	20
8036*	female	20
7830*#	male	18
7831*#	male	18
524*	female	18
503*	female	19
1736*	female	20
7755*	female	25
7718*	male	27
7601*	female	28

11523* (APP23)	male	20

2.1.4 Growing and Maintenance of *C. elegans*

Hermaphrodites were grown on Nematode Growth (NG) plates (preparation of NG plates is described at http://www.wormbook.org/chapters/www_strainmaintain/strainmaintain.html) containing the bacterial (*E. coli*) strain OP50 at either 15°C, 20°C or 25°C. Stock plates were kept at 15°C.

Males were grown on empty NG plates with a low amount of OP50 at 15°C or 20°C. Once per week (if incubated at 20°C every four days) 12 males were mated with three L4s from a stock of the respective strain. To generate new males of a transgenic strain with a fluorescent marker three L4s of the respective strain were first crossed with 12 N2 males. To continue, three fluorescent L4s were picked from a stock of the transgenic strain and crossed with 12 fluorescent males from the last mating plate. The last step was repeated three times before the males were used for example for a cross with another strain.

2.1.5 Strain generation

To generate the double transgenic strain DCD296 overexpressing Aβ and PAR-5, GMC101 males were generated by crossing N2 males to GMC101 hermaphrodites as described at 2.1.4 and by mating the GMC101 males into UE50 hermaphrodites (as described at (Fay 2013), http://www.wormbook.org).

2.1.6 *C. elegans* liquid culture

To obtain large aged-synchronized populations of *C. elegans*, temperature induced sterile *gon-2* mutants (CF2253) were used. The whole procedure was carried out independently four times

to collect four biological replicates with four time points, respectively. The worms were collected at day 2 (reproductive animals), day 6 (at the end of reproduction in wild-type animals), day 10 (around 30% of the population has died) and day 14 (around 50% of the population has died). Age is defined by the number of days of adulthood starting from the last larval stage L4.

2.1.6.1 Propagation of gon-2 mutants to collect the parental generation for the temperature shift

As food source the *E. coli* OP50-1 strain, which has a streptomycin resistance, was streaked out onto a Lysogeny Browth (LB) plate with 50 µg/mL streptomycin and incubated over night at 37°C (as described at http://www.wormbook.org/chapters/www_strainmaintain/ strainmaintain.html). 200 mL LB medium with 50 µg/mL streptomycin were inoculated with one clone OP50-1 and incubated over night at 37°C. 15 High Growth Medium (HGM) plates (diameter 9 cm) with 50 µg/mL streptomycin (later called HGM/streptomycin plates) were inoculated with 0.5 mL OP50-1 which was distributed with a spatula. *Gon-2(-)* animals (not starved for the last two generations) were chunked onto the 15 HGM/streptomycin plates seeded with OP50-1 and maintained at 20°C until plates were confluent with adults and some OP50-1 was still available. Confluent plates were bleached (as described at (Sulston 1988)), eggs were collected in 15 mL-tubes with M9 solution (85 mM NaCl, 42 mM $Na_2HPO_4 \cdot 7\ H_2O$, 22 mM KH_2PO_4) and placed on a nutating mixer overnight at 20°C. Hatched L1s were washed with M9 as follows: L1s were centrifuged at 3000 x g for 30 s, supernatants were discarded and the tubes were filled up to 15 mL mark with M9. This step was repeated twice. The tubes with the resulting worm pellets were filled up to 15 mL mark with M9. The total number of L1s

was evaluated under a dissection microscope by counting the L1s present in 2 µL drops placed on a non-seeded NG plate. The numbers obtained from at least nine drops were averaged and 6500 L1s were added on one HGM/streptomycin plate, which was seeded before with OP50-1 as described above. In total 60 HGM/streptomycin plates were prepared as described and the worms were grown at 20°C until L4 stage.

2.1.6.2 Temperature shift to obtain gonad-less animals for the liquid culture

At L4 stage, the worms were shifted to 25°C until they started to lay eggs and L1s were hatching. To separate the fragile eggs and L1s from the adults and to collect them, sedimentation was used. The plates were washed with M9 by using 5 mL M9 per five plates. Worms were transferred into 50 mL-tubes. Tubes were filled up to 45 mL mark with M9, the adults were sedimented for 10 min, each supernatant was collected in a 50 mL-tube and the step was repeated with the pellets. The supernatants, that contained eggs and L1s, were centrifuged at 3000 x g for 1 min, the L1s were sedimented for 10 min and the supernatants were removed until 15 mL were left. The tubes containing eggs and L1s were placed on a nutating mixer over night at 25°C.

2.1.6.3 Collection of OP50-1 culture as food source

8 L LB medium with a final concentration of 50 µg/mL streptomycin were inoculated with 24 mL OP50-1 from a 200 mL-overnight-culture and incubated at 37°C overnight at 180 rpm. The OP50-1 culture was harvested by centrifugation at 6700 x g for 10 min at 4°C. The supernatant was removed and the pellet was resuspended in 120 mL ice-cold S basal (100 mM NaCl, 50 mM Potassium phosphate pH 6).

2.1.6.4 Liquid cultures to collect gon-2(-) mutants at day 2, day 6, day 10 and day 14

Per condition (four in total), 200 mL S basal was added in a Fernbach culture flask (capacity 2,800 mL). For a final culture volume of 300 mL the following ingredients were added: 10 mM Potassium citrate, pH 6, 3 mL Trace metals solution (5 mM Ethylenediaminetetraacetic acid (EDTA), 2.5 mM $FeSO_4$, 1 mM $MnCl_2$, 1 mM $ZnSO_4$, 0.1 mM $CuSO_4$), 3 mM $MgSO_4$, 3 mM $CaCl_2$, 100 ng/mL carbendazim, 5 µg/mL cholesterole and 50 µg/mL streptomycin.

The L1s obtained as described at 2.1.6.2 were transferred to 15 mL-tubes and centrifuged at 1900 x g for 3 min. The supernatant was removed and the L1s per 2 µL were counted. As mentioned above, four biological replicates with four time points respectively were prepared. The total numbers of worms grown in the four liquid cultures for each replicate are shown in Table 2.4. The following describes the procedure for replicate number four as an example for all replicates: In total 695,000 worms were needed to divide them to four flasks. OP50-1 was added proportionally to the number of worms: Out of 120 mL total OP50-1, each time 20 mL were added to the flask for the day 2 and day 6 worm collections, 30 mL to the flask for the day 10 worm collection and 35 mL to the flask for the day 14 worm collection. The following amount of worms was added to the following worm collection: 170,000 worms to day 2, 150,000 worms to day 6 and day 10 and 225,000 worms to day 14. Each worm culture was completed with S basal to bring the total volume to 300 mL and incubated at 25°C and 150 rpm. An aliquot from each liquid culture was periodically collected and placed on a glass slide. Using a dissection microscope, the bacterial food level in each culture was checked especially during the growth

phase. In advance a 4 L OP50-1 culture was prepared and harvested as described at 2.1.6.3 and a part of it was added to the cultures if necessary. Additionally, the sterility of the animals was analyzed. The majority of animals did not have a gonad, no animals with eggs were observed.

Table 2.4: Amount of worms grown in liquid cultures for different days for each biological replicate (reproduced from Frontiers article).

Replicate	**Day 2**	**Day 6**	**Day 10**	**Day 14**
1	100,000	100,000	150,000	200,000
2	150,000	150,000	200,000	350,000
3	250,000	150,000	175,000	300,000
4	170,000	150,000	150,000	225,000

2.1.6.5 Collection of gon-2(-) mutants by sucrose separation

At day 2, day 6, day 10 and day 14 worms were collected and removed from bacteria and dead worms by sucrose separation. The worm culture from one flask was added into a separatory funnel and the worms were sedimented for 10 min at room temperature. The worms were collected in one 50 mL-tube. The worm pellet was transferred to two 15 mL-tubes and centrifuged at 1900 x g for 5 min at room temperature. To wash the worms, the supernatants were removed and the tubes were filled up to 15 mL mark with M9. The centrifugation was repeated. Finally, the worms were transferred to two 50 mL-tubes and filled up to 20 mL total volume with ice-cold M9. To remove bacteria and dead worms, the two 20 mL diluted worm pellets were added to two 50 mL-tubes filled with 20 mL ice-cold 60% sucrose and centrifuged at 2700 x g for 5 min at 4°C (acceleration 9 and de-

celeration 7). The top worm layers were taken and added directly into 37 mL of M9 with 0.01% Triton X 100 (AppliChem) (called M9+triton) (3 tubes per sucrose tube) prepared on ice. After centrifugation at 2700 x g for 3 min at 4°C (acceleration 9 and deceleration 7), the supernatants were removed and the pellets were divided into four 15 mL-tubes. The worms were washed as follows: The tubes were filled up to 15 mL mark with ice-cold M9+triton and centrifuged at 1900 x g for 1 min at room temperature. The supernatants were removed and the pellets were again filled up to 15 mL mark with ice-cold M9+triton and centrifuged. The last step was repeated with ice-cold M9. The four tubes were combined to two tubes, filled up with M9 at room temperature to a total volume of 4 mL in the 15 mL-tubes and rotated on a nutating mixer at 25 °C for 40 min. This helped the worms to digest any residual bacteria in the gut. The worms were analyzed with a dissection microscope to control that there were no dead ones. The worms were washed twice with ice-cold M9+triton and twice with M9 as described before. At the end the worms were transferred to one tube and washed once in the Reassembly (RAB) high-salt extraction buffer without inhibitors (0.1 M 4-Morpholineethanesulfonic acid (MES), 1 mM Ethyleneglycoltetraacetic acid (EGTA), 0.1 mM Ethylenediaminetetraacetic acid (EDTA), 0.5 mM $MgSO_4$, 0.75 M NaCl, 0.02 M Sodium fluoride (NaF)) before collection. The supernatant was removed until there was no liquid on top of the worm pellet. The volume of the worm pellet was estimated and an identical volume of RAB with inhibitors (2x Complete Protease Inhibitor Cocktail, Roche) was added. Using a Pasteur pipette, worms were drawn up and slowly dripped into a 50 mL-tube half filled with liquid nitrogen placed in dry ice. Frozen worms were stored at -80 °C until further processing.

2.1.6.6 Disruption of animals collected by sucrose separation

The frozen worm pellet of one day was transferred to a mortar that was pre-cooled with liquid nitrogen on dry ice and the pellet was ground for 2.5 min. Liquid nitrogen was added to the powder to cool it down again and the powder was ground for another 2.5 min. With the dissection microscope it was analyzed that the worm bodies were broken. This procedure was repeated for each day and each replicate. The powder was stored at -80 °C.

2.1.6.7 Liquid culture with C. elegans transgenic strain overexpressing Aβ (GMC101)

To obtain a large population of the *C. elegans* transgenic strain GMC101 which overexpresses Aβ as positive control for the FRANK assay, the same protocol as described above was used with the following changes: Worms were grown on 15 HGM plates seeded with OP50 and bleached when plates were confluent. After an L1 arrest overnight at 20°C, 150,000 worms were grown in liquid culture with OP50 at 20°C until day 1 and shifted to 25°C to induce paralysis (McColl et al. 2012). At day 2 worms were collected and disrupted as described.

2.1.7 Insoluble protein extraction for mass spectrometry and FRANK assay with *C. elegans*

To isolate Sodium dodecyl sulfate (SDS)-insoluble proteins for mass spectrometry analysis and the FRANK assay, a sequential extraction was performed with each time point and each replicate. All centrifugation steps were performed at 18,400 x g for 20 min at 4°C. The buffers, that were used for the extraction, are shown in Table 2.5. For mass spectrometry analysis, two times 350 mg ground worms per time point were weighed out on dry ice. To remove the high-salt soluble proteins two volumes of RAB with inhibitors, 1 mM Phenylmethylsulfonyl fluoride (PMSF),

200 U/mL DNaseI (Roche) and 100 µg/mL RNaseA (Promega) per weight (700 µL total) were added to each tube and the powder was solubilized on ice. The suspension was drawn up into a 1 mL syringe (gray needle, 27 G x ½ ", 0.4 mm x 13 mm) 15 times and incubated on ice for 10 min. For the FRANK assay, 50 mg ground worms (*gon-2* mutants or Aβ overexpressing transgenics) per time point were solubilized in 200 µL RAB buffer with inhibitors, PMSF, DNaseI and RNaseA. After centrifugation the supernatant containing high-salt soluble proteins was collected and the fat layer was discarded. After dialysis against PBS, these high-salt soluble proteins of *gon-2* mutants were used as soluble fraction in the FRANK assay. To remove lipids, the pellet was resuspended in two volumes of RAB with inhibitors (without DNaseI and RNaseA) containing 1 M sucrose (respectively 200 µL for the FRANK assay extraction). The suspension was drawn up into a syringe 10 times and incubated on ice for 5 min. After centrifugation all supernatant and lipids were removed and discarded. To remove SDS-soluble proteins, the pellet was resuspended in two volumes of Radioimmunoprecipitation assay (RIPA) buffer (respectively 200 µL for the FRANK assay extraction) (50 mM Tris(hydroxymethyl)aminomethane (Tris) pH 8, 150 mM NaCl, 5 mM EDTA, 0.5% SDS, 0.5% Sodium deoxycholate (SDO), 1% Nonidet P40 (NP40) (Applichem), 1 mM PMSF, 1x Complete Protease Inhibitor Cocktail (Roche)). The suspension was drawn up into a syringe 10 times and incubated for 10 min on ice. After centrifugation the supernatant containing SDS-soluble proteins was collected. The two samples of each condition were pooled together after solubilizing each pellet with 500 µL RIPA buffer (for the FRANK assay the pellet from one condition was solved with 200 µL RIPA buffer). The suspension was drawn up into a syringe 10 times and centrifuged. All supernatant was removed and discarded. The final pellet containing

highly insoluble proteins was resuspended in 400 µL 70% formic acid for mass spectrometry. The suspension was drawn up into a syringe 20 times, incubated for 20 min on ice and centrifuged at 50,000 x g for 20 min at 4°C, to remove worm cuticle debris. For the FRANK assay, the final pellet was resuspended in 100 µL PBS and centrifuged at 3,000 x g for 5 min at 4°C to remove the worm cuticle. The supernatant, that contains highly insoluble proteins, was collected.

2.1.8 Quick protein extraction for western blot analysis

To isolate detergent-soluble and -insoluble proteins for western blot analysis, a simplified protocol was used where 50 mg of ground animals in RAB buffer with inhibitors were directly re-suspended in 150 µL RIPA buffer and the suspension was drawn up into a 1 mL syringe 10 times. SDS-insoluble proteins were isolated by resuspension in RIPA buffer and centrifugation at 18,400 x g for 20 min at 4°C. The pellet was washed once in 100 µL RIPA buffer. Final pellets containing insoluble proteins were recovered in 75 µL 8 M Urea, 2% SDS, 50 mM Dithiothreitol (DTT), 50 mM Tris pH 8 at room temperature.

2.1.9 Mouse brain preparation and insoluble protein extraction for mass spectrometry and FRANK assay

Brains from wild-type mice (Table 2.3) were divided into both hemispheres after the cerebellum had been removed by Dr. Frank Baumann at the Hertie Institute for Clinical Brain Research, Tübingen. The same was done with the mouse brain from a transgenic APP23 mouse (20 months) for the FRANK assay. Two volumes per weight RAB buffer with inhibitors, PMSF, DNaseI and RNaseA (see above and Table 2.5) were added per hemisphere. Each hemisphere was homogenized with the Precellys Ceramic Beads Kit (Cayman Chemical) for two times 10 s

with 10 s pause in between. The homogenate was transferred into a new tube and processed as described for *C. elegans*. During each extraction step, two volumes buffer per weight were used. High-salt soluble proteins were removed by centrifugation at 18,400 x g for 20 min at 4°C. After dialysis against PBS, these high-salt soluble proteins were used as soluble fraction in the FRANK assay. Insoluble proteins were isolated as was performed with *C. elegans*, the final pellet containing highly insoluble proteins was resuspended in 200 µL 70% formic acid for mass spectrometry. For the FRANK assay the resulting pellet was resuspended in 200 µL PBS. The sample was centrifuged at 3,000 x g for 5 min at 4°C and the supernatant containing the detergent-insoluble proteins was used for the FRANK assay.

Table 2.5: Buffers for insoluble protein extraction.

Buffer	**Components**
RAB (with inhibitors, PMSF, DNaseI, RNaseA)	0.1 M MES, 1 mM EGTA, 0.1 mM EDTA, 0.5 mM $MgSO_4$, 0.75 M NaCl, 0.02 M NaF, 2x Complete Protease Inhibitor Cocktail (Roche), 1 mM PMSF, 200 U/mL DNaseI (Roche), 100 µg/mL RNaseA (Promega)
RIPA	50 mM Tris pH 8, 150 mM NaCl, 5 mM EDTA, 0.5% SDS, 0.5% SDO, 1% NP40 (Applichem), 1 mM PMSF, 1x Complete Protease Inhibitor Cocktail (Roche)
Formic acid	70% in ddH_2O
Urea/SDS	8 M Urea, 2% SDS, 50 mM DTT, 50 mM Tris pH 8

2.1.10 Gel electrophoresis and Western blotting

Proteins were separated on 12% SDS-PAGE gels or 4-12% gradient gels (NuPAGE 4-12% BisTris protein gels, Thermo Fisher). 12% SDS-PAGE gels were cast with two layers, the resolving

layer (12% acrylamide solution, 0.385 M Tris-Cl pH 8.8, 0.1% SDS, 0.1% Ammonium persulfate (APS), 0.04% Tetramethylethylenediamine (TEMED)) and the stacking layer (5% acrylamide solution, 0.05 M Tris-Cl pH 6.8, 0,1% SDS, 0.1% APS, 0.1% TEMED). Samples were mixed with 4x NuPAGE LDS sample buffer and 10x sample reducing agent (both from Thermo Fisher). After heating at 70°C for 10 min samples were centrifuged at 18,400 x g for 10 min at room temperature. 5 µl Magic Mark XP Western Protein Standard (Thermo Fisher) or Novex Sharp Pre-Stained Protein Standard (Thermo Fisher) were used as marker. Electrophoresis was carried out with Tris-glycine buffer (25 mM Tris, 250 mM glycine, 0.1% SDS) or, if gradient gels were used, with NuPAGE MES or MOPS SDS running buffer (Thermo Fisher) with 110 V until the samples were stacked and 130 V until the gel running was stopped.

Proteins were transferred onto Polyvinylidene difluoride (PVDF) membrane (PVDF Western Blotting Membranes (Roche) if the Stella 3200 imaging system (raytest) was used for detection, Immobilon-FL PVDF membrane (Merck Millipore) if Odyssey CLx imaging system (LiCor) was used) as follows: The SDS-PAGE gel was added onto the membrane activated with methanol and incubated in transfer buffer (25 mM Tris, 190 mM glycine, 20% methanol) or NuPAGE transfer buffer (Thermo Fisher). Gel and membrane were sandwiched between one layer of Whatman filter paper and sponge and inserted into a transfer tank for wet electroblotting (Bio Rad) filled with transfer buffer. Blotting was carried out with 35 mA over night at 4°C. The blot was washed two times for 10 min with Tris-buffered saline (TBS) with 0.1% Tween 20 (Sigma) (TBST), blocked for 1 h with blocking buffer (4% milk or 5% BSA in TBST or LiCor blocking buffer), washed once for 5 min with TBST and probed with the primary antibody

over night at 4°C. The blot probed with anti-Ubiquitin VU-1 (LifeSensors) was treated differently according to manufacturer's instructions. Unbound primary antibody was removed by washing four times for 5 min with TBST. The blot was re-probed with the appropriate secondary antibody conjugated to horseradish peroxidase (HRP) (anti-mouse IgG, 1:5000, #7076, Cell Signaling Technology) or with IRDye800CW goat anti-mouse (1:15000, LiCor) for 1 h at room temperature. After washing four times for 5 min with TBST the blot was developed with ECL (Amersham ECL Prime Western Blotting Detection Reagent, GE Healthcare) following manufacturer's instructions and detected with Stella 3200 imaging system (raytest) or directly detected after re-probing with the secondary antibody with Odyssey CLx imaging system (LiCor).

2.1.10.1 Total protein gel staining

15 µL SDS-insoluble proteins dissolved in formic acid and dialyzed against 50 mM Tris pH 7.5, 1 mM DTT, 0.1 mM PMSF (as described at 2.1.12.1) were loaded on a 12% SDS gel. Electrophoresis was carried out as described above. The gel was stained with Sypro Ruby protein gel stain following the manufacturer's instructions (Thermo Fisher).

2.1.10.2 Total protein blot staining

For the analysis of post-translational modifications, 6 µl RIPA samples (soluble proteins) and 9 µl Urea/SDS samples (insoluble proteins) of *C. elegans* from 2.1.8 were loaded on a 12% SDS gel.

For the total protein staining of SDS-insoluble proteins of wildtype mouse brains dissolved in formic acid and dialyzed against 50 mM Tris pH 7.5, 1 mM DTT, 0.1 mM PMSF (as described at 2.1.12.1) one tenth of the original volume after dialysis were loaded on a 4-12% gradient gel.

Electrophoresis and electroblotting were carried out as described above. The blots were stained with Sypro Ruby protein blot stain following the manufacturer's instructions (Thermo Fisher).

2.1.10.3 Western blot analysis of PAR-5 (14-3-3)

9 µl Urea/SDS samples (insoluble proteins) from 2.1.8 were loaded on a 4-12% gradient gel. The membrane was probed with anti-14-3-3 (1:5000, SC-1657, Santa Cruz Biotechnology). The quantification was done with ImageJ.

2.1.10.4 Western blot analysis of post-translational modifications

6 µl RIPA samples (soluble proteins) and 9 µl Urea/SDS samples (insoluble proteins) from 2.1.8 were loaded on a 12% SDS gel. The membrane was probed with anti-Phosphotyrosine (1:500, Merck Millipore) or anti-Ubiquitin VU-1 following the manufacturer's instructions (1:1000, VU101, LifeSensors).

2.1.11 FRANK assay (Fibrillization of Recombinant Aβ Nucleation Kinetic)

The FRANK assay was performed by Anika Bühler and supervised by Dr. Frank Baumann at the Hertie Institute for Clinical Brain Research, Tübingen. The seeding potential of soluble or insoluble protein extracts from *C. elegans* and wild-type mouse brains was detected by measuring Thioflavin T (ThT) fibrillization kinetics as described by (Nagarathinam et al. 2013) with the modifications as described in detail in (Marzesco et al. 2016; Nielsen et al. 2001). In brief: All kinetic measurements were carried out with 20 µM soluble recombinant Aβ(1-40) in 50 mM Phosphate buffer pH 7.4 and 150 mM NaCl with 20 µM ThT supplemented with protease inhibitors (Complete Protease Inhibitor Cocktail, Roche). Each assay was performed with freshly monomerized Aβ1-40. Briefly, lyophilized recombinant Aβ1-40

peptide was dissolved to a stock-concentration of 5 mM in 100% DMSO and frozen at - 80°C. Before use, this stock was then freshly diluted in DMSO to 400 µM and sonified for 20 min in a water bath followed by 30 min centrifugation at 22,000 x g at room temperature. The supernatant was then further diluted to reach 200 µM Aβ1-40 in a 50% DMSO stock. In 96-well plates (µclear non-bind plate, Greiner), eight technical replicates were measured for each sample. The plates sealed with film sheets were incubated at 37°C for up to two to three days. The fluorescence measurements were performed from the bottom of the plate on a Fluostar Omega plate reader (BMG Labtech) (excitation: 440 nm, emission: 480 nm) at 30 min interval after double orbital shaking for 30 s at 500 rpm. Increase of fluorescence over time was followed until the maximum was reached. For each sample, five to eight replicates were averaged and the lag times were determined from fitted curves (Nielsen et al. 2001) with GraphPad Prism 5. For this assay, the peptide Aβ(1-40) was expressed and purified as described earlier (Hortschansky et al. 2005) by Prof. Marcus Fändrich at the University Ulm. Bicinchoninic acid (BCA) protein assay was performed to determine the total protein content in the soluble or detergent-insoluble protein fractions. For all experiments (with *C. elegans* and mice) 0.001 µg was used.

2.1.12 Mass spectrometry analysis

SDS-insoluble proteins dissolved in formic acid were further processed for mass spectrometry analysis. Two biological replicates of *C. elegans* (Table 2.4 replicate 1 and 2) with four different time points each (day 2, day 6, day 10, day 14) were analyzed with mass spectrometry. SDS-insoluble protein extracts of three hemispheres of three young and three old wild-type mouse brains (six hemispheres in total) (Table 2.3) were analyzed.

2.1.12.1 Dialysis

Insoluble proteins dissolved in formic acid were dialyzed against 50 mM Tris pH 7.5, 1 mM DTT, 0.1 mM PMSF as follows: Three times 65 µL insoluble protein of one condition were added onto three membranes (Membrane filters 0.025 µM, Millipore) placed on the buffer surface in a 1-liter-beaker. For *C. elegans*, each condition was divided onto six membranes. For mouse brains, each condition was divided onto three membranes. The pH of one sample was analyzed by removing 5 µL and adding it onto a pH strip. The sample was collected at a pH between 7 and 8 (approximately after two hours). Finally, 10 µL dialysis buffer was used to wash the precipitate off each membrane.

2.1.12.2 Preparation for mass spectrometry

The amount of insoluble proteins in the dialyzed samples was evaluated by loading an aliquot onto a 4-12% gradient gel together with a reference sample of known concentration. A Sypro Ruby protein gel staining (Thermo Fisher) was performed according to manufacturer's instructions and the protein amount was quantified with ImageJ. This step was necessary to estimate the amount of trypsin needed for the digestion (described later). The samples were concentrated using a centrifugal evaporator (Concentrator plus, Eppendorf). The insoluble proteins were solubilized in a final concentration of 8 M urea. Tris(2-carboxyethyl)phosphine hydrochloride (TCEP, Serva) was added to a final concentration of 4 mM and incubated for 1 h at 57°C with 300 rpm. Iodoacetamide (Serva) was added to a final concentration of 8.4 mM and incubated for 45 min in the dark at room temperature. The samples were diluted in 150 mM ammonium bicarbonate (Sigma Aldrich) to obtain a final 2 M urea concentration. Proteins were digested with 5% w/w modified trypsin (Promega) overnight at 37°C and 400 rpm. A sample of the

digested proteins was loaded on a 12% SDS gel and Sypro Ruby protein gel or blot staining (Thermo Fisher) (as described at 2.1.10.1 and 2.1.10.2) were performed to analyze if the digestion worked.

2.1.12.3 Mass spectrometry and data analysis with C. elegans samples

Peptides from *C. elegans* at day 2, day 6, day 10 and day 14 from two biological replicates were labelled by 8-plex isobaric tags for relative and absolute quantitation (iTRAQ) following the manufacturer's instructions (Applied Biosystems).

Mass spectrometry and data analysis were performed by Dr. Ka Wan Li, Pim van Nierop and Prof. August B. Smit at the VU University Amsterdam as described (Klemmer et al. 2011). The iTRAQ-tagged samples were pooled, dried and peptides partially separated in a strong cation exchange column (2.1 x 150-mm PolySUFOETHYL A column, PolyLC Inc). Peptides in each collected fractions were further fractionated by capillary reverse phase C18 column (150 mm x 100 µm-inner diameter column packed in house with the Alltima C18 3 µm particle using the pressure injection cell from Next Advance). The eluents were continuously mixed with matrix (α-cyanohydroxycinnamic acid), and deposited off-line to the metal target every 15 s. The peptides were analyzed on the 5800-proteomics analyzer (AB-Sciex). Tandem mass spectrometry (MS/MS) spectra were each collected from 2500 laser shots; a maximum of 25 MS/MS was allowed per spot. Mascot was used to annotate spectra that were searched against *C. elegans* UniprotKB database.

The peak areas of each iTRAQ signature ions were log2-transformed and normalized to the total peak area of the signature peaks. The peak areas in each sample were mean-centered,

which were used to calculate the protein averages. The permutation-derived false discovery rate (q-value) was calculated by the excel plug-in of the Significant Analysis of Microarrays (SAM) program (Van Nierop 2011).

2.1.12.4 Ingenuity Pathway Analysis

Human homologs of early-aggregating proteins and late-aggregating proteins in *C. elegans* (as described at 3.1.3) were identified using cildb 3.0 (http://cildb.cgm.cnrs-gif.fr) and Ensembl genome browser 87 (http://www.ensembl.org/index.html). 83 human homologs of early-aggregating proteins and 116 human homologs of late-aggregating proteins including early-aggregating proteins that continued to aggregate strongly at day 10 and day 14 were analyzed together with 161 minor components of AD pathological aggregates previously published (Ayyadevara, Balasubramaniam, Parcon, et al. 2016; Liao et al. 2004; Wang et al. 2005) using Ingenuity Pathway Analysis (IPA Winter Release 2016, www.ingenuity.com). Fisher's exact test was used to calculate a p-value reflecting the probability that the association between the set of molecules and a given pathway is due to chance alone. The threshold of the p-value for association was set to 0.01. This analysis was performed by our colleague Dr. Chaolie Huang.

2.1.12.5 Mass spectrometry and data analysis with mice samples

Labeling of the samples and nano-liquid chromatography-MS/MS (nanoLC-MS/MS) analysis were performed by Dr. Ana Velic at the Proteome Center Tübingen. Peptides from three young and three old wild-type mouse brains were labelled with heavy and light dimethyl at lysine residues and N-termini as follows (published at (Spat, Macek, and Forchhammer 2015)): Samples were on-column (SepPak C18) dimethylation labeled as described previously (Boersema et al. 2009). In brief, 5 mL of the

respective labeling solutions with CH_2O (Sigma-Aldrich) and $NaBH_3CN$ (Fluka) for light- and $^{13}CD_2O$ (Sigma-Aldrich) and $NaBD_3CN$ (Sigma-Aldrich) for heavy labeling were flushed with 15 min contact time through the column. Labeled peptides were washed with 5 mL HPLC Solvent A (0.5% acetic acid) on the column and eluted with HPLC Solvent B (80% acetonitrile in 0.5% acetic acid). For validation of labeling efficiency and correct mixing of the labeled peptides, two times 5 µg of each labeled sample (based on Bradford measurements) were used for separate measurements or mixed 1:1 and subjected after purification by C18 stage tips (Ishihama, Rappsilber, and Mann 2006) to pilot LC-MS/MS measurements. Based on the obtained label ratios, correction factors were applied for correct mixing of samples.

For nanoLC-MS/MS analyses peptides were loaded onto an in-house packed 15 cm reverse-phase C18 (3 µm; Dr. Maisch) nanoHPLC column on an EasyLC nano-HPLC (Proxeon Biosystems). Separation was performed by 230 min segmented linear gradients with 5–90% HPLC solvent B. Eluted peptides were directly ionized and measured on a LTQ Orbitrap Elite mass spectrometer. Mass spectrometers were operated in the positive ion mode. The LTQ Orbitrap Elite was conducting higher energy collision dissociation (HCD) of the 15 most intense multiply charged ions at the same scan range at resolution 120,000. Dynamic exclusion of sequenced precursor ions for 90 s and the lock mass option (Olsen et al. 2005) for real time recalibration were enabled on both instruments.

All raw MS spectra were processed with MaxQuant software suite (version 1.5.3.12) (Cox et al. 2009) and default settings. Identified peaks were searched against the target-decoy mouse databases of Uniprot (http://www.uniprot.org) with the following database search criteria: trypsin was defined as cleaving

enzyme and up to two missed cleavages were allowed. Carbamido-methylation of cysteines was set as a fixed, and methionine oxidation and protein N-termini acetylation were set as variable modifications. Light- and heavy-dimethylation labeling on peptide N-termini and lysine residues was defined. The initial mass tolerance of precursor ions was limited to 6 ppm and 0.5 ppm for fragment ions. False discovery rates (FDRs) of peptides and proteins were set to 1%, respectively. Quantification of dimethylation labeled peptides required at least two ratio counts. Peptides were only allowed with a posterior error probability (PEP) <1% at the peptide level.

Perseus 1.5.1.6 was used for the statistical analysis of the MaxQuant output. Proteins only identified by site (proteins only identified with modified peptides), by reverse peptides and potential contaminants were removed. Peptide ratios were log2-transformed (as described in 3.1.8). Three replicates were analyzed together, resulting to 617 proteins that can be found in all replicates.

2.1.12.6 Identification of C. elegans homologs of insoluble mouse brain proteins

C. elegans homologs of proteins that aggregate the most in wild-type mouse brains (as described at 3.1.8) were identified using cildb 3.0 (http://cildb.cgm.cnrs-gif.fr) and Ensembl genome browser 87 (http://www.ensembl.org/index.html).

2.1.13 Motility analysis and paralysis assay with *C. elegans* overexpressing Aβ

2.1.13.1 Preparation of Aβ overexpressing worms and speed measurement

To measure the motility of Aβ overexpressing worms (GMC101) compared to N2 worms or to analyze if the motility is influenced

by a knockdown of a specific protein, worms were kept at 20°C until Aβ overexpressing worms started to paralyze (usually at day 5 or day 6) (worms were defined as paralyzed if they only moved their heads when touched with a platinum wire) and transferred on NG plates without bacteria. To transfer rapidly a large number of worms onto NG plates for motility measurement, a previously described protocol (Ramot et al. 2008) was used with slight modifications. 40 worms were picked into M9 buffer with 0.001% Triton X 100 (AppliChem) and shortly centrifuged. 20 µL containing concentrated worms were pipetted onto a stack of four Whatman paper disks (1.7 cm x 1.4 cm). The top disk was inverted onto a NG mini plate (diameter 3.5 cm) prepared with a Whatman filter paper border with inside dimensions of 2 cm x 1.7 cm, resulting to a transfer of around 30 worms. Because worms try to avoid cupper, the border was soaked with 100 mM $CuCl_2$. Worms were kept for 30 min at room temperature. The motility of Aβ overexpressing worms (GMC101) compared to N2 was measured by taking videos two times for 10 min and two times for 20 min (3 frames/s) with StreamPix 6 (Norpix) software and the camera BM 500 (JAI). After the first comparison the settings were changed. Videos were taken 10 times for 30 s with 30 s pauses in between (7.5 frames/s). For the video analysis, the Parallel Worm Tracker software was used with MathWorks MATLAB R2015b (as described at (Ramot et al. 2008)). To be able to use the software published in 2008 some changes were made in the MATLAB code by Björn Müller (CIN, Tübingen) and Angelos Skodras (DZNE, Tübingen). The settings were obtained from Dr. Jan Kubanek (Stanford University, USA) and are shown in 6.2. The first settings were needed to track a video with the new MATLAB version. The second settings were necessary to be able to analyze videos taken for other time periods than 30 s. Each analysis was

controlled manually. If only a few worms were detected and measured by the software the respective video was removed. Because the motility measurements with the Parallel Worm Tracker software were not reproducible, a motility analysis plugin (called "wrMTrck") for ImageJ described by Jesper S. Pedersen (http://www.phage.dk/plugins/download/wrMTrck.pdf) was used with the following settings: Minimum size 50 pixels, maximum size 400 pixels, maximum velocity 50 pixels/frame, maximum area change 100%, minimum track length 10 frames, frames per second 7.5 and set scale 30 pixel/mm.

2.1.13.2 Knockdown of proteins with RNA interference (RNAi) for motility analysis

One to two days in advance, NG plates with 50 µg/mL Carbenicillin (Carb) and 1 mM IPTG (NG/Carb/IPTG) were prepared with control bacteria or RNAi bacteria (Table 2.6) to inhibit the gene of interest (detailed protocol about RNAi in *C. elegans*: JoVE Science Education Database. *Essentials of Biology 1: yeast, Drosophila and C. elegans.* RNAi in *C. elegans*. JoVE, Cambridge, MA, doi: 10.3791/5105 (2017)). Two bacterial libraries (established by Julie Ahringer and Marc Vidal) were used with bacteria expressing the double stranded RNA needed for the RNAi. Once the offspring reached the L4 larval stage, L4s were transferred onto NG/Carb/IPTG plates seeded with control RNAi or RNAi bacteria for the gene of interest and kept at 20°C. The aging worms were transferred away from their progeny to new plates every second day until the end of their reproductive period in order to be able to distinguish them from their offspring. After knockdown of early-aggregating proteins that continued to aggregate strongly at day 10 and day 14 (NEX-1 and LEC-5, Table 2.6), the average speed of worms was measured between day 3

and day 6 as described above. Most of this part was performed by the intern Stavros Vagionitis.

After transferring Aβ overexpressing worms on different control RNAi's (Table 2.6) for the knockdown of *C. elegans* homologs of insoluble proteins that aggregate the most in wild-type mouse brains, the motility was measured at day 6 as described above with the following changes: For each condition (three different control RNAi's) three plates with 20 worms were prepared. Videos were taken five times for 30 s with 30 s pauses, resulting to five videos per plate and 15 videos per condition. For comparison, videos were analyzed with the Parallel Worm Tracker software and ImageJ.

Table 2.6: RNAi bacteria used for motility analysis of Aβ overexpressing worms (GMC101).

RNAi bacteria (gene name)	**Source (JA: Julie Ahringer, MV: Marc Vidal RNAi library)**	**Description**
L4440	JA	Control RNAi, empty vector
GFP	Cynthia Kenyon's lab at UCSF	Control RNAi
her-1	JA	Control RNAi
nex-1 (ZC155.1)	MV	
lec-5 (ZK1248.16)	JA	

2.1.13.3 Paralysis Assay

To compare the paralysis levels of worms overexpressing PAR-5 (UE50), Aβ (GMC101) or both (double transgenic, DCD296), 105 L4s of each overexpressing strain were kept at 20°C. At day 1 of adulthood, worms were transferred to 25°C to induce paralysis

(McColl et al. 2012). The numbers of paralyzed worms were counted from day 2 to day 4 (until most of the double-transgenic worms were paralyzed). Worms were defined as paralyzed if they only moved their heads when touched with a platinum wire.

2.1.13.4 Staining of Aβ-overexpressing worms with K114 and confocal analysis

For the staining of Aβ amyloids in Aβ-overexpressing GMC101 worms with the Congo red analogue (trans, trans)-1-bromo-2,5-bis-(4-hydroxy)styrylbenzene (K114), age-synchronized worms were shifted to 25°C at day 1 and collected when they started to paralyze (day 2). The fixation protocol for confocal analysis was adapted from a fixation protocol previously described (Antibody Staining of *C. elegans* by Michael Koelle, https://medicine.yale.edu/lab/koelle/protocols/Antibody%20Staining_180540_21947.pdf). Worms were picked into 300 µL M9 buffer, shortly centrifuged and the supernatant was removed. Worms were washed once with 500 µL ddH_2O (ddH_2O was added, the tube was rotated, worms were shortly centrifuged and the supernatant was removed) before being resuspended in fixation solution containing 1% PFA (Sigma). After mixing thoroughly, worms were immediately immersed into liquid nitrogen for freezing. Worms were thawed at 70°C and refrozen in dry ice two times and then rotated for 3 h at 4°C. Worms were washed three times as described above with 500 µL PBST-B buffer (1x Phosphate-buffered saline (PBS) pH 7.4, 0.1% Bovine serum albumin (BSA) (Sigma), 0.5% Triton X 100 (AplliChem), 5 mM sodium azide, 1 mM EDTA). Worms were stained with 50 µL 1 mM K114 (VWR) in PBST-A buffer (same as PBST-B buffer except 1% BSA) for 90 min in the dark at room temperature, washed four times with PBST-B and placed on a slide using Fluorescent Mounting Medium (Dako). Worms were examined under

a Leica SP8 confocal microscope with the HC PL APO CS2 63x1.40 oil objective using the Leica HyD hybrid detector. K114 was detected using 405 nm as excitation and an emission range from 450 to 486 nm.

2.1.14 Intracerebral injection of insoluble proteins into young, pre-depositing APP23 transgenic mice

The intracerebral injection and analysis were performed by Ulrike Obermüller and supervised by Dr. Frank Baumann at the Hertie Institute for Clinical Brain Research, Tübingen.

All APP23 transgenic mice used were bred and maintained under pathogen-free conditions at the Hertie Institute for Clinical Brain Research, Tübingen. All studies were performed in accordance with German animal welfare legislation and with approval from the Ethical Commission for animal experimentation of Tübingen, Germany ("Tierversuchsantrag N03/11").

For the injection of insoluble protein extracts into the hippocampi of APP23 transgenic mice a mix of insoluble protein extracts of aged (total volume of 60 µL) or young (total volume of 40 µL) wild-type mouse brains, that were obtained as described for the FRANK assay at 2.1.9, was prepared (Table 2.7). Per hemisphere 2.5 µL of the mix were injected bilaterally stereotacticly into the hippocampi of five recipient mice (injection of extract mix of aged mice) or four recipient mice (injection of extract mix of young mice) (Table 2.8). All recipients were three months of age when injected and were killed, perfused and histologically analyzed six months after injection.

Table 2.7: Mice used as donors for intracerebral injection. Shown are the sex of the mice, age and volume for the mix of insoluble protein extracts.

Mouse	**Sex**	**Age (months)**	**Volume used for injection**
524	female	18	3x 10 µl
503	female	19	1x 10 µl
7830	male	18	1x 10 µl
7831	male	18	1x 10 µl
8418	female	2	1x 10 µl
8419	female	2	1x 10 µl
8628	male	3	1x 10 µl
8629	male	3	1x 10 µl

Table 2.8: Mice used as recipients for intracerebral injections. Shown are the sex of the mice, age when histologically analyzed and injected protein extract (from aged or young mice).

Mouse	**Sex**	**Age (months)**	**Extract**
451	female	10	aged
512	female	10	aged
518	female	10	aged
525	female	10	aged
526	female	10	aged
832	male	10	young
853	male	10	young
864	female	9	young
865	female	9	young

2.1.15 Statistics

For the FRANK Assays significance was tested with unpaired t-test ($p<0.05$), One-way ANOVA ($p<0.05$) or Two-way ANOVA ($p<0.05$) using Graph Pad Prism 7. For Figure 3.1C the relative seeding activity was calculated using the normalization function of Graph Pad Prism 7. The absolute lag times measured for four biological replicates were normalized to those of the standards. The lag time of a soluble extract from day 2 worms (negative control) was defined as 0% and the lag time of an insoluble extract from transgenic *C. elegans* overexpressing Aβ (GMC101, positive control) was defined as 100%.

For the motility analysis of Aβ-overexpressing worms subjected to RNAi bacteria an unpaired t-test ($p<0.05$) or One-way ANOVA ($p<0.05$) was performed using Graph Pad Prism 7.

For the comparison of the paralysis levels of PAR-5 overexpressing worms, Aβ overexpressing worms and the double-transgenic worms overexpressing both proteins, Fisher's exact test was used (http://www.socscistatistics.com/tests/fisher/default2.aspx).

The Spearman r for the correlation between different replicates of quantitative mass spectrometry with insoluble proteins from young and old wild-type mouse brains was calculated with the correlation analysis of Graph Pad Prism 7.

2.2 Investigation whether rapidly-aggregating proteins seed the aggregation of other proteins

2.2.1 *C. elegans* mutant and transgenics

Table 2.9: C. elegans mutant and transgenic strains used in this study.

Strain name	**Genotype**
CF2137	*fem-1(hc17ts)IV*
DCD187	*uqIs19[Pmyo-2::rho-1::hisavi + Pmyo-2:: birAtagRFP]*
DCD243 (CF2137;DCD187)	*fem-1(hc17ts)IV; uqIs19[Pmyo-2::rho-1::hisavi + Pmyo-2::birAtagRFP]*

2.2.2 Bacterial Strains

See 2.1.2.

2.2.3 Growing and Maintenance of *C. elegans*

As described at 2.1.4.

2.2.4 Cloning and strain generation

In order to isolate rapidly-aggregating proteins and their co-aggregating proteins, a tandem-affinity purification strategy in denaturing conditions was used. For this, an aggregation-prone candidate was tagged with a tandem-affinity tag combining a biotin signal with a hexa-histidine sequence (called histidine-avidin tag) (Schaffer et al. 2010; Tagwerker et al. 2006). The avidin tag is known as AviTag, an artificial target motif for biotinylation by the *E. coli* biotin holoenzyme synthetase birA (Schaffer et al. 2010).

For the method development to crosslink, isolate and identify rapidly-aggregating proteins together with their co-aggregating proteins, a transgenic strain was generated overexpressing RHO-1 (a Rho GTPase orthologous to transforming protein RhoA in mammals) with a histidine-avidin tag at the C-terminus together with the biotinylation enzyme birA fused to tagRFP. Cloning was carried out using the Gateway system (Invitrogen, Carlsbad, CA, USA). The promoter *Pmyo2* was obtained from Brian Lee (UCSF, USA) and the cDNA of the *rho-1* gene was obtained from Open Biosystems (Thermo Scientific, Huntsville, AL, USA). The Gateway vector with histidine-avidin tag was generated by Dr. Emily Crawford. The biotinylation enzyme birA was obtained from Dr. Ekkehard Schulze (University Freiburg) with the construct *Pmyo3::birA::mCherry*. The tagRFP gene was obtained from Evrogen (AXXORA, San Diego, CA, USA). Constructs were sequenced at each step.

The transgenic *C. elegans* line expressing RHO-1 tagged with histidine-avidin and birA fused to tagRFP under the control of the pharyngeal muscle-specific promoter *Pmyo-2* was generated as follows: The construct containing *Pmyo2::rho-1::hisavi* was injected at 30 ng/µL together with the plasmid containing *Pmyo2::birAtagRFP* at 100 ng/µL into N2 animals by Katja Widmaier (as described at (Evans 2006), http://www.wormbook.org).

The extrachromosomal array was integrated by UV irradiation with the CL-1000 Ultraviolet Crosslinker (UVP) with 275,000 µJ/cm^2 as follows: 100 young adults of the strain were irradiated, separated to 10 worms per plate and incubated at 20°C. Irradiated adults were transferred to new plates every day until day 3. The progeny was also kept at 20°C. After starvation 100 L1s from each day were picked onto 100 plates and kept at

20°C to produce progeny. Worms were checked for 100% inheritance (100% fluorescence) with a fluorescence microscope. Worms were backcrossed four times with N2 males to remove potential mutations caused by UV irradiation during integration of a transgene, resulting to the strain DCD187, as follows: 12 N2 males and three L4 hermaphrodites of the transgenic strain were mated. From the mating plate three L4s were picked for the next backcross with 12 N2 males. The last step was repeated until the transgenic strain was backcrossed four times with N2 males. Nine L4s were picked from the mating plate onto separate plates to produce progeny. From the progeny 20 L1s were added onto separate plates. The progeny was analyzed for 100% transmission of the transgene.

The *C. elegans* transgenic strain overexpressing RHO-1 tagged with histidine-avidin and overexpressing the biotinylation enzyme birA fused to tagRFP (DCD187) with temperature-induced sterility was generated as follows: N2 males were crossed with temperature induced sterile *fem-1* mutant hermaphrodites (CF2137) as described at 2.1.4. CF2137 males were mated into DCD187 hermaphrodites as described at (Fay 2013), resulting to the strain DCD243.

2.2.5 *C. elegans* liquid culture

The *C. elegans* transgenic strain overexpressing RHO-1 tagged with histidine-avidin, overexpressing the biotinylation enzyme birA and bearing the *fem-1* mutation (DCD243) to get temperature induced sterile worms was used to obtain a large aged-synchronized population. The same protocol was used as described at 2.1.6 with the following changes: To collect the parental generation for the temperature shift, worms were first grown on 10 NG plates seeded with OP50 at 20°C until plates were con-

fluent, washed from the plates with M9 and grown in liquid culture with OP50-1 at 20°C instead of growing the worms on HGM plates.

When most animals were adults and L1s were hatching, eggs and L1s were separated from the adults by sedimentation as described at 2.1.6.2. After L1 arrest overnight at 25°C, L1s were counted and 300,000 L1s were grown with OP50-1 at 25°C. At day 1, worms were collected and removed from bacteria and dead worms by sucrose separation as described at 2.1.6.5. The resulting worm pellet was frozen in liquid nitrogen with an equal volume of RAB high-salt buffer with inhibitors. The frozen worm pellet was ground in a mortar as described at 2.1.6.6.

For the method development of chemical crosslinking and purification non-sterile *C. elegans* transgenic worms overexpressing RHO-1 with histidine-avidin tag and the biotinylation enzyme birA (DCD187) were collected at day 1 as described above and ground in a mortar.

2.2.6 Insoluble protein extraction with chemical crosslinking

2.2.6.1 Method development without chemical crosslinking

To establish the purification protocol protein extractions without crosslinking were performed with non-sterile *C. elegans* transgenic worms overexpressing RHO-1 with histidine-avidin tag and the biotinylation enzyme birA (DCD187) collected at day 1.

After grinding of the frozen worm pellet as described at 2.1.6.6, the protocol for insoluble protein extraction for mass spectrometry with *C. elegans* described at 2.1.7 was followed until resuspension and centrifugation with the RIPA buffer. After centrifu-

gation the supernatants were removed and the two pellets resulting from two times 350 mg powder were resuspended with 300 µL urea buffer each. For the first extraction urea buffer A (8 M urea, 20 mM sodium phosphate pH 7.4, 500 mM NaCl, 10 mM imidazole) was used. For the second extraction for the purification with harsh conditions urea buffer 1 (8 M urea, 300 mM NaCl, 0.5% NP40, 50 mM sodium phosphate, 50 mM Tris pH 8) (Tagwerker et al. 2006) was used. After centrifugation at 18,400 x g for 20 min at 4°C the supernatants of one extraction containing highly insoluble proteins were combined, resulting to 600 µL total volume.

2.2.6.2 Chemical crosslinking with 0.4% Para-Formaldehyde (PFA)

For the first chemical crosslinking with Para-Formaldehyde (PFA, Sigma) the protein extraction was performed as described above but the resuspension and centrifugation were done with a RIPA buffer free of primary amines containing 50 mM 4-(2-hydroxyethyl)-1-piperazineethanesulfonic acid (HEPES) pH 8 instead of Tris. After centrifugation the supernatants were removed and the two samples were pooled together after solubilizing each pellet with 500 µL RIPA buffer (with HEPES). After the suspension was drawn up into a syringe 10 times and centrifuged, all supernatant was removed and discarded. The pellet was resuspended with 700 µL 0.4% PFA in PBS pH 7.4. The suspension was incubated for 10 min at room temperature on a nutating mixer. The reaction was quenched with 700 µL ice-cold 2.5 M glycine in PBS (for a final concentration of 1.25 M glycine). After centrifugation at 18,400 x g for 20 min at 4°C the supernatant was removed. The final pellet was resolved with 600 µL urea buffer 1 and centrifuged at room temperature. The supernatant containing crosslinked SDS-insoluble proteins was trans-

ferred to a new tube. The pellet was resolved with 100 µL 2x SDS gel-loading buffer (100 mM Tris pH 6.8, 4% SDS, 0.2% bromophenol blue, 20% glycerol, 200 mM DTT) and heated at 95°C for 5 min for SDS gel or western blot analysis.

2.2.6.3 Chemical crosslinking with Disuccinimidyl glutarate (DSG)

Because the chemical crosslinking with PFA was to strong, a crosslinking with Disuccinimidyl glutarate (DSG, Thermo Scientific) was performed as described for PFA with the following changes: After resuspension and centrifugation with RIPA buffer (with HEPES) for the second time, the pellet was resuspended with 700 µL 0.25 mM DSG, 0.025 mM DSG or 0.0025 mM DSG in PBS pH 7.4. The crosslinker was incubated for 30 min at room temperature on a nutating mixer. The reaction was quenched with 700 µL 100 mM Tris pH 7.5 (for a final concentration of 50 mM Tris) for 15 min and centrifuged as described for PFA. The final pellet was resolved with 600 µL urea buffer 1 and centrifuged at room temperature.

2.2.7 Protein purification with Nickel affinity chromatography

All purifications were performed with the ÄKTA Pure 25 System and UNICORN control software (GE Healthcare) with a flow rate of 1 mL/min.

2.2.7.1 Purification with imidazole

For the first purification, the volume of the sample containing highly insoluble proteins of worms overexpressing RHO-1 with histidine-avidine tag (DCD187) was increased with urea buffer A to 800 µL. Before loading the sample onto a His-Trap™ FF column (column volume 1 mL, GE Healthcare), the sample was centrifuged at 18,400 g for 20 min at 4°C to remove any particles. The column was equilibrated and the sample was loaded onto

the column with 20 column volumes (CV) urea buffer A, respectively. The column was washed with 30 CV urea buffer A. The elution was performed with a linear gradient from urea buffer A to urea buffer B (8 M urea, 20 mM sodium phosphate pH 7.4, 500 mM NaCl, 500 mM imidazole) over 20 CV. During all steps 1 mL-fractions ("flow through" and "elution") or 3 mL-fractions ("wash") were collected.

2.2.7.2 Purification with harsh conditions

The purification under harsh conditions was performed as described at 2.2.7.1, with the following changes: The column was equilibrated and the sample was loaded onto the column with 20 column volumes (CV) urea buffer 1, respectively. The column was washed with 10 CV urea buffer 1, 10 CV urea buffer 1 pH 6.3 and 10 CV urea buffer 1 pH 6.3 and 10 mM imidazole. The elution was performed with a linear gradient from urea buffer 1 pH 6.3 and 10 mM imidazole to urea buffer 2 (8 M urea, 200 mM NaCl, 50 mM sodium phosphate, 2% SDS, 10 mM EDTA, 100 mM Tris pH 4.3) over 20 CV. During all steps 1 mL-fractions ("flow through" and "elution") or 5 mL-fractions ("wash") were collected.

2.2.8 Gel electrophoresis and Western blotting

Gel electrophoresis and Western blotting were performed as described at 2.1.10. Before the samples (load, flow through, wash and elution fractions) were loaded onto a 4-12% gradient gel they were mixed with NuPage sample buffer as described and heated at 65°C for 10 min.

2.2.8.1 Western blot analysis of histidine-avidin tagged proteins

10 µL samples collected during purification were loaded on a 4-12% gradient gel. The membrane was probed with horseradish

peroxidase (HRP)-conjugated Streptavidin (1:10,000, OC181939, Thermo Scientific).

2.2.8.2 Silver staining

The same volumes of samples were loaded as described at 2.2.8.1. Silver staining was performed with the Pierce™ Silver Stain Kit (Thermo Scientific) according to the manufacturer's instructions.

3 Results

3.1 Identifying age-dependent heterologous seeds for amyloid-β aggregation

Results and figures are mainly reproduced from:

Groh N, Bühler A, Huang C, Li KW, van Nierop P, Smit AB, Fändrich M, Baumann F and David DC (2017) Age-Dependent Protein Aggregation Initiates Amyloid-β Aggregation. Front. Aging Neurosci. 9:138. Doi: 10.3389/fnagi.2017.00138

3.1.1 Protein aggregates formed during normal *C. elegans* aging seed Aβ aggregation *in vitro*

To investigate whether age-dependent protein aggregates formed during aging in *C. elegans* have the potential to seed the aggregation of synthetic Aβ *in vitro*, highly detergent-insoluble proteins from young and aged *C. elegans* were isolated as described at 2.1.7. *C. elegans* has been extensively characterized as a model for aging (Antebi 2007) and widespread protein aggregation with age has been repeatedly documented (David et al. 2010; Reis-Rodrigues et al. 2012; Walther et al. 2015). As extensive protein aggregation occurs in the reproductive tissues (David et al. 2010), a gonad-less *C. elegans* strain was used to investigate only somatic age-dependent protein aggregation. To identify seeding, changes in the lag time preceding the formation of Aβ(1-40) fibrils *in vitro* were examined using the FRANK assay (Fibrillisation of Recombinant Aβ Nucleation Kinetic) (Figure 1.3B). This assay has been successfully used to quantify the seeding activity of different cellular extracts containing Aβ seeds (Fritschi et al. 2014; Marzesco et al. 2016; Nagarathinam et al. 2013).

Insoluble protein extracts from aged *C. elegans* (day 14, ~50% dead) significantly shortened the lag time of Aβ aggregation compared to extracts from young animals (day 2, 0% dead) (Figure 3.1A, p=0.039). Similar to a classical western blot, it is only meaningful to compare absolute lag time values evaluated in the same assay plate. However, despite variations between experiments, the difference in seeding activity between insoluble extracts from young and aged animals was highly reproducible (Figure 3.1). Consistent with the nature of a seed, only 0.001 µg of insoluble proteins from aged animals were needed to seed Aβ aggregation. To distinguish whether seeding is a general characteristic of the aged proteome or specific to aggregated proteins, high-salt soluble proteins were evaluated with the *in vitro* assay. The lag time for Aβ aggregation remained similar for soluble proteins from aged and young animals and comparable to that observed with insoluble extracts from young animals (Figure 3.1A). Together, these results demonstrate that protein aggregates appearing during normal aging can serve as heterologous seeds for Aβ aggregation.

3.1.2 Seeding activity appears in the later stages of life

Sporadic AD is a late-onset disease affecting humans over age 65. However, it remains unclear when pathogenesis starts in the patients' brains. To determine when the seeds triggering Aβ aggregation appear, insoluble extracts from different stages of adulthood were analyzed. For this, four time points were chosen: young animals (day 2), early middle-aged animals (day 6, at the end of reproduction in wild-type animals), late middle-aged animals (day 10, ~30% of the population has died) and old animals (day 14, ~50% of the population has died). To collect large numbers of individuals for all time points, *C. elegans* were cultured in liquid. The whole procedure was performed four times to obtain

four different biological replicates. In order to compare the seeding activities of all insoluble extracts measured in two separate assay plates, two standard extracts were included: a soluble extract as negative control and an insoluble extract from transgenic *C. elegans* overexpressing Aβ as positive control. The relative seeding activity was calculated by normalizing the absolute lag times measured for each biological replicate to those of the standards with 0% being the lag time of the negative control and 100% being the lag time of the positive control. Sypro Ruby staining of insoluble proteins on an SDS gel showed accelerated protein aggregation with increasing age, especially between day 10 and day 14 (Figure 3.1B). Evaluation of the relative seeding activity did not reveal a significant increase in seeding between day 2 and day 6 (Figure 3.1C, $p= 0.57$). Instead, a large increase in seeding activity at day 10 was found ($p= 0.0086$ compared to day 2). The seeding potential was not further increased in insoluble extracts from 14-day-old animals. When extrapolated to human aging, the appearance of heterologous protein aggregate seeds for Aβ aggregation at the later stages of life rather than early middle age would be consistent with the late-onset of AD dementia.

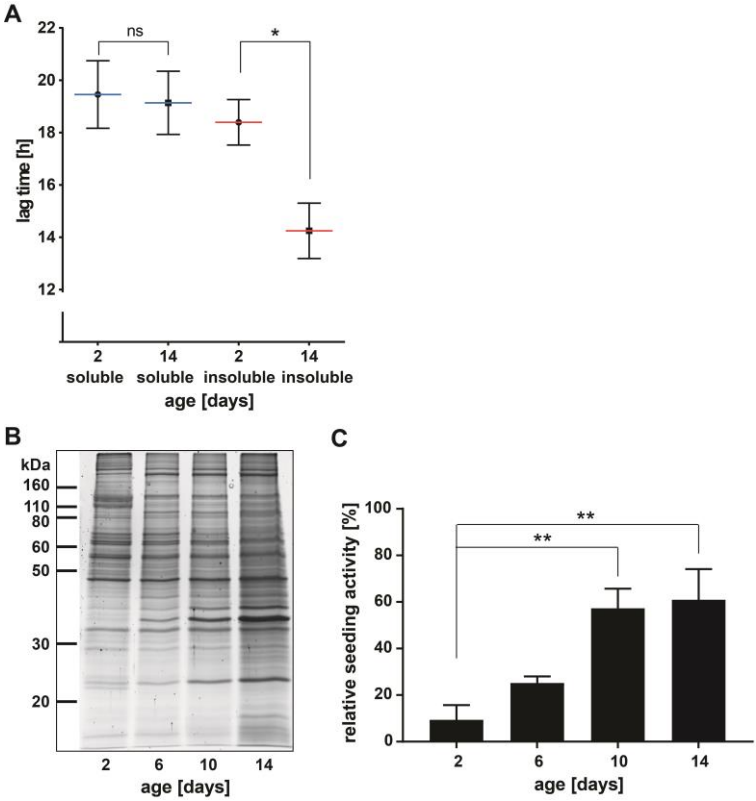

Figure 3.1: Insoluble protein extracts from aged C. elegans seed Aβ aggregation in vitro (reproduced from Frontiers article).
*A: Lag times measured for Aβ aggregation in the presence of 0.001 µg C. elegans soluble and detergent-insoluble protein extracts (day 2 and day 14). Mean values (blue lines soluble, red lines insoluble) with respective SEM of 3 biological replicates are represented (each including a minimum of five technical replicates). Two-tailed p-value: day 2 insoluble vs. day 14 insoluble *p= 0.039.*
B: SDS gel of insoluble protein extracts from different ages stained with Sypro Ruby protein gel stain.
C: Relative seeding activity measured for Aβ aggregation in the presence of 0.001 µg insoluble protein extracts from different ages. Mean values of four biological replicates (each including five technical replicates) are

*shown. Data were normalized with 0% being the lag time of the negative control (soluble extract, day 2) and 100% being the lag time of the positive control (insoluble extract from C. elegans transgenics expressing Aβ). One-way ANOVA: day 2 vs. day 10 **p= 0.0086 and day 2 vs. day 14 **p= 0.0051.*

3.1.3 Identification of early- and late-aggregating proteins during aging

The results from the *in vitro* assay imply that changes in aggregation between day 6 and day 10 are responsible for seeding. Quantitative mass spectrometry was performed using the stable-isotope iTRAQ reagents to identify these changes with two independent biological repeats. 845 quantifiable aggregation-prone proteins were found. Of these, 460 were identified in a previous study (David et al. 2010). This large overlap attests to the quality of the present mass spectrometry analysis. After normalization, the proteins were ranked depending on their relative change in aggregation levels focusing on proteins with the highest change in aggregation with age, i.e. in the top 25th percentile in both repeats. Early-aggregating proteins were defined as present in the top 25th percentile of day 6 compared to day 2 and late-aggregating proteins as present in the top 25th percentile of day 10 or day 14 compared to day 6 (Figure 3.2). 133 proteins were detected at day 6 in the top aggregating fractions in both replicates. Significantly among these early-aggregating proteins, the rate of aggregation continued to increase strongly for 23 proteins at day 10 (in the top 25th percentile) as well as 30 proteins at day 14 (Figure 3.2; as opposed to 3.3 by chance, Table 3.1). Consequently, these latter proteins could also be responsible for seeding Aβ. At day 10 and day 14, 65 and 107 late-aggregating proteins were detected, respectively. Of these, 42 proteins (as opposed to 3.3 by chance, Table 3.1) were prone to aggregate

strongly at both later ages compared to day 6. As seeding activity appears in day 10 animals, these late-aggregating proteins are prime candidates.

To identify functional groups associated with the early- and late-aggregating proteins, an Ingenuity Pathway Analysis (IPA) was performed with the human homologs. Then, pathways that were also significantly associated with the minor components in AD pathological aggregates were investigated. This analysis highlighted eight pathways that tend to harbor both late-aggregating proteins and disease-related aggregate components, namely: proteins related to 14-3-3 mediated signaling, PI3K/AKT signaling, ERK/MAPK signaling, Calcium Transport I as well as proteins related to the ubiquitination pathway, aryl hydrocarbon receptor signaling, NRF2-mediated oxidative stress response and xenobiotic metabolism signaling (Table 3.2). The latter four categories were also significantly associated with early-aggregating proteins. These results predict that interactions between Aβ or tau with these pathway components could potentially induce or accelerate their aggregation.

In addition to the pathway analysis, late-aggregating proteins that were also minor components in AD were identified. At day 10 and/or day 14 the homologs of the following ten proteins were identified in amyloid plaques and/or NFTs: PAR-5, UBA-1, SPC-1, LMN-1, NEX-3, HIS-1, NKB-3, FRM-1, MCA-3 and GPD-1 (Table 3.3). Importantly, seeding activity of the late-aggregating protein, 14-3-3 (human homolog of PAR-5), has already been demonstrated both *in vitro* and in cell culture, whereby 14-3-3 initiates tau fibril formation (Hernandez, Cuadros, and Avila 2004; Li and Paudel 2016; Qureshi et al. 2013). Western blot analysis confirmed that PAR-5 was highly prone to aggregate at day 10 compared to day 6 (3.2 fold, Figure 3.3). Conversely, six

minor components of amyloid plaques and/or NFTs were among the early-aggregating proteins in *C. elegans*. Of note, only one of these early-aggregating minor components, GST-1, continued to aggregate strongly at day 10 and day 14 and therefore could also play a role in Aβ seeding.

To summarize, this quantitative proteomic analysis of the *C. elegans* aggregating proteome at different ages brings insight into which minor components of pathological protein aggregates could directly seed disease-associated aggregation.

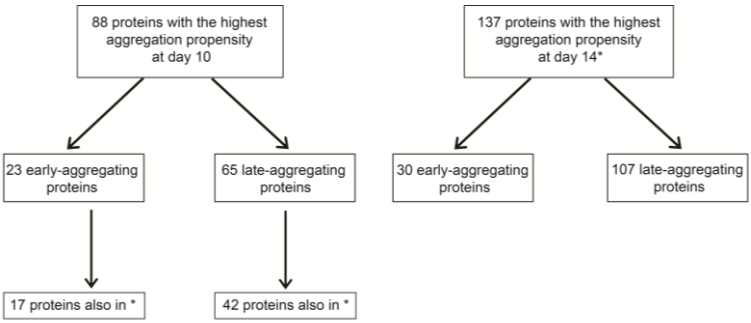

*Figure 3.2: Schematic summarizing numbers of early- and late-aggregating C. elegans proteins detected by quantitative mass spectrometry (reproduced from Frontiers article). Proteins with the highest aggregation propensity at day 10 or day 14 are defined as proteins quantified in the top 25th percentile compared to day 6. Proteins with the highest aggregation propensity at day 6 are defined as proteins quantified in the top 25th percentile compared to day 2. Quantification was performed with two biological replicates and all numbers represent only proteins in the top 25th percentiles from both replicates. *Proteins also among the 137 proteins with the highest aggregation propensity at day 14 (in top right box).*

Table 3.1: Comparison of actual and expected numbers of proteins in the top 25th percentile of two biological replicates (reproduced from Frontiers article).

Proteins ranked in (two replicates)	**actual**	**expected#**	**Chi-Square Test***
Top 25th percentile of day 6	133	52.8	4.38E-30
Not in top 25th percentile of day 6	712	792.2	
Top 25th percentile of day 10	88	52.8	5.71E-07
Not in top 25th percentile of day 10	757	792.2	
Top 25th percentile of day 14	137	52.8	5.45E-33
Not in top 25th percentile of day 14	708	792.2	
Top 25th percentile of day 6 and day 10	23	3.3	1.71E-27
Not in top 25th percentile of day 6 and day 10	822	841.7	
Top 25th percentile of day 6 and day 14	30	3.3	4.49E-49
Not in top 25th percentile of day 6 and day 14	815	841.7	
Top 25th percentile of day 10 and day 14	42	3.3	4.59E-101
Not in top 25th percentile of day 10 and day 14	803	841.7	

#Calculation: the expected probability of proteins to be ranked in the top 25th percentile of two replicates is 1/16. In addition the expected probability of these proteins to be ranked in the top 25th percentile of two different days is 1/256.
** Chi-Square Test has been performed with Excel formula CHITEST.*

Table 3.2: Ingenuity Canonical Pathways identified in the set of late- or early-aggregating proteins and their association with minor components found in AD pathological aggregates (highlighted in grey) (–log(p-value) > 2) (reproduced from Frontiers article).

	-log(p-value)	
Ingenuity Canonical Pathways	**Late-aggregating proteins**	**Minor components**
Protein Ubiquitination Pathway	6.82	2.57
Aryl Hydrocarbon Receptor Signaling	4.93	3.19
Glutathione-mediated Detoxification	4.75	
EIF2 Signaling	4.54	
tRNA Charging	4.23	
mTOR Signaling	3.96	
LPS/IL-1 Mediated Inhibition of RXR Function	3.67	
Regulation of eIF4 and p70S6K Signaling	3.66	
PI3K/AKT Signaling	3.23	5.37
ERK/MAPK Signaling	3.11	3.18
Citrulline Biosynthesis	3.09	
Calcium Transport I	2.89	7.47
Death Receptor Signaling	2.79	
Superpathway of Citrulline Metabolism	2.59	
NRF2-mediated Oxidative Stress Response	2.38	4.96
Xenobiotic Metabolism Signaling	2.31	2.92

14-3-3-mediated Signaling	2.25	13.4
Endoplasmic Reticulum Stress Pathway	2.24	
Glutathione Redox Reactions I	2.20	
Lipid Antigen Presentation by CD1	2.06	
Ingenuity Canonical Pathways	**Early-aggregating proteins**	**Minor components**
EIF2 Signaling	5.68	
Protein Ubiquitination Pathway	5.22	2.57
Cell Cycle Control of Chromosomal Replication	4.87	
Aryl Hydrocarbon Receptor Signaling	4.78	3.19
NRF2-mediated Oxidative Stress Response	4.01	4.96
Creatine-phosphate Biosynthesis	3.84	
Glutathione-mediated Detoxification	3.73	
Leucine Degradation I	3.29	
Xenobiotic Metabolism Signaling	3.08	2.92
Unfolded protein response	2.93	
eNOS Signaling	2.52	
Aldosterone Signaling in Epithelial Cells	2.42	2.05
Glutamine Biosynthesis I	2.42	
Prostate Cancer Signaling	2.25	
Choline Degradation I	2.12	

Table 3.3: Minor components of AD pathological aggregates identified as late- or early-aggregating proteins in C. elegans (reproduced from Frontiers article).

C. elegans **entry name**	***C. elegans*** **Uniprot ID**	***C. elegans*** **gene name**	***Homo sapiens*** **protein name**
Late-aggregating proteins			
14331_CAEEL[x,†]	P41932	*par-5*	14-3-3 proteins ß/α; δ
C1P636_CAEEL[x,*]	C1P636	*uba-1*	Ubiquitin-like modifier-activating enzyme 1
G4S034_CAEEL[x,*]	G4S034	*spc-1*	Spectrin α-chain, non-erythrocytic protein 1
LMN1_CAEEL[x,*]	Q21443	*lmn-1*	Lamin A/C
Q27473_CAEEL[‡,*]	Q27473	*nex-3*	Annexin A5
H4_CAEEL[‡]	P62784	*his-1*	H4 histone family, member C
AT1B3_CAEEL[‡]	Q9XUY5	*nkb-3*	Sodium/potassium-transporting ATPase beta-1 chain
G5EEG8_CAEEL[x]	G5EEG8	*frm-1*	Band 4.1-like protein 1
Q95XP6_CAEEL[x]	Q95XP6	*mca-3*	Plasma membrane Ca++-transporter ATPase 1
G3P1_CAEEL[‡]	P04970	*gpd-1*	Glyceraldehyde-3-phosphate dehydrogenase
Early-aggregating proteins			
GSTP1_CAEEL[x,+]	P10299	*gst-1*	Glutathione S-transferases Mu 3, Mu 5
DYHC_CAEEL[x,†]	Q19020	*dhc-1*	Cytoplasmic dynein 1 heavy chain 1
HSP90_CAEEL[x,†]	Q18688	*daf-21*	Protein HSP90-β

G5ECP9_CAEEL[x]	G5ECP9	*vab-10*	Plectin
HSP7A_CAEEL[‡]	P09446	*hsp-1*	Heat shock cognate 71 kDa protein
KARG2_CAEEL[‡]	Q27535	ZC434.8	Creatine kinase B-type

[x] Minor components identified in both amyloid plaques and NFTs in (Ayyadevara, Balasubramaniam, Parcon, et al. 2016).
[†] Minor components identified in amyloid plaques in (Liao et al. 2004).
[‡] Minor components identified in NFTs in (Wang et al. 2007).
[*] Minor components identified as late aggregating proteins in both day 10 and day 14.
[+] Minor component identified as early-aggregating protein with a high increase in aggregation at both day 10 and day 14.

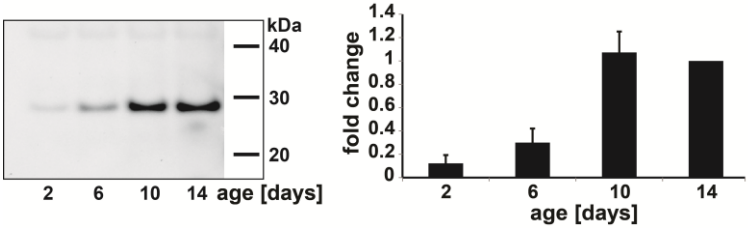

Figure 3.3: PAR-5 (14-3-3) is highly prone to aggregate at day 10 (reproduced from Frontiers article). Representative immunoblot detecting PAR-5 in insoluble protein extracts from different ages of C. elegans. Right: Immunoblot quantification of PAR-5. Band intensities were normalized to day 14. N= 4 (biological repeats), SEM depicted.

3.1.4 Motility analysis and paralysis assay with *C. elegans* overexpressing Aβ in the body-wall muscle

3.1.4.1 Motility measurements of C. elegans overexpressing Aβ

In *C. elegans*, Aβ toxicity in the body-wall muscle causes the animals to paralyze (Link 1995; McColl et al. 2012). To investigate whether a knockdown of early-aggregating proteins that continued to aggregate strongly at day 10 and day 14 would rescue the reduced motility of Aβ overexpressing worms, motility meas-

urements of worms subjected to different RNAi's were performed. When comparing wild-type (N2) with Aβ overexpressing worms by eye at day 5 (when Aβ overexpressing worms started to paralyze at 20°C), worms overexpressing Aβ were obviously slower. The motility measurement with the Parallel Worm Tracker software did not confirm this observation (Figure 3.4A). Next, Aβ overexpressing worms were subjected to two different control RNAi's (GFP and L4440) and RNAi against two different early-aggregating proteins with a high increase in aggregation at both day 10 and day 14, namely LEC-5 and NEX-1. Animals were kept at 20°C and the motility measurements were performed at different days (between day 3 and day 6, Figure 3.4B) to analyze if a knockdown of LEC-5 or NEX-1 proteins lead to a detectable improvement of the motility. With age Aβ overexpressing worms were getting slower, which can be demonstrated by the comparison of day 4 to day 6 old worms after exposure to GFP RNAi. This result could not be confirmed with the second control RNAi. The worms subjected to L4440 RNAi showed a significant increase in their speed between day 4 and day 6. Also the knockdown of NEX-1 resulted to a significant increase of the motility between day 3 and day 4 and day 3 and day 6, but no increase could be observed when day 4 and day 6 were compared. The knockdown of LEC-5 did not lead to a significant difference in motility between day 3 and day 6. Because the exposure of worms to two different control RNAi's led to contrary results they were not compared with the other worms. All measurements were performed with Aβ overexpressing worms kept at 20°C to delay the onset of paralysis. But the motility defect was not clear enough with age to be detectable by the software.

Changes in aggregation between day 6 and day 10 are responsible for seeding, as demonstrated in Figure 3.1C. Therefore, the

question whether early-aggregating proteins that continued to aggregate strongly at day 10 and day 14 would influence the motility of Aβ overexpressing worms arose. The knockdown of these proteins and the subsequent motility measurements with the Parallel Worm Tracker software did not contribute to answer this question.

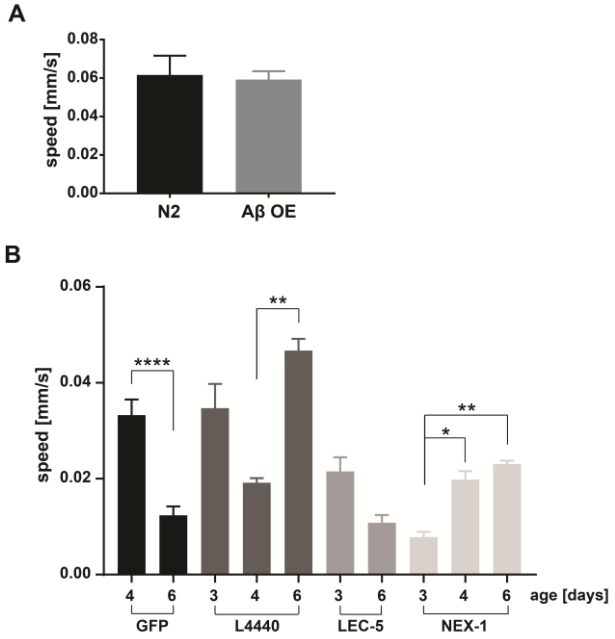

Figure 3.4: Motility measurements of Aβ overexpressing worms (Aβ OE) subjected to different RNAi bacteria.
A: Average speed with respective SEM of N2 worms and Aβ overexpressing worms subjected to OP50. With both strains videos were taken two times for 10 min and two times for 20 min at day 5 and the average speeds were calculated. Two-tailed p-value: N2 vs. Aβ OE not significant.
B: Average speed with respective SEM of Aβ overexpressing worms subjected to control RNAi (GFP, L4440) or RNAi against two different early-aggregating proteins with a high increase in aggregation at both day 10 and day 14 (LEC-5 or NEX-1). Videos were taken 10 times for 30 s with

*30 s pauses in between at different days and the average speed was calculated for each day and each condition. One-way ANOVA: GFP day 4 vs. day 6 ****p< 0.0001, L4440 day 4 vs. day 6 **p= 0.0032, NEX-1 day 3 vs. day 4 *p= 0.0427, NEX-1 day 3 vs. day 6 **p= 0.0027.*

3.1.4.2 Paralysis assay of C. elegans overexpressing Aβ and PAR-5

Because the knockdown of aggregating proteins and the subsequent motility analysis could not contribute to investigate whether aggregating proteins influence Aβ toxicity, an overexpression of the late-aggregating protein PAR-5 (*C. elegans* homolog of 14-3-3) was performed. Previously it has been shown that a knockdown of PAR-5 rescued paralysis induced by Aβ (Ayyadevara, Balasubramaniam, Parcon, et al. 2016). This led to the speculation that overexpression of the aggregation-prone protein PAR-5 would accelerate the rate of paralysis. Indeed, a significant increase in the number of double transgenics paralyzed compared to those solely expressing Aβ was observed in three biological replicate experiments (Figure 3.5A and data not shown). This effect cannot be explained by a general toxicity due to PAR-5 overexpression as these animals displayed negligible levels of paralysis in the absence of Aβ. Additionally, transgenics solely overexpressing Aβ were stained with K114, a Congo red analogue that stains amyloid structures (Zhuang et al. 2001), to show the formation of Aβ amyloids in the body-wall muscle (Figure 3.5B). As already mentioned, seeding activity of 14-3-3 was demonstrated previously. The data presented here confirmed that 14-3-3 accelerated Aβ toxicity.

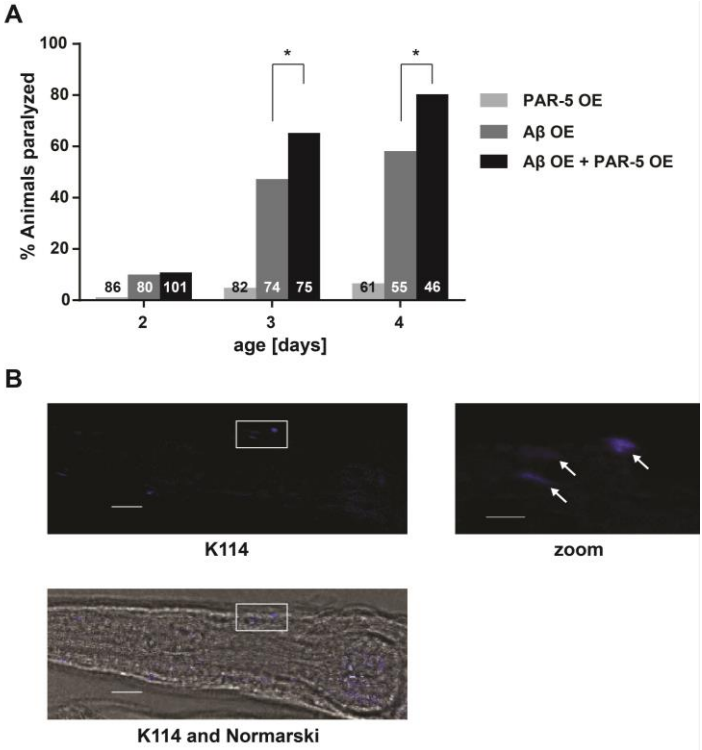

Figure 3.5: Late-aggregation-prone protein PAR-5 (14-3-3) accelerates Aβ toxicity in C. elegans.
*A: Paralysis levels of worms that overexpress PAR-5 (PAR-5 OE), Aβ (Aβ OE) or both (double transgenic, Aβ OE + PAR-5 OE) (reproduced from Frontiers article). Shown are the percentages of worms paralyzed at different days. The numbers in the bars represent the total numbers of worms analyzed. Fisher's exact test: Aβ OE vs. Aβ OE + PAR-5 OE, day 3 *p= 0.032 and day 4 *p= 0.019.*
B: Staining of Aβ aggregates. Paralyzed worms overexpressing Aβ were stained at day 2 with K114. Left: Head of a paralyzed worm with Aβ aggregates in the body-wall muscle (box). Right, zoom: Arrows highlight Aβ aggregates. Scale bars: Left 10 µm, right: zoom, 3 µm.

3.1.5 Insoluble proteins show an increase of specific post-translational modifications with age in *C. elegans*

A number of post-translational modifications (PTMs) have been identified in disease-associated aggregates, and a recent study detected carbonylation in the mouse age-dependent insoluble proteome (Tanase et al. 2016). Therefore, it is possible that PTMs occurring with age influence the seeding ability of late-aggregating proteins as well as early-aggregating proteins that continue to become more insoluble with age. Western blot analysis confirmed that detergent-insoluble proteins show an increase of ubiquitination (Figure 3.6A, right) and phosphorylation of tyrosines (Figure 3.6B, right) with age in *C. elegans.* The increase in PTMs was stronger compared to the increase in insolubility with age for all proteins, shown by the total protein staining (Figure 3.6A and B, left part). Regarding the soluble proteins no obvious differences in PTMs between young (day 2) and old (day 14) worms can be detected (Figure 3.6A and B, right part). These results were confirmed with a second repeat with protein extracts from another timeline. Additionally, dimethylation of arginines, citrullination (irreversible conversion of arginine into citrullin) and phosphorylation of serines and threonines were analysed, but no differences with age could be detected. However, only a few faint bands were visible (data not shown).

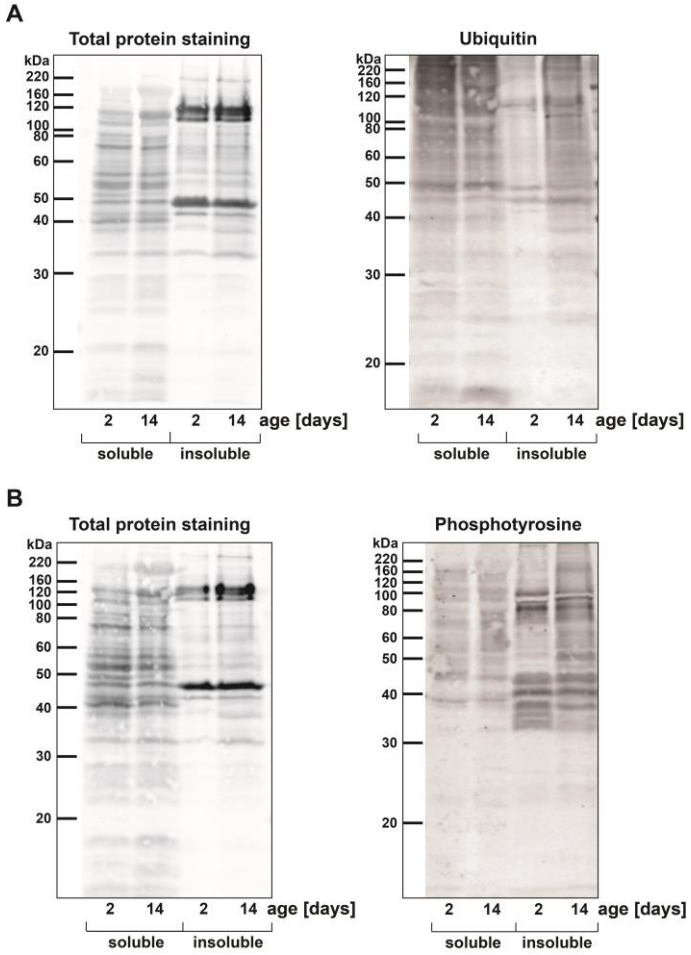

Figure 3.6: Insoluble proteins show an increase of post-translational modifications (PTMs) with age in C. elegans.
Left: Blot of soluble and insoluble protein extracts from young (day 2) and old (day 14) worms stained with Sypro Ruby protein blot stain. Right: Immunoblot detecting A: ubiquitinated proteins (mono- and poly-ubiquitin) or B: proteins with phosphorylated tyrosine in soluble and insoluble protein extracts from young (day 2) and old (day 14) worms.

3.1.6 Aged mouse brains contain protein aggregates that seed Aβ aggregation *in vitro*

To confirm that insoluble proteins present in mammals also have the potential to seed Aβ aggregation, the same *in vitro* assay as described above was performed with homogenates of wild-type mouse brains. Of note, previous studies did not detect seeding activity in aged wild-type mouse brains (Fritschi et al. 2014; Nagarathinam et al. 2013). However, total brain homogenates were tested without any enrichment for insoluble proteins. Here, detergent-insoluble protein extracts from young (2-3 months) and aged (18-20 months) mouse brains were measured. Compared to young extracts, insoluble protein extracts from aged mouse brains led to a significant decrease of the lag time preceding Aβ aggregation (Figure 3.7, p= 0.0073). No further increase in seeding potential was detected when examining insoluble extracts from 25-28 month old mice (Figure 3.7, p= 0.0067 compared to 2-3 months). This is consistent with the similar seeding activity of insoluble protein extracts from late-middle aged and old *C. elegans*. For comparison, the insoluble extract from an APP23 transgenic mouse, which contains Aβ seeds, and the soluble extract from an aged wild-type mouse brain were included.

Collectively, these results demonstrate, that cross-seeding of Aβ aggregation by age-dependent protein aggregation is conserved from *C. elegans* to mammals.

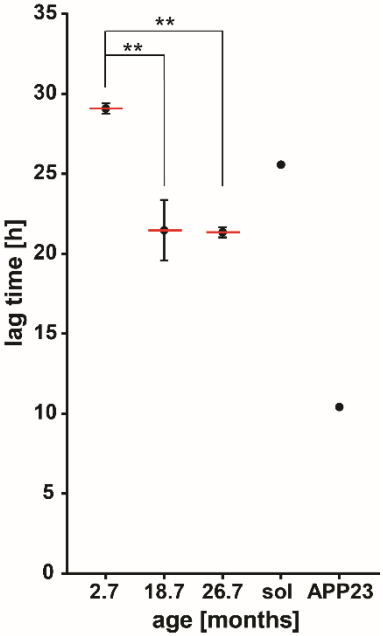

*Figure 3.7: Insoluble protein extracts from aged wild-type mouse brains seed Aβ aggregation in vitro (reproduced from Frontiers article). Lag times measured for Aβ aggregation in the presence of 0.001 µg detergent-insoluble protein extracts from wild-type mouse brains at different ages. Mean values (red lines) with respective SEM of three biological replicates (each including five technical replicates) from on average 2.7 month-, 18.7 month- and 26.7 month-old mouse brain insoluble extracts. Lag time of an 18 month-old mouse brain soluble extract (sol, negative control) and a 20 month-old mouse brain insoluble extract from an APP23 transgenic mouse (APP23, positive control). One-way ANOVA: 2.7 months vs. 18.7 months **p= 0.0073, 2.7 months vs. 26.7 months **p= 0.0067.*

3.1.7 Formation of Aβ plaques in APP23 transgenic mouse brains after injection of insoluble proteins from aged mouse brains

To analyze whether insoluble proteins can also seed Aβ aggregation *in vivo,* detergent-insoluble proteins from young or old wild-type mouse brains were injected into the hippocampus of young (3 months of age) APP23 transgenic mice. In transgenic mouse models, injection of whole brain extracts containing Aβ seeds is sufficient to lead to the formation and spreading of Aβ plaques (Kane et al. 2000; Meyer-Luehmann et al. 2006), whereas after injection of whole brain extracts from control patients without AD or wild-type mice no Aβ plaques were observed. An extract containing an enrichment of insoluble proteins from wild-type mouse brains was not analyzed so far. Six months after injection of detergent-insoluble proteins from 18.3 month-old wild-type mouse brains, the formation of Aβ plaques can be observed in three out of five mice (Figure 3.8, left). Injection of insoluble proteins from young mouse brains (2.5 months) did not lead to plaque formation (Figure 3.8, right). Only in one mouse a possible plaque formation can be seen (Figure 3.8 zoom, blue arrow). These results suggest, that insoluble proteins from old wild-type mouse brains seed Aβ aggregation *in vivo* although only a few plaques were observed.

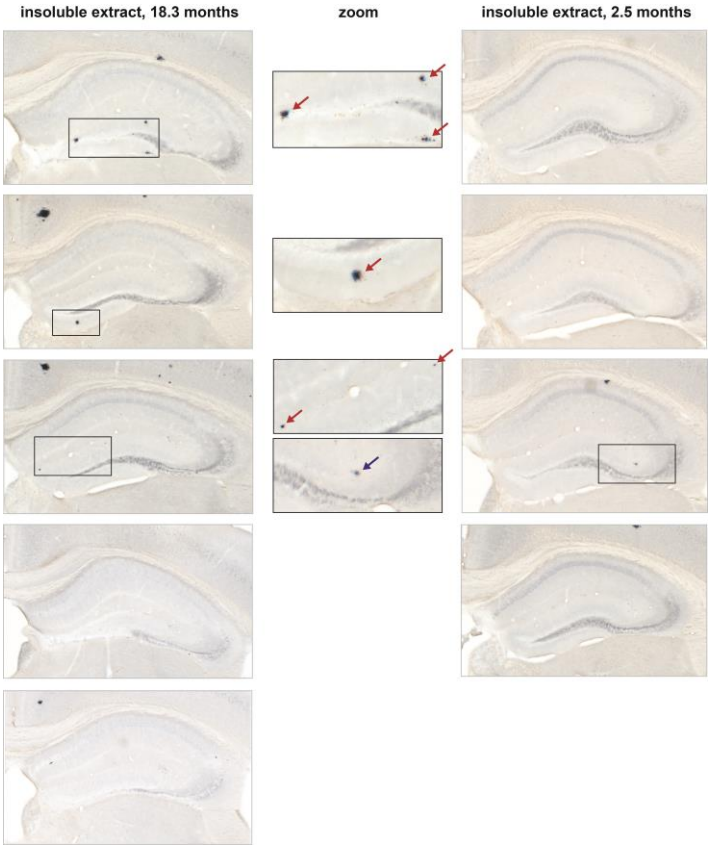

Figure 3.8: Insoluble protein extracts from aged wild-type mouse brains seed Aβ aggregation in vivo.
Left: Hippocampi of five APP23 transgenic mice injected with insoluble protein extracts from 18.3 month old mice.
Middle: Zoom, formation of Aβ plaques. Red arrows indicate plaques developed after injection of insoluble protein extracts from old mice, blue arrow indicates possible plaque formation after injection of insoluble protein extracts from young mice.
Right: Hippocampi of four APP23 transgenic mice injected with insoluble protein extracts from 2.5 month old mice (control).
All mice were three months of age when injected and were histologically analyzed six months after injection.

3.1.8 Identification of insoluble proteins in wild-type mouse brains

Because of the demonstrated seeding potential of proteins that were highly insoluble with age, a quantitative mass spectrometry study was performed to identify the change in aggregation with age of the insoluble proteins in wild-type mouse brains. Detergent-insoluble proteins of three young (2.7 months on average) and three old (18.7 months on average) wild-type mouse brains were probed with heavy or light dimethyl-labeling to analyze whether each protein shows an increase or decrease in insolubility with age (total protein staining of the analyzed protein extracts is shown in Figure 3.9). During one measurement insoluble protein extracts from one young mouse brain and from one old mouse brain were compared. 617 quantifiable aggregation-prone proteins were identified in all three biological replicates. Figure 3.10A shows a comparison of the log2-transformed ratios of insoluble proteins from young versus old mice between each replicate. Because the ratios are normalized, only changes in insolubility with age versus the mean change can be analyzed. With the data presented here, just a few changes compared to the mean can be observed. To analyze if the replicates can be correlated to each other, the log2-transformed ratios of each insoluble protein from young mice versus old mice of two replicates were plotted against each other (Figure 3.10B-D). Independent of which replicates were compared no close correlation could be detected (Spearman $r < 0.15$). Already the total protein staining of the different insoluble protein extracts shows a high variability within the young mice and the old mice (Figure 3.9). Comparing two young mice with two aged mice, an increase in insolubility with age can be detected (Figure 3.9, left), but be-

tween another young and old mouse a decrease can be seen (Figure 3.9, right).

We identified 14 proteins within the top 25th percentile in all three replicates, i.e. with the highest change in aggregation with age. To analyze which proteins have the potential to seed Aβ aggregation, a knockdown of homologs of these mouse brain proteins in *C. elegans* in Aβ overexpressing worms and a subsequent motility analysis should be performed. 12 *C. elegans* homologs were identified. Interestingly, one of these proteins was TDP-1 (*C. elegans* homolog of TDP-43). TDP-43 has already been shown to cross-seed Aβ (Fang et al. 2014). But immunoblot detection with a TDP-43 antibody did not confirm the change in aggregation with age (data not shown). To analyze if a knockdown of homologs of mouse brain proteins with the highest increase in insolubility with age could influence the motility of Aβ overexpressing worms, a first experiment was performed with different control RNAi's and two different motility analysis programs (Appendix Table 6.1). During the comparison of minimum and maximum speeds of the worms subjected to control RNAi's a big difference within one control can be detected (for example a six-fold difference between minimum and maximum speed for HER-1 independently of the analysis program). For some videos only a few worms could be detected and analyzed by the programs. Even the adjustment of the parameters did not improve the analysis. Because the measurements with different control RNAi's were not reproducible, the motility analysis was not continued and the question whether proteins with the highest change in insolubility with age in mouse brains could be responsible for seeding Aβ aggregation could not be answered.

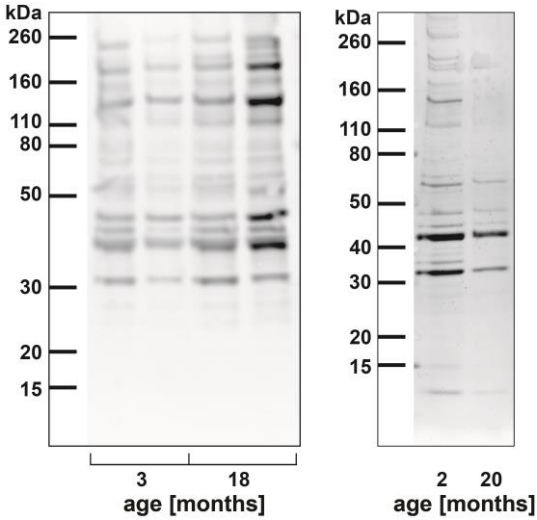

Figure 3.9: Total protein staining of insoluble protein extracts from young and old mice stained with Sypro Ruby protein blot stain.

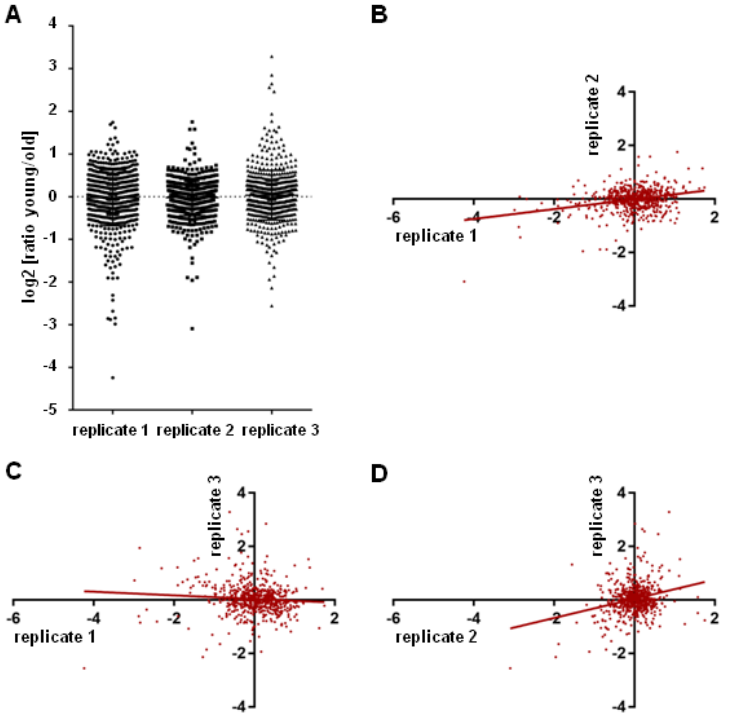

Figure 3.10: Quantitative mass spectrometry results of insoluble proteins of brains from young (2.7 months) versus old (18.7 months) mice. Three replicates with one insoluble protein extract from a young mouse brain and one insoluble protein extract from an old mouse brain each were measured.
A: Log2 ratio of insoluble proteins from young mouse brains versus old mouse brains for each replicate. Each point represents the ratio of one protein.
B-D: Correlation of log2 ratio of insoluble proteins from young mouse brains versus old mouse brains between the different replicates. Each point represents the ratio of one protein. B: Spearman r= 0.1475, C: Spearman r= -0.1454, D: Spearman r= 0.1349.

3.1.9 Summary

To summarize, it was shown in 3.1 that age-dependent protein aggregates can initiate Aβ aggregation and that this cross-seeding is conserved from nematodes to mammals. One of the late-aggregating proteins that is also a minor component in AD pathological aggregates, 14-3-3 (PAR-5), was demonstrated to enhance paralysis of worms overexpressing Aβ and PAR-5. Moreover, an increase in specific PTMs was detected in insoluble proteins with age in *C. elegans*.

3.2 Investigation whether rapidly-aggregating proteins seed the aggregation of other proteins

In parallel to the finding that age-dependent protein aggregates seed the aggregation of Aβ, as demonstrated in 3.1, our goal was to investigate whether rapidly-aggregating proteins could lead to the aggregation of other non-disease related proteins in *C. elegans*. The idea was to chemically crosslink an early-aggregating protein, identified in 3.1.3, together with its co-aggregating proteins, to purify them and to identify them by mass spectrometry.

During the preparation of the *C. elegans* samples for the mass spectrometry analysis and the evaluation of the mass spectrometry results described in 3.1, a tandem-affinity purification strategy in denaturing conditions was established to isolate and identify rapidly-aggregating proteins together with their co-aggregates. The aggregation-prone protein RHO-1, a Rho GTPase orthologous to transforming protein RhoA in mammals, is known to aggregate fast when it is overexpressed in *C. elegans* (already at day 1). RHO-1 was tagged with a tandem-affinity tag combining a histidine tag (hexa-histidine) for Nickel affinity purification with a biotinylation sequence (avidin tag) for subse-

quent avidin purification (Schaffer et al. 2010; Tagwerker et al. 2006). The avidin tag is an artificial target motif for biotinylation by the *E. coli* biotin holoenzyme synthetase birA (Schaffer et al. 2010). To be able to purify protein aggregates, denaturing conditions (8 M urea) were needed. Therefore, the tandem-affinity tag was chosen, because it tolerates two-step purification under fully denaturing conditions (Tagwerker et al. 2006). The first purification step was shown to efficiently remove endogenous biotinylated proteins. With the second purification step with avidin beads, highly purified samples should be achieved because of the high affinity between biotin and avidin. The avidin tag published by (Schaffer et al. 2010) was used for the study presented here, because they demonstrated a succesfull purification of proteins with the avidin tag from *C. elegans* lysates and the subsequent mass spectrometry analysis. Additionally, the worms expressed birA under the same promoter as the tagged protein. Therefore, tissue specificity is obtained and proteins could be selectively purified from a target cell type. To collect large numbers of individuals, *C. elegans* overexpressing the tagged RHO-1 together with the biotinylation enzyme birA were cultured in liquid. We postulated that during aging the rapidly-aggregating protein (potential seeding protein) co-aggregates with other proteins. To identify the co-aggregating proteins, our plan was to remove the detergent-soluble proteins from a homogenate of worms overexpressing the tagged RHO-1 and chemically crosslink the detergent-insoluble proteins (Figure 3.11). RHO-1 together with the crosslinked proteins would then be solved in urea and purified with Nickel affinity chromatography to be able to identify the proteins by mass spectrometry in the end.

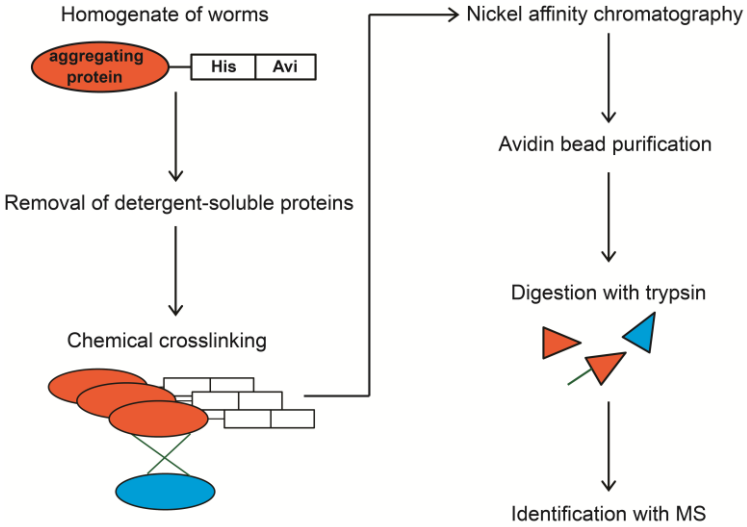

Figure 3.11: Schematic showing the procedure of chemical crosslinking of rapidly-aggregating proteins (red) (tagged with a histidine-avidin tag) with their co-aggregating proteins (blue), the subsequent purification, digestion with trypsin and identification of tryptic peptides with mass spectrometry.

3.2.1 Purification of RHO-1 without crosslinking

3.2.1.1 Purification with imidazole

To establish the purification protocol for rapidly-aggregating proteins, RHO-1 without crosslinking was purified with Nickel affinity chromatography using a high imidazole concentration in the elution buffer as it is recommended for the purification with the nickel column. Figure 3.12 shows an immunoblot of the first purification of RHO-1 detecting biotinylated avidin of the histidine-avidin tag of RHO-1 in the fraction, that was loaded onto the column (load), in the fractions that were collected during the sample was loaded (flow through) and during the column was washed (wash) and in the elution fractions (number three to

number nine). Because a high protein amount of RHO-1 can be detected in the flow through fractions, a lot of RHO-1 did not bind to the column. One possibility is that the protein amount was too high so that the column could not bind additional proteins anymore. Moreover, it can be seen that RHO-1 was washed away from the column, which means that it was not bound properly. Performing the elution with a linear gradient to a high imidazole concentration resulted to a broad elution peak with many fractions containing RHO-1. It seemed like RHO-1 was continuously washed and eluted from the column. Most of RHO-1 was eluted with 28% elution buffer (145 mM imidazole, fraction number E6).

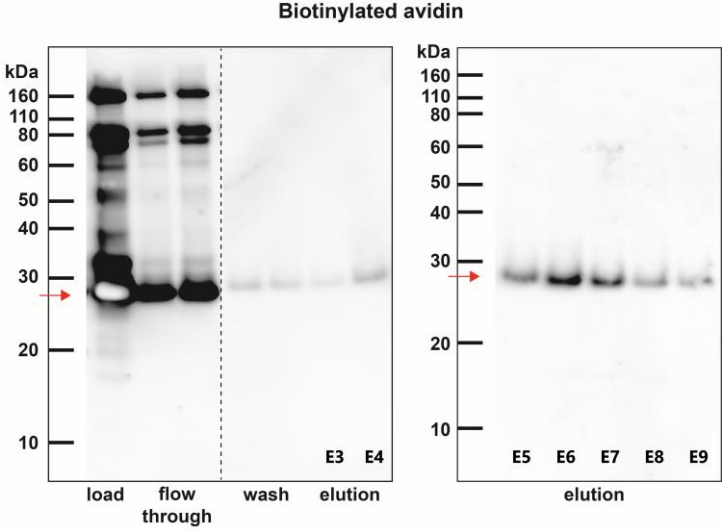

Figure 3.12: Purification with Nickel affinity chromatography of RHO-1 with histidine-avidin tag. Elution was performed with a linear gradient to 500 mM imidazole. Shown is an immunoblot detecting biotinylated avidin in the collected fractions. Load: Insoluble protein extract from C. elegans overexpressing RHO-1 that was loaded on the column. Flow through: First two out of 20 fractions that were collected during the extract was loaded on the column. Wash: First two out of 10 fractions that were collected during the column was washed. Elution: Seven out of 20 eluted samples. E3 to E9: Elution fractions number three to nine. Arrow: RHO-1 with histidine-avidin tag.

3.2.1.2 Purification under harsh conditions

Because the first purification of RHO-1 with a high imidazole concentration in the elution buffer led to a broad elution of RHO-1, a different purification was used to establish the purification protocol for rapidly-aggregating proteins. RHO-1 without cross-linking was purified with Nickel affinity chromatography using a harsh elution buffer published by (Tagwerker et al. 2006). They state that stringent purification conditions remove non-

crosslinked, interacting proteins. Therefore, unspecific binding is reduced. Figure 3.13A shows an immunoblot with the collected fractions of the purification of RHO-1 with the published buffers. In Figure 3.13B a silver stained SDS gel of another purification with the same conditions can be seen. Because there is less RHO-1 in the flow through fractions visible, a lot of RHO-1 was bound to the column. Moreover, most of RHO-1 can be eluted in only two fractions with the harsh elution buffer. The elution fractions were very pure, because there were only a few other faint bands visible (Figure 3.13B). Most of RHO-1 was eluted with 83% or 78% elution buffer (Figure 3.13A fraction number E17 or Figure 3.13B fraction number E16). In general, this second purification protocol seemed to be useful to purify rapidly-aggregating proteins.

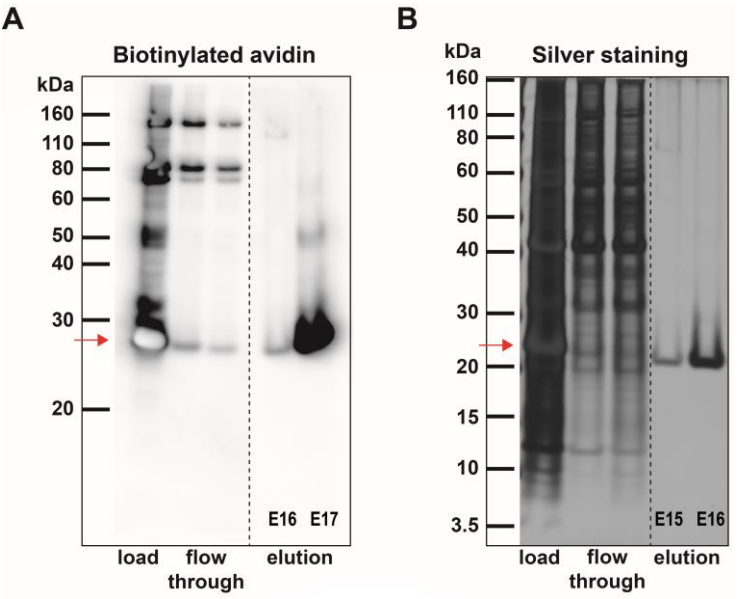

Figure 3.13: Purification with Nickel affinity chromatography of RHO-1 with histidine-avidin tag. Elution was performed with a linear gradient and harsh conditions (elution buffer with 2% SDS, 10 mM EDTA, 100 mM Tris pH 4.3). Load: Insoluble protein extract from C. elegans overexpressing RHO-1 that was loaded on the column. Flow through: First two out of 20 fractions that were collected during the extract was loaded on the column. Elution: Two out of 20 eluted samples. Arrow: RHO-1 with histidine-avidin tag.
A: Immunoblot detecting biotinylated avidin in the collected fractions. E16, E17: Elution fractions number 16 and 17.
B: Silver stained SDS gel with collected fractions of another purification. E15, E16: Elution fractions number 15 and 16.

3.2.2 Purification of RHO-1 crosslinked with 0.4% Para-Formaldehyde (PFA)

After the establishment of the purification protocol under harsh conditions, RHO-1 was crosslinked with 0.4% Para-Formaldehye (PFA), which is a common crosslinker and very reactive towards

primary amines. But two different problems appeared. First, crosslinked RHO-1 could not be eluted from the column (Figure 3.14A and B). The immunoblot detection shows only faint bands in the elution fractions (Figure 3.14A). With a silver staining only some bigger proteins (~ 60 kDa) are visible (Figure 3.14B). Even with the harsh elution buffer, RHO-1 was still bound to the column.

To investigate what happened with RHO-1 after crosslinking, resolving in urea and centrifugation, the final pellet (not solubilized by urea) was compared with the final pellet without crosslinking of RHO-1 and the following second problem was detected: A lot of RHO-1 remained in the urea-insoluble pellet fraction compared to the fraction without crosslinking (Figure 3.14C). Therefore, it is likely that most of RHO-1 becomes so insoluble after crosslinking that it cannot be disrupted by urea.

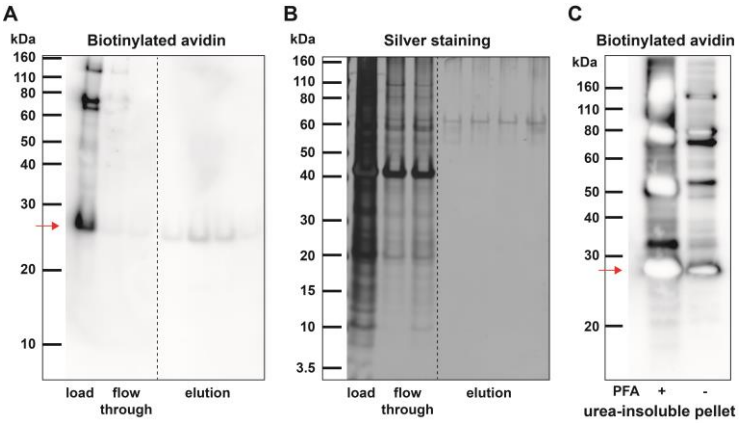

Figure 3.14: Purification with Nickel affinity chromatography of RHO-1 with histidine-avidin tag crosslinked with 0.4% PFA. Elution was performed with a linear gradient and harsh conditions (elution buffer with 2% SDS, 10 mM EDTA, 100 mM Tris pH 4.3). A-B: Load: Crosslinked insoluble protein extract from C. elegans overexpressing RHO-1 that was loaded on the column. Flow through: First two out of 20 fractions that were collected during the extract was loaded on the column. Elution: Four out of 20 eluted samples. Arrow: RHO-1 with histidine-avidin tag.
A: Immunoblot detecting biotinylated avidin in the collected fractions.
B: Silver stained SDS gel with collected fractions.
C: Immunoblot detecting biotinylated avidin in the urea-insoluble pellet from the insoluble protein extraction after crosslinking and centrifugation (+) or in the urea-insoluble pellet without crosslinking (-).

3.2.3 Purification of RHO-1 crosslinked with Disuccinimidyl glutarate (DSG)

Because the crosslinking with PFA prevented the solubilisation of aggregated RHO-1 proteins in urea, we investigated whether another crosslinker would be more appropriate. Disuccinimidyl glutarate (DSG) reacts with primary amines on the N-termini and ε-amine of lysine residues forming an amide bond. Concentrations between 0.25 mM and 0.0025 mM were used. The crosslinked detergent-insoluble protein extracts and the urea-

insoluble pellets were analysed with an immunoblot, shown in Figure 3.15. The lowest protein amount of detergent-insoluble proteins and the highest protein amount in the urea-insoluble pellet were detected in the sample with the highest DSG concentration suggesting too high crosslinking similar to the results with PFA. When comparing the sample without crosslinking with the samples with low DSG concentrations, no difference can be seen, which raised the question whether the crosslinking did not work with low concentrations. Therefore, a purification was performed with the extract crosslinked with the highest concentration (0.25 mM DSG), but no improvement could be detected in comparison to the treatment with PFA. Nothing could be seen in the elution fractions, which suggests that RHO-1 could not be eluted from the column (Figure 3.16) and there was still a high amount of RHO-1 in the urea-insoluble pellet fraction, as already shown in Figure 3.15B.

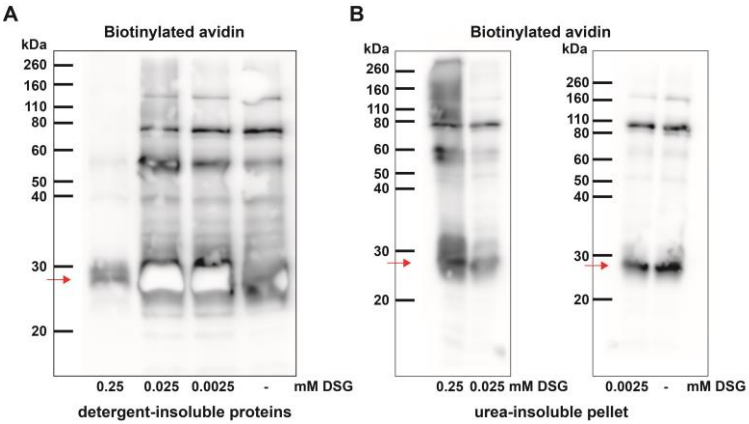

Figure 3.15: Immunoblots detecting biotinylated avidin of histidine-avidin tag of crosslinked RHO-1. Arrow: RHO-1 with histidine-avidin tag.
A: Detergent-insoluble protein extracts from C. elegans overexpressing RHO-1 after crosslinking with different concentrations of DSG or without crosslinking (-).
B: Urea-insoluble pellet from the insoluble protein extraction after cross-linking with different concentrations of DSG or without crosslinking (-).

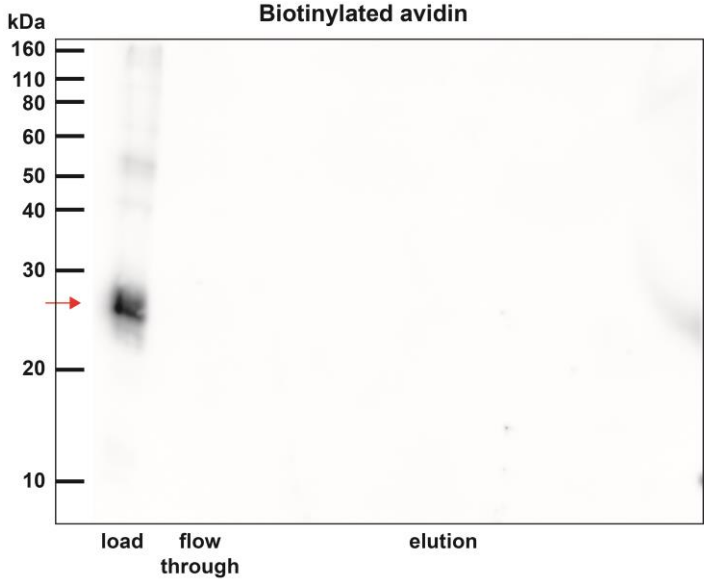

Figure 3.16: Purification with Nickel affinity chromatography of RHO-1 with histidine-avidin tag crosslinked with 0.25 mM DSG. Elution was performed with a linear gradient and harsh conditions (elution buffer with 2% SDS, 10 mM EDTA, 100 mM Tris pH 4.3). Shown is an immunoblot detecting biotinylated avidin in the collected fractions. Load: Crosslinked insoluble protein extract from C. elegans overexpressing RHO-1 that was loaded on the column. Flow through: First two out of 20 fractions that were collected during the extract was loaded on the column. Elution: Nine out of 20 eluted samples. Arrow: RHO-1 with histidine-avidin tag.

3.2.4 Summary

To summarize, RHO-1 aggregates solved in urea can be purified with Nickel affinity chromatography using a harsh elution buffer. After crosslinking of RHO-1 it could not be eluted from the column anymore under harsh conditions independent of the type and the amount of the crosslinker. Moreover, with increasing amounts of crosslinker most of RHO-1 becomes so insoluble that

it cannot be disrupted by urea. Because the problems with the crosslinking of RHO-1 could not be solved, we were not able to analyze co-aggregating proteins.

4 Discussion

4.1 Identifying age-dependent heterologous seeds for amyloid-β aggregation

This chapter includes a part of the discussion reproduced from:

Groh N, Bühler A, Huang C, Li KW, van Nierop P, Smit AB, Fändrich M, Baumann F and David DC (2017) Age-Dependent Protein Aggregation Initiates Amyloid-β Aggregation. Front. Aging Neurosci. 9:138. Doi: 10.3389/fnagi.2017.00138

The discovery of widespread protein aggregation with age has raised the question whether these assemblies influence disease-related protein aggregation. The study described here demonstrates, that a direct interaction between insoluble proteins from aged *C. elegans* or aged mouse brains initiates Aβ aggregation *in vitro*. These results could have important implications for our understanding of the initial pathogenesis steps in AD, particular in late-onset cases.

A recent study revealed that wild-type spinal cord homogenates injected into transgenic mice expressing α-synuclein with the A53T mutation induced early α-synuclein pathology (Sacino et al. 2016). As cortical homogenates from wild-type mice had no effect, the authors speculate that higher levels of myelinated white matter in the spinal cord could be responsible. A myelin component is unlikely to be the seeding agent in the data presented here. First, a very stringent procedure was performed to isolate highly-insoluble proteins while removing the lipids using sucrose flotation and then high concentrations of strong detergents including SDS. Second, brain homogenates without spinal cord, brain stem and cerebellum were used. Third, the effect

observed is age-dependent and therefore unlikely to be due to the basic composition of the brain tissue used. Fourth, numbers of oligodendrocytes decrease with age (Pelvig et al. 2008). Therefore, it is reasonable to conclude that the induction of Aβ seeding in the present study is due to highly-insoluble proteins rather than a lipid contaminant. In addition, the findings presented here cannot be explained by age-related changes in endogenous Aβ (Mahler et al. 2015) as *C. elegans* lack homologs of BACE and no Aβ-like peptides have been detected.

Previous *in vitro* studies have shown cross-seeding between Aβ and other disease-associated aggregating proteins including α-synuclein, scrapie prion protein (PrP^{Sc}), human islet amyloid polypeptide (hIAPP), tau and TAR DNA-binding protein 43 (TDP-43) (Fang et al. 2014; Morales, Moreno-Gonzalez, and Soto 2013; Vasconcelos et al. 2016). Interestingly, acetylcholinesterase, a minor component in Aβ plaques, was also shown to accelerate Aβ aggregation *in vitro* (Inestrosa et al. 1996). This raised the possibility that minor components in disease-associated aggregates could also play a role in seeding the main component. Recently, this hypothesis has gained support with the discovery that these minor components are significantly over-represented in the age-dependent insoluble proteome (David et al. 2010). Therefore, a large number of minor components are themselves aggregation-prone. The present data support the notion that misfolding and aggregation of minor components during age constitute heterologous seeding events for disease-associated aggregation. A recent study examined the expression levels of minor components found in plaques and NFTs in healthy brains (Freer et al. 2016). Interestingly, the regions known to be the first affected by NFT pathology in AD displayed higher levels of these minor aggregate components compared to non-affected

regions. Of the 16 minor components identified as late- or early-aggregating proteins in the analysis presented here, seven out of 10 evaluated in the study by (Freer et al. 2016) followed this pattern. Therefore, it is possible that higher levels of age-dependent seeds accumulate in these regions and induce tissue-specific vulnerability to disease protein aggregation in AD. Overall, it will be important to determine which proteins and in which locations have seeding activity.

The presented proteomic timeline analysis highlights several minor plaque or NFT components that should be prime candidates as initiators of Aβ or tau seeding events to be investigated in future studies. One of these candidates, 14-3-3, has already been confirmed as a heterologous seed for tau aggregation (Li and Paudel 2016). It was also shown that a knockdown of 14-3-3 rescued Aβ toxicity in *C. elegans* (Ayyadevara, Balasubramaniam, Parcon, et al. 2016). Importantly, the present study shows that 14-3-3 overexpression accelerated Aβ toxicity in a *C. elegans* model for Aβ aggregation. With a staining of these paralyzed double-transgenic worms with an amyloid-specific dye (K114) or an Aβ-specific antibody (6E10) no obvious difference in the abundance of Aβ was detected compared to the staining of worms solely overexpressing Aβ (data not shown). However, the staining was variable between worms in each strain. A quantification of the fluorescence intensity was also not possible, because of the high background. To analyze whether paralyzed worms overexpressing Aβ together with the *C. elegans* homolog of 14-3-3 (PAR-5) have more Aβ aggregates than worms solely overexpressing Aβ and whether a co-localization of Aβ and PAR-5 could be observed, the staining has to be improved. In addition, we did not see any obvious differences in the insoluble Aβ levels detected by western blot. For the future, the next step would be

to analyze whether insoluble protein extracts of worms overexpressing PAR-5 accelerate the aggregation of Aβ *in vitro*. Moreover, it would be interesting to perform an *in vitro* tau seeding assay to analyze whether detergent-insoluble protein extracts from aged wild-type individuals can also seed the aggregation of tau *in vitro*.

Another possibility to explain why insoluble proteins become effective seeds with age is that changes in the structure of these proteins could occur. It would be interesting to analyze whether minor plaque or NFT components, which were identified as late-aggregating proteins, are in an amyloid state.

As some seeding proteins may not be sufficiently abundant to be detected in disease aggregates, it will be relevant to investigate the other late-aggregating proteins as well as early-aggregating proteins that continue to become more insoluble with age. With a first analysis presented here we wanted to investigate whether a knockdown of two different early-aggregating proteins that continued to aggregate strongly at day 10 and day 14 (NEX-1 and LEC-5) would rescue the reduced motility of Aβ overexpressing worms. But motility measurements at different time points of Aβ overexpressing worms subjected to RNAi against NEX-1 or LEC-5 with the Parallel Worm Tracker software (Ramot et al. 2008) led to contrary results. Already for the controls different results were obtained, with one control showing a decrease in motility with age as expected and one showing an increase. The main problem was, that very often only a few worms were detected automaticaly by the software. This resulted to big differences in speed between the single tracks and less reproducibility. We tried to adjust the minimum and maximum size of an object that will be identified as a single worm, as suggested in the publication. But even the adjustment of the software parameters did not

improve the detection of the worms. The reason why we wanted to establish a motility assay was to be able to analyze a lot of different conditions in short time. For the assay Aβ overexpressing worms were used that were kept at 20°C to delay the onset of paralysis, but the motility defect was not clear enough with age. The model is only useful to study paralysis rates after switching the worms to 25°C at day 1. Because the worms start to paralyze one day after the temperature shift, we are not able to see effects of preventing age-dependent protein aggregation by RNAi. Still, it would be interesting to continue with the analysis of late-aggregating proteins (and also early-aggregating proteins that continue to become more insoluble with age). In particular, proteins associated with the eight pathways highlighted by the IPA analysis should be promising candidates. For future studies a paralysis assay could be performed as demonstrated for the worms overexpressing Aβ and PAR-5. Therefore, double-transgenic worms overexpressing Aβ and one of the candidates need to be generated to analyze whether an increase in paralysis can be seen. Then the respective protein would be a good candidate for a dangerous aggregating protein that seed Aβ aggregation.

Moreover, the finding that aggregating proteins co-localize would help to demonstrate that they interact with each other. To analyze whether co-localization between Aβ and an inherent aggregating protein in *C. elegans* could be observed, strains expressing Aβ and a protein that is known to aggregate in the body-wall muscle should be generated. Preliminary results suggest that low numbers of Aβ aggregates and variability between animals will make the analysis challenging (data not shown).

Another point that should be considered is the possibility that post-translational modifications (PTMs) occurring with age in-

fluence the seeding ability of late-aggregating proteins as well as early-aggregating proteins that continue to become more insoluble with age. A number of PTMs have been identified in disease-associated aggregates, and a recent study detected carbonylation in the mouse age-dependent insoluble proteome (Tanase et al. 2016). (Tanase et al. 2016) determined, that PTMs are conductive of aggregate formation. PTMs could lead to unfolding of proteins and exposure of their hydrophobic sites which increases their tendency to aggregate. In humans, phosphorylation of tyrosine residues, catalyzed by tyrosine kinases, plays a role in cellular signal transduction (as described in the human metabolome database (Wishart et al. 2013)). Phosphorylation of tyrosines of proteins with age could change their structural stability leading to their unfolding and at least to their aggregation. Ubiquitination directs proteins for degradation by the proteasome or by lysosomes (as described in 1.). Ubiquitinated unfolded proteins often assemble in large aggregates. The present data demonstrate by western blot analysis, that insoluble proteins from *C. elegans* show an increase in phosphorylation of tyrosines and ubiquitination with age. Moreover, three other PTMs were analyzed: dimethylation of arginines, citrullination (irreversible conversion of arginine into citrullin) and phosphorylation of serines and threonines. No difference could be detected. However, only a few faint bands were visible. Either the western blot protocol has to be improved or different antibodies should be tried out. For the future it would be interesting to analyze whether other PTMs could be detected or whether these findings could be confirmed with the insoluble proteins of mouse brains. Besides the identification of changes in aggregation with age of the insoluble mouse brain proteome by mass spectrometry as discussed later, changes in PTMs with age could be analyzed. For the PTM analysis of insoluble proteins of young and

aged mouse brains by mass spectrometry, the results presented here cannot be used, because the methodology to analyze PTMs is different including an enrichment strategy of the proteins or peptides.

Because of the demonstrated seeding potential of highly insoluble proteins from aged mouse brains, we performed a quantitative mass spectrometry study of young and aged wild-type mouse brains to identify the change in aggregation with age of the insoluble proteome. Overall, there was no general increase in insolubility with age and our results suggest variabilities in the insoluble protein fraction preparation. After normalization, we found very little correlations between fold changes in levels of insoluble proteins between the three replicates. This is similar to the previous findings where only a limited number of proteins changing their insolubility with age was observed (Ottis et al. 2013). (Ottis et al. 2013) demonstrated, that absolute changes in the levels of insoluble proteins of hippocampal proteomes from rats were small compared to the findings in the whole *C. elegans* insoluble proteome. Moreover, (Walther and Mann 2011) performed a proteomic analysis of three brain regions as well as heart and kidney in mice aged five or 26 months without any enrichment for insoluble proteins. They showed that mean protein abundance changes of more than twofold between young and old mice were detected in less than 1% of all proteins and very few of these were statistically significant. Still, to continue with the mass spectrometry results presented here, 14 proteins that aggregate the most with age in all three replicates were determined with 12 homologues in *C. elegans*. One of the identified proteins was TDP-43. Inclusions of TDP-43 are hallmarks of frontotemporal lobar dementia (FTLD) and amyotrophic lateral sclerosis (ALS). Intriguingly, human TDP-43 was shown to form

oligomers that cross-seed Aβ to form amyloid oligomers (Fang et al. 2014). Because these proteins seemed to be interesting candidates for seeding, the goal was to perform a motility analysis of Aβ overexpressing worms subjected to RNAi against homologues of all 12 proteins. During the first experiment only worms subjected to control RNAi's were analyzed with two different motility analysis programs. The measured speeds were variable and not reproducible within the same group and differed between the worms subjected to different control RNAi's independent of the software used, as discussed previously. Therefore, the analysis was not continued with the candidates.

An important aspect to be addressed was to determine the seeding activity of age-dependent protein aggregation *in vivo*. Therefore, an established mouse model for Aβ seeding was used, in which past experiments showed that intracerebral injection of Aβ-rich brain extracts in young APP-transgenic mice induced Aβ plaque formation prior to the appearance of endogenous Aβ deposits (Meyer-Luehmann et al. 2006). In the present study insoluble protein extracts from aged mouse brains were injected. After six months the formation of some Aβ plaques was observed in three out of five mice. Of note, it was unclear whether this *in vivo* model would be sufficiently sensitive to detect heterologous seeding by the age-dependent insoluble proteome within the time window preceding the emergence of endogenous plaques and cerebral amyloid-β angiopathy. Indeed, the low amount of detected Aβ plaques could be explained by the *in vitro* data showing a reproducible but relatively low seeding activity compared to Aβ seeds and therefore successful *in vivo* seeding studies may require repeated injections of insoluble extracts and/or very long incubation times.

In summary, the study described here shows that protein aggregates formed during normal aging in *C. elegans* and in mouse brains initiate Aβ aggregation *in vitro*. In agreement with the late onset of neurodegeneration in humans, cross-seeding activity appears in the later stages of life in *C. elegans*. The study demonstrates that several minor components identified previously in NFTs and amyloid plaques in AD are prone to aggregate with age. Additionally, overexpression of one of these proteins, PAR-5 (*C. elegans* homolog of 14-3-3), accelerates Aβ toxicity in *C. elegans*.

Together, the present findings emphasize the need to understand better why protein insolubility is prevalent in older age and how the cellular quality-control systems fail to prevent it. Abrogating the formation of heterologous seeds could significantly reduce disease-associated seeding events and delay the onset of AD. As perspective it would be interesting to map the aggregating proteome throughout the brain in healthy individuals and in patients with neurodegeneration to clarify whether aging seeds associate with specific disease types in specific anatomical areas.

4.2 Investigation whether rapidly-aggregating proteins seed the aggregation of other proteins

A variety of neurodegenerative diseases are associated with the aggregation of specific proteins. Moreover, aging is a major risk factor for neurodegeneration. In recent years protein aggregation with age, in the absence of disease, has been investigated by several groups (David et al. 2010; Reis-Rodrigues et al. 2012; Walther et al. 2015). In parallel to the first study presented here, showing that age-dependent protein aggregates seed the aggregation of Aβ (3.1), a second study was performed to investigate

whether rapidly-aggregating proteins lead to the aggregation of other non-disease related proteins in *C. elegans*. Our goal was to crosslink proteins in an aggregate, purify them in denaturing conditions and to identify the co-aggregating proteins by mass spectrometry. Finally, we intended to quantify changes in co-aggregating proteins with age. To establish the protocol for tandem-affinity purification under denaturing conditions for the isolation and identification of rapidly-aggregating proteins with co-aggregating proteins, an aggregation-prone protein was used. RHO-1, a Rho GTPase orthologous to transforming protein RhoA in mammals, is known to aggregate fast when it is overexpressed in *C. elegans.* Therefore, transgenic worms were generated over-expressing RHO-1 tagged with a tandem-affinity tag combining a histidine tag for Nickel affinity purification with a biotinylation sequence (avidin tag) for subsequent avidin purification (Schaffer et al. 2010; Tagwerker et al. 2006).

First of all, an insoluble protein extraction with the homogenate of RHO-1 overexpressing worms and a subsequent purification of RHO-1 with Nickel-affinity chromatography was performed. A well-established elution buffer with a high imidazole concentration was used. In theory, imidazole competes with the histidine tag of the protein for the binding to nickel and therefore lead to the elution of the protein that is bound on the column. The first purification presented here resulted to a broad elution of RHO-1 in many fractions. To analyze whether this purification method could be used for other proteins, the purification of KIN-19 (a serine/threonine kinase orthologous to human Casein Kinase I), that is also known to aggregate fast if it is overexpressed in *C. elegans*, was performed. But, as a preliminary result, KIN-19 could not be eluted from the column (data not shown). Because using high imidazole concentrations led to a broad elution of

RHO-1 and another protein, KIN-19, could not be eluted, a different protocol with harsh conditions was chosen (Tagwerker et al. 2006). Using the harsh elution buffer, we were able to elute RHO-1 in only a few fractions. Next, RHO-1 was chemically crosslinked with its co-aggregates with the common crosslinker PFA (Sutherland, Toews, and Kast 2008) and purified as established for RHO-1 without crosslinking under harsh conditions. But the following two problems appeared: First, the protein RHO-1 could not be eluted from the column anymore. The elution buffer contained EDTA which removes the nickel ions from the column and therefore should also remove RHO-1 that was bound with its histidine tag to nickel. But in the elution fractions no RHO-1 could be detected. PFA is a strong crosslinker. Even with low PFA amounts it seemed that most of RHO-1 was getting highly insoluble and accumulates to big aggregates (together with the co-aggregates) that stick on the column and cannot be removed. The assumed formation of large intractable aggregates could also lead to the second problem: a high amount of crosslinked RHO-1 could not be loaded onto the column because the aggregates cannot be disrupted, even with high urea concentrations.

To continue, the second crosslinker DSG was used, which also reacts with primary amines like PFA, but the results could not be improved. Still, we were not able to elute RHO-1 from the column or to get more RHO-1 aggregates solved before loading it onto the column. Additionally, lower DSG concentrations were used, but no crosslinking could be observed anymore.

To conclude, the demonstrated purification protocol under harsh conditions can be used to purify non-crosslinked RHO-1, but the protocol is not applicable to crosslinked proteins. For future studies the following possibilities are suggested: First, another crosslinker could be tried out that is reactive to different groups

compared to PFA or DSG, for example Bis(maleimido)hexane (BMH) that crosslinks sulfhydryl groups. Second, to avoid unspecific crosslinking, the pellet after removal of detergent-soluble proteins could be diluted in a low amount of urea (1 M) before crosslinking and then the crosslinked proteins are solubilized with the high amount of urea (8 M). Another possibility is to perform the crosslinking already with the detergent-soluble proteins. This could help to avoid the formation of huge crosslinked aggregates that cannot be disrupted by urea anymore.

(Ayyadevara et al. 2015) isolated and characterized protein components of Q40 aggregates using a *C. elegans* strain expressing Q40 as a model of polyglutamine array diseases such as Huntington's. They found three Q40-associated proteins that were inferred to promote aggregation. The knockdown of one of these proteins, CRAM-1, reduced the Q40 aggregates up to 86%. Recently, it was shown that a knockdown of six human muscle-aggregate orthologs, that significantly decreased protein aggregate counts of Q40 and increased muscle mass, also consistently rescued worms from amyloid paralysis (Ayyadevara, Balasubramaniam, Suri, et al. 2016). (Fonte et al. 2002) used *C. elegans* expressing human Aβ to identify proteins that interact with intracellular Aβ and demonstrated that one of these proteins, HSP-16, co-localizes with Aβ. If co-aggregating proteins of RHO-1 were successfully identified it would be possible to overexpress RHO-1 together with an interesting candidate in *C. elegans* and evaluate co-localization or changes in their aggregation pattern. Moreover, lifespan analysis can be performed with worms overexpressing a rapidly-aggregating protein or with worms subjected to RNAi against a rapidly-aggregating protein to investigate whether a decrease or an increase in lifespan could be observed. Then, this protein (for example RHO-1) would be a

candidate for a dangerous aggregating protein that could lead to the aggregation of other proteins.

After the establishment, the protocol could be used to analyse whether early-aggregating proteins, identified in 3.1.3, lead to aggregation of other proteins. Co-aggregating proteins from young and aged worms could be compared by the quantification of differences in co-aggregation with age with mass spectrometry. Because we recently showed that KIN-19 accelerates PAB-1 (polyadenylate-binding protein 1) aggregation in *C. elegans* and that both proteins co-localize in large aggregates in double-transgenic animals (Lechler et al. 2017), we think that co-aggregation and seeding of protein aggregation by inherent-aggregating proteins can occur with age. Our goal is to discover proteins that lead to further aggregation as a reason for cellular dysfunction during aging. This investigation would give insights into the general mechanisms of protein aggregation with age and therefore could help to understand better the mechanisms involved in neurodegenerative diseases.

In conclusion, the results of both studies presented in this thesis help to advance our understanding of aging in the absence of disease. Moreover, the first study helps to understand the influence of aging on pathophysiology. How age-dependent protein aggregation and disease-associated protein aggregation influence each other, is still an open question. The first study supports the hypothesis of a direct interaction whereby disease-associated proteins and age-dependent aggregation-prone proteins co-aggregate. We were able to show that misfolded proteins aggregating with age form heterologous seeds that initiate Aβ aggregation *in vitro*. As a prevention strategy, heterologous

seeds could be targeted before the onset of the disease. In general, the investigation of physiological age-dependent protein aggregation could give insights into molecular and cellular mechanisms that regulate protein aggregation and could help to understand the effect of protein insolubility on organisms health.

5 References

Alvarez, A., R. Alarcon, C. Opazo, E. O. Campos, F. J. Munoz, F. H. Calderon, F. Dajas, M. K. Gentry, B. P. Doctor, F. G. De Mello, and N. C. Inestrosa. 1998. 'Stable complexes involving acetylcholinesterase and amyloid-beta peptide change the biochemical properties of the enzyme and increase the neurotoxicity of Alzheimer's fibrils', *J Neurosci*, 18: 3213-23.

Anckar, J., and L. Sistonen. 2011. 'Regulation of HSF1 function in the heat stress response: implications in aging and disease', *Annu Rev Biochem*, 80: 1089-115.

Antebi, A. 2007. 'Genetics of aging in Caenorhabditis elegans', *PLoS Genet*, 3: 1565-71.

Ayyadevara, S., M. Balasubramaniam, Y. Gao, L. R. Yu, R. Alla, and R. Shmookler Reis. 2015. 'Proteins in aggregates functionally impact multiple neurodegenerative disease models by forming proteasome-blocking complexes', *Aging Cell*, 14: 35-48.

Ayyadevara, S., M. Balasubramaniam, P. A. Parcon, S. W. Barger, W. S. Griffin, R. Alla, A. J. Tackett, S. G. Mackintosh, E. Petricoin, W. Zhou, and R. J. Shmookler Reis. 2016. 'Proteins that mediate protein aggregation and cytotoxicity distinguish Alzheimer's hippocampus from normal controls', *Aging Cell*, 15: 924-39.

Ayyadevara, S., M. Balasubramaniam, P. Suri, S. G. Mackintosh, A. J. Tackett, D. H. Sullivan, R. J. Shmookler Reis, and R. A. Dennis. 2016. 'Proteins that accumulate with age in human skeletal-muscle aggregates contribute to declines in muscle mass and function in Caenorhabditis elegans', *Aging (Albany NY)*, 8: 3486-97.

Ayyadevara, S., F. Mercanti, X. Wang, S. G. Mackintosh, A. J. Tackett, S. V. Prayaga, F. Romeo, R. J. Shmookler Reis, and J. L. Mehta. 2016. 'Age- and Hypertension-Associated Protein Aggregates in Mouse Heart Have Similar Proteomic Profiles', *Hypertension*, 67: 1006-13.

Balch, W. E., R. I. Morimoto, A. Dillin, and J. W. Kelly. 2008. 'Adapting proteostasis for disease intervention', *Science*, 319: 916-9.

Balchin, D., M. Hayer-Hartl, and F. U. Hartl. 2016. 'In vivo aspects of protein folding and quality control', *Science*, 353: aac4354.

Boersema, P. J., R. Raijmakers, S. Lemeer, S. Mohammed, and A. J. Heck. 2009. 'Multiplex peptide stable isotope dimethyl labeling for quantitative proteomics', *Nat Protoc*, 4: 484-94.

Bucciantini, M., E. Giannoni, F. Chiti, F. Baroni, L. Formigli, J. Zurdo, N. Taddei, G. Ramponi, C. M. Dobson, and M. Stefani. 2002. 'Inherent toxicity of aggregates implies a common mechanism for protein misfolding diseases', *Nature*, 416: 507-11.

Burkewitz, K., K. Choe, and K. Strange. 2011. 'Hypertonic stress induces rapid and widespread protein damage in C. elegans', *Am J Physiol Cell Physiol*, 301: C566-76.

Chondrogianni, N., K. Georgila, N. Kourtis, N. Tavernarakis, and E. S. Gonos. 2015. '20S proteasome activation promotes life span extension and resistance to proteotoxicity in Caenorhabditis elegans', *FASEB J*, 29: 611-22.

Corsi, A. K., B. Wightman, and M. Chalfie. 2015. 'A Transparent window into biology: A primer on Caenorhabditis elegans', *WormBook*: 1-31.

Cox, J., I. Matic, M. Hilger, N. Nagaraj, M. Selbach, J. V. Olsen, and M. Mann. 2009. 'A practical guide to the MaxQuant computational platform for SILAC-based quantitative proteomics', *Nat Protoc*, 4: 698-705.

David, D. C. 2012. 'Aging and the aggregating proteome', *Front Genet*, 3: 247.

David, D. C., N. Ollikainen, J. C. Trinidad, M. P. Cary, A. L. Burlingame, and C. Kenyon. 2010. 'Widespread protein aggregation as an inherent part of aging in C. elegans', *PLoS Biol*, 8: e1000450.

Demontis, F., and N. Perrimon. 2010. 'FOXO/4E-BP signaling in Drosophila muscles regulates organism-wide proteostasis during aging', *Cell*, 143: 813-25.

Dobson, C. M. 1999. 'Protein misfolding, evolution and disease', *Trends Biochem Sci*, 24: 329-32.

———. 2003. 'Protein folding and misfolding', *Nature*, 426: 884-90.

Eisenberg, D., and M. Jucker. 2012. 'The amyloid state of proteins in human diseases', *Cell*, 148: 1188-203.

Evans, T. C. 2006. 'Transformation and microinjection', *WormBook*: 1-15.

Fang, Y. S., K. J. Tsai, Y. J. Chang, P. Kao, R. Woods, P. H. Kuo, C. C. Wu, J. Y. Liao, S. C. Chou, V. Lin, L. W. Jin, H. S. Yuan, I. H. Cheng, P. H. Tu, and Y. R. Chen. 2014. 'Full-length TDP-43 forms toxic amyloid oligomers that are present in frontotemporal lobar dementia-TDP patients', *Nat Commun*, 5: 4824.

Fay, D. S. 2013. 'Classical genetic methods', *WormBook*: 1-58.

Fersht, A. R. 2000. 'Transition-state structure as a unifying basis in protein-folding mechanisms: contact order, chain topology, stability, and the extended nucleus mechanism', *Proc Natl Acad Sci U S A*, 97: 1525-9.

Fire, A., S. Xu, M. K. Montgomery, S. A. Kostas, S. E. Driver, and C. C. Mello. 1998. 'Potent and specific genetic interference by double-stranded RNA in Caenorhabditis elegans', *Nature*, 391: 806-11.

Fonte, V., W. J. Kapulkin, A. Taft, A. Fluet, D. Friedman, and C. D. Link. 2002. 'Interaction of intracellular beta amyloid peptide with chaperone proteins', *Proc Natl Acad Sci U S A*, 99: 9439-44.

Freer, R., P. Sormanni, G. Vecchi, P. Ciryam, C. M. Dobson, and M. Vendruscolo. 2016. 'A protein homeostasis signature in healthy brains recapitulates tissue vulnerability to Alzheimer's disease', *Sci Adv*, 2: e1600947.

Fritschi, S. K., A. Cintron, L. Ye, J. Mahler, A. Buhler, F. Baumann, M. Neumann, K. P. Nilsson, P. Hammarstrom, L. C. Walker, and M. Jucker. 2014. 'Abeta seeds resist inactivation by formaldehyde', *Acta Neuropathol*, 128: 477-84.

Guo, J. L., D. J. Covell, J. P. Daniels, M. Iba, A. Stieber, B. Zhang, D. M. Riddle, L. K. Kwong, Y. Xu, J. Q. Trojanowski, and V. M.

Lee. 2013. 'Distinct alpha-synuclein strains differentially promote tau inclusions in neurons', *Cell*, 154: 103-17.

Haass, C., and D. J. Selkoe. 2007. 'Soluble protein oligomers in neurodegeneration: lessons from the Alzheimer's amyloid beta-peptide', *Nat Rev Mol Cell Biol*, 8: 101-12.

Hartl, F. U., A. Bracher, and M. Hayer-Hartl. 2011. 'Molecular chaperones in protein folding and proteostasis', *Nature*, 475: 324-32.

Hernandez, F., R. Cuadros, and J. Avila. 2004. 'Zeta 14-3-3 protein favours the formation of human tau fibrillar polymers', *Neurosci Lett*, 357: 143-6.

Hortschansky, P., V. Schroeckh, T. Christopeit, G. Zandomeneghi, and M. Fandrich. 2005. 'The aggregation kinetics of Alzheimer's beta-amyloid peptide is controlled by stochastic nucleation', *Protein Sci*, 14: 1753-9.

Inestrosa, N. C., A. Alvarez, C. A. Perez, R. D. Moreno, M. Vicente, C. Linker, O. I. Casanueva, C. Soto, and J. Garrido. 1996. 'Acetylcholinesterase accelerates assembly of amyloid-beta-peptides into Alzheimer's fibrils: possible role of the peripheral site of the enzyme', *Neuron*, 16: 881-91.

Ishihama, Y., J. Rappsilber, and M. Mann. 2006. 'Modular stop and go extraction tips with stacked disks for parallel and multidimensional Peptide fractionation in proteomics', *J Proteome Res*, 5: 988-94.

Jean, L., B. Thomas, A. Tahiri-Alaoui, M. Shaw, and D. J. Vaux. 2007. 'Heterologous amyloid seeding: revisiting the role of acetylcholinesterase in Alzheimer's disease', *PLoS One*, 2: e652.

Jucker, M., and L. C. Walker. 2011. 'Pathogenic protein seeding in Alzheimer disease and other neurodegenerative disorders', *Ann Neurol*, 70: 532-40.

———. 2013. 'Self-propagation of pathogenic protein aggregates in neurodegenerative diseases', *Nature*, 501: 45-51.

Kane, M. D., W. J. Lipinski, M. J. Callahan, F. Bian, R. A. Durham, R. D. Schwarz, A. E. Roher, and L. C. Walker. 2000. 'Evidence for seeding of beta -amyloid by intracerebral infusion of Alzheimer brain extracts in beta -amyloid

precursor protein-transgenic mice', *J Neurosci*, 20: 3606-11.

Kaushik, S., and A. M. Cuervo. 2015. 'Proteostasis and aging', *Nat Med*, 21: 1406-15.

Khlistunova, I., J. Biernat, Y. Wang, M. Pickhardt, M. von Bergen, Z. Gazova, E. Mandelkow, and E. M. Mandelkow. 2006. 'Inducible expression of Tau repeat domain in cell models of tauopathy: aggregation is toxic to cells but can be reversed by inhibitor drugs', *J Biol Chem*, 281: 1205-14.

Klemmer, P., R. M. Meredith, C. D. Holmgren, O. I. Klychnikov, J. Stahl-Zeng, M. Loos, R. C. van der Schors, J. Wortel, H. de Wit, S. Spijker, D. C. Rotaru, H. D. Mansvelder, A. B. Smit, and K. W. Li. 2011. 'Proteomics, ultrastructure, and physiology of hippocampal synapses in a fragile X syndrome mouse model reveal presynaptic phenotype', *J Biol Chem*, 286: 25495-504.

Kuret, J., E. E. Congdon, G. Li, H. Yin, X. Yu, and Q. Zhong. 2005. 'Evaluating triggers and enhancers of tau fibrillization', *Microsc Res Tech*, 67: 141-55.

Lapierre, L. R., C. D. De Magalhaes Filho, P. R. McQuary, C. C. Chu, O. Visvikis, J. T. Chang, S. Gelino, B. Ong, A. E. Davis, J. E. Irazoqui, A. Dillin, and M. Hansen. 2013. 'The TFEB orthologue HLH-30 regulates autophagy and modulates longevity in Caenorhabditis elegans', *Nat Commun*, 4: 2267.

Lechler, M. C., E. D. Crawford, N. Groh, K. Widmaier, R. Jung, J. Kirstein, J. C. Trinidad, A. L. Burlingame, and D. C. David. 2017. 'Reduced Insulin/IGF-1 Signaling Restores the Dynamic Properties of Key Stress Granule Proteins during Aging', *Cell Rep*, 18: 454-67.

Li, T., and H. K. Paudel. 2016. '14-3-3zeta Mediates Tau Aggregation in Human Neuroblastoma M17 Cells', *PLoS One*, 11: e0160635.

Liao, L., D. Cheng, J. Wang, D. M. Duong, T. G. Losik, M. Gearing, H. D. Rees, J. J. Lah, A. I. Levey, and J. Peng. 2004. 'Proteomic characterization of postmortem amyloid plaques

isolated by laser capture microdissection', *J Biol Chem*, 279: 37061-8.

Link, C. D. 1995. 'Expression of human beta-amyloid peptide in transgenic Caenorhabditis elegans', *Proc Natl Acad Sci U S A*, 92: 9368-72.

Mahler, J., J. Morales-Corraliza, J. Stolz, A. Skodras, R. Radde, C. C. Duma, Y. S. Eisele, M. J. Mazzella, H. Wong, W. E. Klunk, K. P. Nilsson, M. Staufenbiel, P. M. Mathews, M. Jucker, and B. M. Wegenast-Braun. 2015. 'Endogenous murine Abeta increases amyloid deposition in APP23 but not in APPPS1 transgenic mice', *Neurobiol Aging*, 36: 2241-7.

Marzesco, A. M., M. Flotenmeyer, A. Buhler, U. Obermuller, M. Staufenbiel, M. Jucker, and F. Baumann. 2016. 'Highly potent intracellular membrane-associated Abeta seeds', *Sci Rep*, 6: 28125.

McColl, G., B. R. Roberts, T. L. Pukala, V. B. Kenche, C. M. Roberts, C. D. Link, T. M. Ryan, C. L. Masters, K. J. Barnham, A. I. Bush, and R. A. Cherny. 2012. 'Utility of an improved model of amyloid-beta (Abeta(1)(-)(4)(2)) toxicity in Caenorhabditis elegans for drug screening for Alzheimer's disease', *Mol Neurodegener*, 7: 57.

Meyer-Luehmann, M., J. Coomaraswamy, T. Bolmont, S. Kaeser, C. Schaefer, E. Kilger, A. Neuenschwander, D. Abramowski, P. Frey, A. L. Jaton, J. M. Vigouret, P. Paganetti, D. M. Walsh, P. M. Mathews, J. Ghiso, M. Staufenbiel, L. C. Walker, and M. Jucker. 2006. 'Exogenous induction of cerebral beta-amyloidogenesis is governed by agent and host', *Science*, 313: 1781-4.

Morales, R., L. D. Estrada, R. Diaz-Espinoza, D. Morales-Scheihing, M. C. Jara, J. Castilla, and C. Soto. 2010. 'Molecular cross talk between misfolded proteins in animal models of Alzheimer's and prion diseases', *J Neurosci*, 30: 4528-35.

Morales, R., I. Moreno-Gonzalez, and C. Soto. 2013. 'Cross-seeding of misfolded proteins: implications for etiology and pathogenesis of protein misfolding diseases', *PLoS Pathog*, 9: e1003537.

Nagarathinam, A., P. Hoflinger, A. Buhler, C. Schafer, G. McGovern, M. Jeffrey, M. Staufenbiel, M. Jucker, and F. Baumann.

2013. 'Membrane-anchored Abeta accelerates amyloid formation and exacerbates amyloid-associated toxicity in mice', *J Neurosci*, 33: 19284-94.

Nielsen, L., R. Khurana, A. Coats, S. Frokjaer, J. Brange, S. Vyas, V. N. Uversky, and A. L. Fink. 2001. 'Effect of environmental factors on the kinetics of insulin fibril formation: elucidation of the molecular mechanism', *Biochemistry*, 40: 6036-46.

O'Nuallain, B., A. D. Williams, P. Westermark, and R. Wetzel. 2004. 'Seeding specificity in amyloid growth induced by heterologous fibrils', *J Biol Chem*, 279: 17490-9.

Olsen, J. V., L. M. de Godoy, G. Li, B. Macek, P. Mortensen, R. Pesch, A. Makarov, O. Lange, S. Horning, and M. Mann. 2005. 'Parts per million mass accuracy on an Orbitrap mass spectrometer via lock mass injection into a C-trap', *Mol Cell Proteomics*, 4: 2010-21.

Olzscha, H., S. M. Schermann, A. C. Woerner, S. Pinkert, M. H. Hecht, G. G. Tartaglia, M. Vendruscolo, M. Hayer-Hartl, F. U. Hartl, and R. M. Vabulas. 2011. 'Amyloid-like aggregates sequester numerous metastable proteins with essential cellular functions', *Cell*, 144: 67-78.

Oskarsson, M. E., J. F. Paulsson, S. W. Schultz, M. Ingelsson, P. Westermark, and G. T. Westermark. 2015. 'In vivo seeding and cross-seeding of localized amyloidosis: a molecular link between type 2 diabetes and Alzheimer disease', *Am J Pathol*, 185: 834-46.

Ottis, P., B. Topic, M. Loos, K. W. Li, A. de Souza, D. Schulz, A. B. Smit, J. P. Huston, and C. Korth. 2013. 'Aging-induced proteostatic changes in the rat hippocampus identify ARP3, NEB2 and BRAG2 as a molecular circuitry for cognitive impairment', *PLoS One*, 8: e75112.

Partridge, L. 2011. 'Some highlights of research on aging with invertebrates, 2010', *Aging Cell*, 10: 5-9.

Pelvig, D. P., H. Pakkenberg, A. K. Stark, and B. Pakkenberg. 2008. 'Neocortical glial cell numbers in human brains', *Neurobiol Aging*, 29: 1754-62.

Peters, T. W., M. J. Rardin, G. Czerwieniec, U. S. Evani, P. Reis-Rodrigues, G. J. Lithgow, S. D. Mooney, B. W. Gibson, and

R. E. Hughes. 2012. 'Tor1 regulates protein solubility in Saccharomyces cerevisiae', *Mol Biol Cell*, 23: 4679-88.

Qureshi, H. Y., T. Li, R. MacDonald, C. M. Cho, N. Leclerc, and H. K. Paudel. 2013. 'Interaction of 14-3-3zeta with microtubule-associated protein tau within Alzheimer's disease neurofibrillary tangles', *Biochemistry*, 52: 6445-55.

Ramot, D., B. E. Johnson, T. L. Berry, Jr., L. Carnell, and M. B. Goodman. 2008. 'The Parallel Worm Tracker: a platform for measuring average speed and drug-induced paralysis in nematodes', *PLoS One*, 3: e2208.

Reis-Rodrigues, P., G. Czerwieniec, T. W. Peters, U. S. Evani, S. Alavez, E. A. Gaman, M. Vantipalli, S. D. Mooney, B. W. Gibson, G. J. Lithgow, and R. E. Hughes. 2012. 'Proteomic analysis of age-dependent changes in protein solubility identifies genes that modulate lifespan', *Aging Cell*, 11: 120-7.

Sacino, A. N., J. I. Ayers, M. M. Brooks, P. Chakrabarty, V. J. Hudson, 3rd, J. K. Howard, T. E. Golde, B. I. Giasson, and D. R. Borchelt. 2016. 'Non-prion-type transmission in A53T alpha-synuclein transgenic mice: a normal component of spinal homogenates from naive non-transgenic mice induces robust alpha-synuclein pathology', *Acta Neuropathol*, 131: 151-4.

Schaffer, U., A. Schlosser, K. M. Muller, A. Schafer, N. Katava, R. Baumeister, and E. Schulze. 2010. 'SnAvi--a new tandem tag for high-affinity protein-complex purification', *Nucleic Acids Res*, 38: e91.

Scheuner, D., C. Eckman, M. Jensen, X. Song, M. Citron, N. Suzuki, T. D. Bird, J. Hardy, M. Hutton, W. Kukull, E. Larson, E. Levy-Lahad, M. Viitanen, E. Peskind, P. Poorkaj, G. Schellenberg, R. Tanzi, W. Wasco, L. Lannfelt, D. Selkoe, and S. Younkin. 1996. 'Secreted amyloid beta-protein similar to that in the senile plaques of Alzheimer's disease is increased in vivo by the presenilin 1 and 2 and APP mutations linked to familial Alzheimer's disease', *Nat Med*, 2: 864-70.

Schulz, A. M., and C. M. Haynes. 2015. 'UPR(mt)-mediated cytoprotection and organismal aging', *Biochim Biophys Acta*, 1847: 1448-56.

Spat, P., B. Macek, and K. Forchhammer. 2015. 'Phosphoproteome of the cyanobacterium Synechocystis sp. PCC 6803 and its dynamics during nitrogen starvation', *Front Microbiol*, 6: 248.

Spires-Jones, T. L., K. J. Kopeikina, R. M. Koffie, A. de Calignon, and B. T. Hyman. 2011. 'Are tangles as toxic as they look?', *J Mol Neurosci*, 45: 438-44.

Sturchler-Pierrat, C., D. Abramowski, M. Duke, K. H. Wiederhold, C. Mistl, S. Rothacher, B. Ledermann, K. Burki, P. Frey, P. A. Paganetti, C. Waridel, M. E. Calhoun, M. Jucker, A. Probst, M. Staufenbiel, and B. Sommer. 1997. 'Two amyloid precursor protein transgenic mouse models with Alzheimer disease-like pathology', *Proc Natl Acad Sci U S A*, 94: 13287-92.

Sulston, J. & Hodgkin, J. . 1988. *The Nematode Caenorhabditis elegans* (Cold Spring Harbor Laboratory Press: Cold Spring Harbor).

Sutherland, B. W., J. Toews, and J. Kast. 2008. 'Utility of formaldehyde cross-linking and mass spectrometry in the study of protein-protein interactions', *J Mass Spectrom*, 43: 699-715.

Suzuki, N., T. T. Cheung, X. D. Cai, A. Odaka, L. Otvos, Jr., C. Eckman, T. E. Golde, and S. G. Younkin. 1994. 'An increased percentage of long amyloid beta protein secreted by familial amyloid beta protein precursor (beta APP717) mutants', *Science*, 264: 1336-40.

Tabara, H., A. Grishok, and C. C. Mello. 1998. 'RNAi in C. elegans: soaking in the genome sequence', *Science*, 282: 430-1.

Tagwerker, C., K. Flick, M. Cui, C. Guerrero, Y. Dou, B. Auer, P. Baldi, L. Huang, and P. Kaiser. 2006. 'A tandem affinity tag for two-step purification under fully denaturing conditions: application in ubiquitin profiling and protein complex identification combined with in vivocross-linking', *Mol Cell Proteomics*, 5: 737-48.

Tanase, M., A. M. Urbanska, V. Zolla, C. C. Clement, L. Huang, K. Morozova, C. Follo, M. Goldberg, B. Roda, P. Reschiglian, and L. Santambrogio. 2016. 'Role of Carbonyl Modifications on Aging-Associated Protein Aggregation', *Sci Rep*, 6: 19311.

Teschendorf, D., and C. D. Link. 2009. 'What have worm models told us about the mechanisms of neuronal dysfunction in human neurodegenerative diseases?', *Mol Neurodegener*, 4: 38.

Timmons, L., and A. Fire. 1998. 'Specific interference by ingested dsRNA', *Nature*, 395: 854.

Van Nierop, P., Loos, M. . 2011. *Bioinformatics procedures for analysis of quantitative proteomics experiments using iTRAQ.* (Humana Press).

Vasconcelos, B., I. C. Stancu, A. Buist, M. Bird, P. Wang, A. Vanoosthuyse, K. Van Kolen, A. Verheyen, P. Kienlen-Campard, J. N. Octave, P. Baatsen, D. Moechars, and I. Dewachter. 2016. 'Heterotypic seeding of Tau fibrillization by pre-aggregated Abeta provides potent seeds for prion-like seeding and propagation of Tau-pathology in vivo', *Acta Neuropathol*, 131: 549-69.

Vilchez, D., I. Morantte, Z. Liu, P. M. Douglas, C. Merkwirth, A. P. Rodrigues, G. Manning, and A. Dillin. 2012. 'RPN-6 determines C. elegans longevity under proteotoxic stress conditions', *Nature*, 489: 263-8.

Walter, P., and D. Ron. 2011. 'The unfolded protein response: from stress pathway to homeostatic regulation', *Science*, 334: 1081-6.

Walther, D. M., P. Kasturi, M. Zheng, S. Pinkert, G. Vecchi, P. Ciryam, R. I. Morimoto, C. M. Dobson, M. Vendruscolo, M. Mann, and F. U. Hartl. 2015. 'Widespread Proteome Remodeling and Aggregation in Aging C. elegans', *Cell*, 161: 919-32.

Walther, D. M., and M. Mann. 2011. 'Accurate quantification of more than 4000 mouse tissue proteins reveals minimal proteome changes during aging', *Mol Cell Proteomics*, 10: M110 004523.

Wang, Q., R. L. Woltjer, P. J. Cimino, C. Pan, K. S. Montine, J. Zhang, and T. J. Montine. 2005. 'Proteomic analysis of neurofibrillary tangles in Alzheimer disease identifies GAPDH as a detergent-insoluble paired helical filament tau binding protein', *FASEB J*, 19: 869-71.

Wang, Y. P., J. Biernat, M. Pickhardt, E. Mandelkow, and E. M. Mandelkow. 2007. 'Stepwise proteolysis liberates tau fragments that nucleate the Alzheimer-like aggregation of full-length tau in a neuronal cell model', *Proc Natl Acad Sci U S A*, 104: 10252-7.

Wishart, D. S., T. Jewison, A. C. Guo, M. Wilson, C. Knox, Y. Liu, Y. Djoumbou, R. Mandal, F. Aziat, E. Dong, S. Bouatra, I. Sinelnikov, D. Arndt, J. Xia, P. Liu, F. Yallou, T. Bjorndahl, R. Perez-Pineiro, R. Eisner, F. Allen, V. Neveu, R. Greiner, and A. Scalbert. 2013. 'HMDB 3.0--The Human Metabolome Database in 2013', *Nucleic Acids Res*, 41: D801-7.

Zhuang, Z. P., M. P. Kung, C. Hou, D. M. Skovronsky, T. L. Gur, K. Plossl, J. Q. Trojanowski, V. M. Lee, and H. F. Kung. 2001. 'Radioiodinated styrylbenzenes and thioflavins as probes for amyloid aggregates', *J Med Chem*, 44: 1905-14.

6 Appendix

6.1 Abbreviations

Aβ	Amyloid-beta
AD	Alzheimer's disease
APP	Amyloid precursor protein
APS	Ammonium persulfate
BMH	Bis(maleimido)hexane
BSA	Bovine serum albumin
$CaCl_2$	Calcium chloride
C. elegans	*Caenorhabditis elegans*
CV	Column volume
Da	Dalton
DSG	Disuccinimidyl glutarate
dsRNA	Double-stranded RNA
DTT	Dithiothreitol
E. coli	*Escherichia coli*
EDTA	Ethylenediaminetetraacetic acid
EGTA	Ethyleneglycoltetraacetic acid
ER	Endoplasmic reticulum
FDR	False discovery rate
FRANK	Fibrillization of Recombinant Aβ Nucleation Kinetic

GFP	Green fluorescent protein
HCD	Higher energy collision dissociation
HEPES	4-(2-hydroxyethyl)-1-piperazineethanesulfonic acid
HGM	High Growth Medium
HRP	Horseradish peroxidase
HSP	Heat-shock protein
iTRAQ	isobaric tags for relative and absolute quantitation
K114	(*trans*,*trans*)-1-bromo-2,5-bis-(4-hydroxy) styrylbenzene
LB	Lysogeny broth
LC	Liquid chromatography
MES	4-Morpholineethanesulfonic acid
mRNA	Messenger RNA
MS	Mass spectrometry
MS/MS	Tandem mass spectrometry
NaCl	Sodium chloride
NaF	Sodium fluoride
NG	Nematode growth
NP40	Nonidet P40
N2	Wild-type *C. elegans* strain
PBS	Phosphate-buffered saline
PEP	Posterior error probability

PFA	Para-Formaldehyde
PMSF	Phenylmethylsulfonyl fluoride
PrP^{Sc}	Scrapie prion protein
PS-1, -2	Presenilin-1, -2
PVDF	Polyvinylidene difluoride
RAB	Reassembly
RFP	Red fluorescent protein
RIPA	Radioimmunoprecipitation assay
RNA	Ribonucleic acid
RNAi	RNA interference
rpm	rounds per minute
SAM	Significant Analysis of Microarrays
SDO	Sodium deoxycholate
SDS	Sodium dodecyl sulfate
SEM	Standard error of the mean
TBS	Tris-buffered saline
TBST	TBS with 0.1% Tween20
TDP-43	Transactive response (TAR) DNA-binding protein 43
TEMED	Tetramethylethylenediamine
ThT	Thioflavin T
Tris	Tris(hydroxymethyl)aminomethane

UPR	Unfolded protein response
x g	times gravity

6.2 Motility analysis

6.2.1 Settings for The Parallel Worm Tracker software

Settings were obtained from Dr. Jan Kubanek (Stanford University, USA).

6.2.1.1 Settings to track worm videos with MATLAB R2015b

```
%open
outmovie = sprintf('tracked.mp4');
MovieOutObj = VideoWriter(outmovie, 'MPEG-4'); MovieOutObj.FrameRate = framerate; open(MovieOutObj);

%read
hasFrame(MovieObj); %touch the frame pointer MovieFrame = readFrame(MovieObj);

%write
framepar.resolution = [RES_H, RES_V];
frame = fig2frame(gcf, framepar);
writeVideo(MovieOutObj, frame);

%close
close(MovieOutObj);
```

6.2.1.2 Settings to analyze videos taken for other time periods than 30 s

```
function TrackWorms()

% 2015-05-04 Updated to accept movie formats beyond .avi, using
% VideoReader (introduced in R2010b)
% Author: Jan Kubanek (kubanek@go.wustl.edu)

recordbw = 0; %whether to record the video as bw instead of gray

WormTrackerPrefs.MinWormArea = 300;
WormTrackerPrefs.MaxWormArea = 2000;
WormTrackerPrefs.MaxDistance = 50;
WormTrackerPrefs.SizeChangeThreshold = 500;
WormTrackerPrefs.MinTrackLength = 100;
WormTrackerPrefs.AutoThreshold = 1;
WormTrackerPrefs.ManualSetLevel = 0.5;
WormTrackerPrefs.DarkObjects = 0;
WormTrackerPrefs.PlotRGB = 0;
WormTrackerPrefs.PauseDuringPlot = 0;
WormTrackerPrefs.PlotObjectSizeHistogram = 0;
```

```
% WormTrackerPrefs.CorrectFactor = 0.3;
WormTrackerPrefs.CorrectFactor = 0.09;
%image resolution
RES_H = 2048;
RES_V = 1536;
framerate = 20; %fps
NumberOfFrames = 139; %total number of video frames

%----------------------
%clipping

%clip to a rectangle; no clip if empty
rectangularclip = [];
%   rectangularclip = [20,310,180,480];

%clip to a circle; no clip if empty

%focus 2015-10-05 nobact
%focuspar = [310, 130, 6];

%2015-10-12
focuspar = [220, -40, 7];
```

```
center_x = RES_H / 2 - focuspar(1);

center_y = RES_V / 2 - focuspar(2);

radius = RES_V / focuspar(3);

circularclip = [center_x, center_y, radius]; %center_x, center_y, radius

%    circularclip = []; %


% Setup figure for plotting tracker results

% ----------------------------------------

WTFigH = findobj('Tag', 'WTFIG');

if isempty(WTFigH)

   WTFigH = figure('Name', 'Tracking Results', ...

      'NumberTitle', 'off', ...

      'Tag', 'WTFIG');

else

   figure(WTFigH);

end


%settings for movie output

% axis tight;

% set(gca,'nextplot','replacechildren');

% set(gcf,'Renderer','zbuffer');
```

```
% Start Tracker
% -------------
for MN = 1, %for all movies

%    MovieObj = VideoReader(MovieNames{MN});
   Tracks = [];

   % can use the information if necessary
%    NumberOfFrames = MovieObj.NumberOfFrames;

   %initiate video output
   %can use the following R2014b+ (see more comments on that
below)
%    outmovie = sprintf('tracked.mp4');
%    MovieOutObj = VideoWriter(outmovie, 'MPEG-4');
%    MovieOutObj.FrameRate = framerate;
%    open(MovieOutObj);

   %in R2015a, use avifile
   hFig = figure('Visible','off');
   set(hFig, 'PaperPositionMode','auto', 'InvertHardCopy','off')
   aviobj = avifile('tracked.avi', 'fps', framerate);
```

```
  % if circular clipping, precompute the clip area (use it as a multiplication mask)
  if ~isempty(circularclip),
    cx = round(circularclip(1));
    cy = round(circularclip(2));
    ra = round(circularclip(3));

% MovieFrame = read(MovieObj, 1); %if read() is still supported (R2014a doensn't have readFrame yet)

    SX = RES_H;
    SY = RES_V;

    mask = ones(SY, SX, 1);
    for xx = 1 : SX
      for yy = 1 : SY
        if (xx - cx)^2 + (yy - cy)^2 > ra^2, %outside the circle
          mask(yy, xx, :) = 0;
        end
      end
    end
    mask = uint8(mask);
  end
```

```
% Analyze Movie
% -------------
firstframe = 1;
for frameno = firstframe : NumberOfFrames,
  fprintf('Processing frame no %d\n', frameno);

  try
%       MovieFrame = read(MovieObj, frameno); %if read() is still supported (R2014a doensn't have readFrame yet)
    MovieFrame = imread(sprintf('Image_%d.bmp', frameno));
  catch
    hasFrame(MovieObj); %touch the frame pointer
    MovieFrame = readFrame(MovieObj); %if read is no more supported, readFrame will (readFrame doesn't need the frameno argument; it just reads the next frameno; haven't tested though!)
  end

  if ~isempty(rectangularclip),
    MovieFrame = MovieFrame(rectangularclip(1) : rectangularclip(2), rectangularclip(3) : rectangularclip(4), :);
  end
```

```
    %record the stimulus (LED at the very edge of the image)
    stimval = double(MovieFrame(end, end, :));

    if ~isempty(circularclip),
      %apply the circular mask
      MovieFrame = MovieFrame .* mask;

      %reduce the size
      MovieFrame = MovieFrame(cy - ra : cy + ra, cx - ra : cx + ra,
:);
    end
%     [a, MSGID] = lastwarn();
%     warning('off', MSGID);

    if frameno == firstframe,
      figure;
      imshow(MovieFrame);
%       pause;
    end

    % Convert frame to a binary image
    if WormTrackerPrefs.AutoThreshold       % use auto thresh-
olding
```

```
    Level = graythresh(MovieFrame) + WormTracker-
Prefs.CorrectFactor;
    Level = max(min(Level,1) ,0);
  else
    Level = WormTrackerPrefs.ManualSetLevel;
  end
  if WormTrackerPrefs.DarkObjects
    BW = ~im2bw(MovieFrame, Level);  % For tracking dark
objects on a bright background
  else
    BW = im2bw(MovieFrame, Level);  % For tracking bright
objects on a dark background
  end

  % Identify all objects
  [L,NUM] = bwlabel(BW);
  STATS = regionprops(L, {'Area', 'Centroid', 'FilledArea', 'Ec-
centricity'});

  % Identify all worms by size, get their centroid coordinates
  WormIndices = find([STATS.Area] > WormTracker-
Prefs.MinWormArea & ...
    [STATS.Area] < WormTrackerPrefs.MaxWormArea);
  NumWorms = length(WormIndices);
```

```
    WormCentroids = [STATS(WormIndices).Centroid];
    WormCoordinates = [WormCentroids(1:2:2*NumWorms)',
WormCentroids(2:2:2*NumWorms)'];
    WormSizes = [STATS(WormIndices).Area];
    WormFilledAreas = [STATS(WormIndices).FilledArea];
    WormEccentricities = [STATS(WormIndices).Eccentricity];


    % Track worms
    % -----------
    if ~isempty(Tracks)
      ActiveTracks = find([Tracks.Active]);
    else
      ActiveTracks = [];
    end


    % Update active tracks with new coordinates
    for i = 1:length(ActiveTracks)
      Tracks(ActiveTracks(i)).Stimulus =
[Tracks(ActiveTracks(i)).Stimulus; stimval];
      DistanceX = WormCoordinates(:,1) -
Tracks(ActiveTracks(i)).LastCoordinates(1);
      DistanceY = WormCoordinates(:,2) -
Tracks(ActiveTracks(i)).LastCoordinates(2);
      Distance = sqrt(DistanceX.^2 + DistanceY.^2);
```

```
        [MinVal, MinIndex] = min(Distance);

        if (MinVal <= WormTrackerPrefs.MaxDistance) & ...

            (abs(WormSizes(MinIndex) -
Tracks(ActiveTracks(i)).LastSize) < WormTracker-
Prefs.SizeChangeThreshold)

            Tracks(ActiveTracks(i)).Path =
[Tracks(ActiveTracks(i)).Path; WormCoordinates(MinIndex, :)];

            Tracks(ActiveTracks(i)).LastCoordinates = WormCoor-
dinates(MinIndex, :);

            Tracks(ActiveTracks(i)).Frames =
[Tracks(ActiveTracks(i)).Frames, frameno];

            Tracks(ActiveTracks(i)).Size =
[Tracks(ActiveTracks(i)).Size, WormSizes(MinIndex)];

            Tracks(ActiveTracks(i)).LastSize =
WormSizes(MinIndex);

            Tracks(ActiveTracks(i)).FilledArea =
[Tracks(ActiveTracks(i)).FilledArea, WormFilledAre-
as(MinIndex)];

            Tracks(ActiveTracks(i)).Eccentricity =
[Tracks(ActiveTracks(i)).Eccentricity, WormEccentrici-
ties(MinIndex)];

            WormCoordinates(MinIndex,:) = [];

            WormSizes(MinIndex) = [];

            WormFilledAreas(MinIndex) = [];

            WormEccentricities(MinIndex) = [];

        else
```

```
        Tracks(ActiveTracks(i)).Active = 0;
        if length(Tracks(ActiveTracks(i)).Frames) < WormTrackerPrefs.MinTrackLength
          Tracks(ActiveTracks(i)) = [];
          ActiveTracks = ActiveTracks - 1;
        end
      end
    end

    % Start new tracks for coordinates not assigned to existing tracks
    NumTracks = length(Tracks);
    for i = 1:length(WormCoordinates(:,1))
      Index = NumTracks + i;
      Tracks(Index).Active = 1;
      Tracks(Index).Path = WormCoordinates(i,:);
      Tracks(Index).LastCoordinates = WormCoordinates(i,:);
      Tracks(Index).Frames = frameno;
      Tracks(Index).Size = WormSizes(i);
      Tracks(Index).LastSize = WormSizes(i);
      Tracks(Index).FilledArea = WormFilledAreas(i);
      Tracks(Index).Eccentricity = WormEccentricities(i);
      Tracks(Index).Stimulus = double(0.0);
```

```
    end


    % Display every FrameRate'th frame
    if ~mod(frameno, 1)
      if recordbw,
        mov.cdata = BW;
        mov.colormap = [];
      else
        mov.cdata = MovieFrame;
        mov.colormap = colormap;
      end
      PlotFrame(WTFigH, mov, Tracks);
      FigureName = sprintf('Tracking Results for frame %d   ',
frameno);
      set(WTFigH, 'Name', FigureName);


      if WormTrackerPrefs.PlotRGB
        RGB = label2rgb(L, @jet, 'k');
        figure(6)
        set(6, 'Name', FigureName);
        imshow(RGB);
        hold on
        if ~isempty(Tracks)
```

```
        ActiveTracks = find([Tracks.Active]);
    else
        ActiveTracks = [];
    end
    for i = 1:length(ActiveTracks)
        plot(Tracks(ActiveTracks(i)).LastCoordinates(1), ...
            Tracks(ActiveTracks(i)).LastCoordinates(2), 'wo');
    end
    hold off
end

if WormTrackerPrefs.PlotObjectSizeHistogram
    figure(7)
    hist([STATS.Area],300)
    set(7, 'Name', FigureName);
    title('Histogram of Object Sizes Identified by Tracker')
    xlabel('Object Size (pixels')
    ylabel('Number of Occurrences')
end

if WormTrackerPrefs.PauseDuringPlot
    pause;
```

```
        end


        %write frame to video
        %frame = getframe(gcf); %getframe sucks, capture anything
        %that's on the screen


        %the following is an alternative to getframe, but only works in
        %R2014b+; But R2015b has issue with exporting eps (exports triangular objects) so not using it;
        %try to see whether R2015 fixes that; in that case, can use the
        %following code:
%           framepar.resolution = [RES_H, RES_V];
%           [frame] = fig2frame(gcf, framepar);
%           writeVideo(MovieOutObj,frame);

%so for now, use the deprecated avifile (may slow things down)
        aviobj = addframe(aviobj, gcf);
    end


  end    % END for frameno = 1:MovieObj.NumFrames
```

```
    %save the video
    %use in R2014b+
    %close(MovieOutObj);
    %for the moment (R2014a), use:
    aviobj = close(aviobj);

    % Get rid of invalid tracks
    DeleteTracks = [];
    for i = 1:length(Tracks)
      if length(Tracks(i).Frames) < WormTracker-
Prefs.MinTrackLength
        DeleteTracks = [DeleteTracks, i];
      end
    end
    Tracks(DeleteTracks) = [];

    % Save Tracks
    SaveFileName = sprintf('wormcords.mat');
    save(SaveFileName, 'Tracks');

    close all; %close fig
end
```

6.2.2 Motility analysis of Aβ overexpressing *C. elegans* subjected to control RNAi

Table 6.1: Motility analysis of Aβ overexpressing worms subjected to different control RNAi's (L4440, HER-1, GFP). Shown are the speeds of the worms (mm/s) after analysis with MatLab or ImageJ. For both analysis programs the minimum speed is highlighted in red and the maximum speed is highlighted in green. The average speed is shown bold.

L4440		**HER-1**		**GFP**	
MatLab	ImageJ	MatLab	ImageJ	MatLab	ImageJ
0.014846	0.021533333	0.0056622	0.011294118	0.014553	0.021375
0.012329	0.0175	0.0061692	0.011470588	0.015467	0.030636364
0.012123	0.019875	0.0050093	0.0094	0.010147	0.013
0.010499	0.016647059	0.0050337	0.010111111	0.010635	0.017555556
0.0097831	0.012866667	0.0067667	0.011166667	0.011438	0.0305
0.01975	0.038157895	0.022927	0.06325	0.0069989	0.013928571
0.0154	0.0331	0.0055339	0.0269	0.0057541	0.0124
0.011947	0.021	0.0051462	0.025777778	0.0057969	0.012833333
0.011763	0.023	0.022897	0.028071429	0.0057378	0.012153846
0.0089456	0.019263158	0.022708	0.0314	0.0058266	0.011923077
0.020185	0.0288125	0.024152	0.0481	0.015416	0.023166667
0.010325	0.0228125	0.010978	0.042642857	0.0084805	0.02
0.011594	0.019625	0.037393	0.0495	0.010284	0.0151
0.010209	0.0153125	0.014137	0.03625	0.010398	0.016125
0.010137	0.01475	0.018501	0.017785714	0.0079139	0.013125
0.012656	**0.0202625**	**0.014201**	**0.027320994**	**0.0096564**	**0.017588161**

6.3 Statement of contributions

All experiments and data analyses described for the first project with the title "Identifying age-dependent heterologous seeds for amyloid-β aggregation" were performed by myself besides the ones that are listed in the next paragraph. Briefly, I performed the following experiments and analyses: strain generation of DCD296, *C. elegans* liquid culture, insoluble protein extraction and quick protein extraction, gel electrophoresis and western blotting, mass spectrometry analysis with *C. elegans* samples (dialysis, preparation, labeling), mass spectrometry analysis with mice samples (dialysis and data analysis), motility analysis, paralysis assay and staining of *C. elegans* with K114.

Anika Bühler performed the FRANK Assay, in detail the preparation of the Assay plate and the measurements, supervised by Dr. Frank Baumann who also evaluated the data. Both worked at the Hertie Institute for Clinical Brain Research, Tübingen. For the FRANK assay, the peptide Aβ(1-40) was expressed and purified by Prof. Marcus Fändrich (University Ulm). Dr. Frank Baumann removed the mouse brains for the FRANK Assay or mass spectrometry analysis. The intracerebral injection into APP23 transgenic mice and analysis were performed by Ulrike Obermüller and supervised by Dr. Frank Baumann (Hertie Institute for Clinical Brain Research, Tübingen). Mass spectrometry and data analysis with samples from *C. elegans* were performed by Dr. Ka Wan Li, Pim van Nierop and Prof. August B. Smit (VU University Amsterdam). Mass spectrometry analysis with mice samples, in detail the labeling of the samples and nano-liquid chromatography-MS/MS analysis, were performed by Dr. Ana Velic (Proteome Center Tübingen). The Ingenuity Pathway Analysis was performed by Dr. Chaolie Huang (DZNE, Tübingen). The intern Stavros Vagionitis performed the motility analysis after knock-

down of early-aggregating proteins that continued to aggregate strongly at day 10 and day 14 (DZNE, Tübingen). To be able to use the Parallel Worm Tracker software changes were made in the MATLAB code by Björn Müller (CIN, Tübingen) and Angelos Skodras (DZNE, Tübingen).

The following colleagues contributed to the second project described in this thesis with the title "Investigation whether rapidly-aggregating proteins seed the aggregation of other proteins": Dr. Emily Crawford developed the tandem-affinity purification strategy and generated a Gateway vector with histidine-avidin tag. Katja Widmaier performed the construct injection into N2 animals to generate the transgenic *C. elegans* line used for the project. Both worked at the DZNE, Tübingen.

All other experiments and data analyses described for the second project were performed by myself. Briefly, I performed the cloning and strain generation (besides the construct injection), *C. elegans* liquid culture, insoluble protein extraction with and without chemical crosslinking, protein purification with nickel affinity chromatography, gel electrophoresis and western blotting.

7 Acknowledgements/Danksagungen

Hiermit möchte ich mich bei der Arbeitsgruppe "Aggregation and Aging" des DZNE Tübingen für ihre Unterstützung und die nette Zusammenarbeit bedanken.

Vor allem bedanke ich mich bei Dr. Della David für die Betreuung meiner Doktorarbeit, sowie bei Prof. Stehle und Prof. Ueffing für das Feedback und ihre Ratschläge während der Advisory Board Meetings.

Dr. Frank Baumann und Anika Bühler gilt ebenfalls mein Dank für die kollegiale Zusammenarbeit.

Abschließend möchte ich meinem Mann und meiner gesamten Familie danken. Sie haben mich während meines Studiums und der Erarbeitung meiner Dissertation immer motiviert und unterstützt.